ABSTRACT

CHAFIN, CLIFFORD. Thermodynamics, Hydrodynamics and Damping in Ultracold Gases. (Under the direction of Thomas Schäfer.)

Ultracold gases have provided experimental systems that span microscopic to macroscopic regimes of behavior and over a range of internal energy scales and interaction strengths that drive behavior from ballistic to hydrodynamic and degenerate to correlated. Here we will examine these systems from several points of view. First, we present a discussion from the standpoint of the evolution of a single many body wavefunction. In support of this picture we examine the longstanding vagueness surrounding measurement and thermalization and show the situation here is significantly better from this point of view than generally presented. The implications for how well defined a temperature can be achieved by various trap manipulation is discussed along with proposed experiments to distinguish these cases. Since hydrodynamic methods have worked well in some cases we then discuss the unitary limit for fermions with contact limited interactions. The scale invariance of the system implies limits on hydrodynamic behavior from which we extract bounds on viscous damping from free expansion and trap oscillation experiments. Linear response theory is used to probe the effect of quantum fluctuations on the viscosity and some nonuniversal contributions are derived. These show that the classical gradient expansion of hydrodynamics breaks down at lower than Burnett order, where problems with the classical expansions typically occur.

Thermodynamics, Hydrodynamics and Damping in Ultracold Gases

by
Clifford Chafin

A dissertation submitted to the Graduate Faculty of
North Carolina State University
in partial fulfillment of the
requirements for the Degree of
Doctor of Philosophy

Physics

Raleigh, North Carolina

2013

APPROVED BY:

Dean Lee	Lubos Mitas
Michael Shearer	Thomas Schäfer Chair of Advisory Committee

DEDICATION

To my mother, Darla, and sister, Cathy.

BIOGRAPHY

Clifford Chafin was born in Arizona. A cross country drive from Boston to California by his mother ended with car failure in Phoenix. She transferred her broadcasting knowledge from radio to local television and made it her new home. The suspicious choice of his firmly Democratic father to attend the local meetings of the young Republicans club and his well functioning car led to a successful courtship. Soon the new family moved to El Paso where his prolific π-reciting dad started an electronics retail company. After 10 years in west Texas, Clifford realized that he was neither Latino nor making any progress in that direction. Except for cosmetic differences, this was a minor problem. Larger ones were an arrogant doctor's role in brain damaging his sister, the one month concussion a neighbor gave him at three, another neighbor stabbing him in the eye at seven and his middle-aged father's decision to embrace the libertine lifestyle of the day.

He and his mother returned to her home in northern Maine one winter day when the ΔT between the source and terminus of their trip was 105° F. This gave him the opportunity to discover that snow could last months not just hours, that he was as bad at French as Spanish and that not even other white people were interested in calculators, slide rules or the McGraw-Hill Encyclopedia of Science and Technology. After building a computer from scratch and later winning the state science fair in chemistry he was voted "most individual" in his high school and considered one of the most likable dorks anyone had ever met. At seventeen, he left home on his bicycle and rode to West Virginia and worked through the winter on a family hog farm. Returning to Maine he started a career as a wooden boatbuilder. From here things become confusing.

The director of his particular shop, Robert Ives, had experienced higher education at Bowdoin college before becoming a hippie-preacher and devoting his life to good deeds, transforming the lives of the poor in Lincoln county, and meddling in the lives of otherwise happy people. He convinced the impressionable young man that college would be a wise choice. Clifford matriculated at Middlebury college where he hitchhiked among the Green mountains and worked at a local co-op. He majored in physics, minored in Hebrew, attended the famous summer immersion Arabic language program. Despite the disadvantage of coming from a small rural high school and competing with peers from powerful preparatory institutions he managed to win a prestigious Dana scholarship to cover his education and graduate magna cum laude. This was helped by the fact that many of his peers, after so much work in prep school, were really ready for a long rest and celebration and college provided the perfect opportunity. In his spare time he was on the student body council, the head officer in the Armadillos political discussion group, secretary of Environmental Quality and a member of Hillel.

Things were seeming to go well for Clifford but his health was mysteriously failing. He enrolled in UNC for physics graduate school but continued to decline and withdrew. Accepting that he was not going to live much longer he pursued his personal passions, studying number theory and attending graduate mathematics classes. He also worked counseling victims of HIV/AIDS and young people about smart sexual choices. Eventually he was diagnosed with celiac sprue and made a complete recovery. Experiencing some ire at UNC hospitals where he had previously sought care, he enrolled at NCSU. This turned out to be the perfect opportunity. The excellent physics program was diverse, positive and unpolitical, the students industrious and inspired and the support staff heroic. He did experimental work in granular physics and acoustics then theoretical work in many body quantum theory and hydrodynamics. The entrepreneurial spirit of the school and resources of the "garage" has brought him in contact with many dynamic and creative people that motivate, humble and inspire him and leave him ever more grateful.

ACKNOWLEDGEMENTS

It is a bit daunting to try to understand, much less adequately acknowledge, all the debts one has acquired at such a threshold in one's life and education. Certainly, there is a debt to North Carolina State University, the state of North Carolina and the physics department for their initial faith and the opportunity to pursue such a transformative path in knowledge, intellectual growth and career potential. The National Science Foundation provided financial support that allowed me some measure of financial freedom through my adviser. Because of them, my circle of obligations extends to the entire country.

Michael Paesler was my first interview here at NC State and his humility, positivity and enthusiasm convinced me that this department had, not just the academics, but the working environment and favorable politics for success. He tapped me for a special NSF TUES proposal project, eTALK, that helped support me and gave me an exciting experience in physics education research.

David Aspnes, while not a coworker, gave me a practically life-transforming year of Jackson based electromagnetism that has colored, inspired and haunted everything I have done since. After all his experience and professional success, his maxim, "If it's not simple, I don't believe it" drives me to understand things in terms of the simplest and most illustrative examples as foils for complex derivations. Only through a synthesis of both of these can I ever navigate the soup of computational success and failure that is the state of the physics literature.

My adviser, Thomas Schäfer has been kind, supportive, patient-as-a-saint as I have climbed, crashed, tilted at windmills and had almost existential crises over physics in my very skeptical approach to science. Hopefully, he has few regrets of entertaining a student so shy of credulity and faith in our physics fathers. I will always treasure our multi-hour arguments.

It is impossible for me to name all the faculty and peers that helped, inspired, shared an ear of support or served as foils for uncertain and unformed notions but I will list a few: Harald Ade, C-R Ji, Dean Lee, Lubos Mitas, James York Jr., Dave Fallest, Letitia McLaughlin, and Don Warren.

The support of family and friends is too important and too numerous to do justice. My mother, Darla S. Chafin, has always had faith in me, despite regular evidence that this wasn't always justified. My sister, Cathy, reminds me how to have dignity and humor in the face of disaster. Surviving and recovering from Lyme disease in the middle of my PhD was nearly the end of my resolve. No one more than she reminded me to laugh and keep on going. Special thanks to Julian and Elsie Hall, John and Marilyn MacDuffie, Bo Hemphill and Renee Foster, Pamela Taylor, Myron Feinstein and the whole tango crowd. Special thanks to Jill Menard for the dinners, laughs, life of the circus and hopes for the future.

TABLE OF CONTENTS

LIST OF FIGURES

Chapter 1

Introduction

1.1 Cold Quantum Gases

Over the past twenty years intensive research has been devoted to the behavior of dilute quantum gases of bosonic and fermionic atoms. These systems probe equilibrium and non-equilibrium thermodynamic properties of matter in a new regime:

- The systems are genuine quantum fluids. The thermal de Broglie wave length $\lambda = \hbar(\frac{2\pi}{mk_BT})^{1/2}$ is bigger than the average spacing between particles $n^{-1/3}$. Previously, the only bulk quantum fluids that could be studied in the laboratory are the two isotopes of helium, ^{4}He and ^{3}He.

- The interaction between particles can be tuned with the help of Fano-Feshbach resonances. This means that we can study the transition from weakly coupled quantum gases to strongly coupled quantum fluids. We can also study such phenomena as the transition from weak pairing of highly overlapping states, as in Bardeen-Cooper-Schrieffer (BCS) superconductivity, to Bose-Einstein condensation (BEC) of tightly bound molecular pairs.

- Trapped atomic gases bridge the gap between quantum mechanical few body systems, with $N \sim (3 - 100)$ particles, and truly macroscopic systems, with $N \sim N_A \sim 10^{23}$ particles. Typical experiments involve $N \sim (10^3 - 10^7)$ particles.

In this thesis we will concentrate on the thermodynamics and fluid dynamics of trapped fermionic gases, with a special emphasis on the unitary Fermi gas. The unitary Fermi gas refers to the limit in which the s-wave scattering length is taken to infinity. In this limit the quantum mechanical scattering amplitude saturates the s-wave unitarity bound (hence the name "unitary"). The unitary Fermi gas is interesting because the system is dilute but very

strongly correlated, and because the interactions do not spoil the exact scale invariance of the non-interacting gas.

Specifically, we will explore whether methods of non-equilibrium thermodynamics can be applied to trapped unitary Fermi gases. We will study the consequences of quantum statistics and strong correlations for equilibrium and transport properties of these systems. An important motivation for these studies comes from the idea that the unitary Fermi gas in an example of a system in which dissipative phenomena, in particular shear viscosity, are limited by quantum effects. The shear viscosity η is a measure of the rate of momentum diffusion. In kinetic theory this rate can be estimated as

$$\eta \sim n\bar{p}l_{mfp}\,, \tag{1.1}$$

where n is the particle density, $\bar{p}$ is the mean particle momentum, and l_{mfp} is the mean free path. In a strongly correlated quantum fluid, it is suspected that the product $\bar{p}l_{mfp}$ approaches the limit set by the quantum mechanical uncertainty relation and $\eta/n \sim \hbar$. We will discuss the limitations on the possibilities of mapping general many-body wavefunction evolution onto a hydrodynamic set of variables.

Hydrodynamic ideas about quantum limited transport have been made more precise using methods of string theory and the AdS/CFT correspondence. In particular, one can find a class of fluids for which in the strong coupling limit $\eta = \frac{\hbar s}{4\pi k_B}$, where s is the entropy density. We will show that linear response theory for the unitary Fermi gas approaches this bound, and discuss some of the implications of this very low viscosity for fluid dynamics in ultracold gases.

1.2 Thermodynamics and Fluid Dynamics

Much of our analysis is based on the methods of thermodynamics and fluid dynamics. Thermodynamics is based on the idea that a complicated many body system probed on spatial scales much larger than the inter-particle spacing and on temporal scales much longer than microscopic time scales can be described in terms of coarse grained thermodynamic variables. Instead of the classical description in terms of $6N$ coordinates on phase space, or the quantum mechanical description based on a wave function dependent on $3N$ coordinates, we characterize the system in terms of a set of thermodynamic variables such as temperature T, chemical potential μ, etc., that fix the globally conserved quantities like energy, particle number, etc. Whenever this description is possible we say that the system is in thermal equilibrium.

If the microscopic dynamics of the system is known, thermodynamic properties can be derived from the classical or quantum mechanical partition function. In the quantum case

$$Z(T,\mu) = \mathrm{Tr}\left[e^{-(H-\mu N)/T}\right]\,, \tag{1.2}$$

where H is the Hamiltonian, N is the particle number operator, and Tr denotes a sum over all states of the system and we have now let $k_B = 1$. The partition function is related to the pressure

$$P(T,\mu) = -\frac{T}{V}\log Z(T,\mu)\,, \tag{1.3}$$

where V is the volume. Derivatives of the pressure determine other thermodynamic quantities, like the entropy and the particle density. The pressure also determines possible phase changes, and fluctuations of thermodynamic quantities around their mean values.

Fluid dynamics is based on the idea that small deviations from equilibrium are governed by local conservations laws. In the case of a non-relativistic fluid the conserved charges are the mass density ρ, the momentum density $\vec{\pi} = \rho\vec{v}$, and the energy density $\mathcal{E}$. Here, $\vec{v}$ is the local fluid velocity. The conservation laws are

$$\frac{\partial\rho}{\partial t} + \vec{\nabla}\cdot(\rho\vec{v}) = 0, \tag{1.4}$$

$$\frac{\partial(\rho v_i)}{\partial t} + \nabla_j\Pi_{ij} = 0, \tag{1.5}$$

$$\frac{\partial\mathcal{E}}{\partial t} + \vec{\nabla}\cdot\vec{\jmath}^{\,\epsilon} = 0. \tag{1.6}$$

The total energy density is the sum of the internal energy density and kinetic energy density, $\mathcal{E} = \mathcal{E}_0 + \frac{1}{2}\rho v^2$. The mass current is $\vec{\jmath} = \rho\vec{v}$. The equations close once we supply constitutive relations for the remaining currents, the stress tensor Π_{ij} and the energy current $\jmath_i^{\,\epsilon}$. Near thermal equilibrium the currents can be expressed systematically in terms of local thermodynamic variables and their derivatives. The stress tensor is given by

$$\Pi_{ij} = \rho v_i v_j + P\delta_{ij} + \delta\Pi_{ij}\,, \tag{1.7}$$

where $\delta\Pi_{ij}$ contains gradients. Neglecting these terms leads to ideal fluid dynamics. Taking into account gradients amounts to including dissipative effects. At first order in derivatives the most general form of the stress tensor consistent with Galilean and rotational invariance is

$$\delta\Pi_{ij} = -\eta\sigma_{ij} - \zeta(\vec{\nabla}\cdot\vec{v}) \tag{1.8}$$

with

$$\sigma_{ij} = \nabla_i v_j + \nabla_j v_i - \frac{2}{3}\delta_{ij}(\vec{\nabla}\cdot\vec{v})\,, \tag{1.9}$$

where η is the shear viscosity and ζ is the bulk viscosity. Requiring $\eta, \zeta \geq 0$ ensures that the second las of thermodynamics is satisfied. The equation of momentum conservation at first

order in derivatives is called the Navier-Stokes equation. The energy current is

$$\jmath_i^\epsilon = v_i w + \delta\jmath_i^\epsilon \,, \tag{1.10}$$

where $w = \mathcal{E}_0 + P$ is the enthalpy density. The dissipative energy current is

$$\delta\jmath_i^\epsilon = \delta\Pi_{ij} v_j - \kappa\nabla_i T \,, \tag{1.11}$$

where T is the temperature and κ is the thermal conductivity.

We note that the equations of fluid dynamics make no assumptions about the microscopic degrees of freedom or the phase structure of the fluid. The equations apply equally to gases, plasmas, and liquids (both quantum or classical). Modifications are required if there are additional conserved quantities, or if some of the symmetries are spontaneously broken, as is the case in superfluids or solids.

1.3 Limitations of Fluid Dynamics

Fluid dynamics is a remarkably general and powerful approach but it is difficult to derive fluid dynamics from first principles. In the classical case, the mechanical motion is simply a statement on the conservation of momentum [33]. Higher momentum expansions of kinetic theory [32] yield the Navier-Stokes equations and specific values for the transport coefficients and microscopic definitions of the thermodynamic functions. In certain limiting cases such as the limits of very weak or very strong coupling, one can derive fluid dynamic behavior for low energy configurations (as in the case of the Gross-Pitaevskii equation), however, it is clear that general wavefunctions exist that have no sensible or propagated mapping onto the much more restrictive hydrodynamic formalism. The extent to which relaxation to such states will occur will be discussed. In the following we will discuss some of the conceptual issues that arise in relating general quantum evolution to fluid dynamics and the well-posedness of the thermodynamic limit.

In hydrodynamics, the ways vorticity can enter a system is constrained. In the absence of density gradients, viscosity can only pull vorticity in through the surface [12]. Quantum systems (i.e. wavefunctions) also are very restricted with respect to vorticity. However, here vorticity for an N-body ψ can only exist in the form of singular 3N-2 dimensional hypercurves where the wavefunction's norm possesses a discontinuity in its gradient. For certain strongly interacting cases, like superfluid Helium, these exhibit a coherence so that these give zeros in the one body density function. It is interesting to note that a long standing problem in hydrodynamics is the immortality of solutions, specifically the nonsingular existence of solutions to Navier-Stokes for all time [86]. This has been shown to reduce to the equivalent property of never forming

singular vorticity in finite time. Ironically, quantum systems only show singular vorticity for all time. Some bridge that represents classical fluids as limits of special quantum systems might shed light on this old problem.

Much of the work on ultracold gases has centered on finding equations of state and transport functions for hydrodynamic and thermodynamic expressions in their description[91]. There is, however, an alternate and under discussed point of view that such systems might be a powerful lever in the investigation of some of the old and languishing problems at the heart of physics: measurement theory and the unification of classical and quantum dynamics, ensembles as a foundation for statistical mechanics and thermodynamics and the justification and consistency of quantum statistical mechanics. These points are not purely academic. To some degree, quantum mechanics, classical mechanics, and thermodynamics exist as independent pillars of a physics that are still unreconciled. This leaves questions about their consistency in doubt and, since they are related by ansatz and prescriptions, how to proceed in nonequilibrium cases and on scales that are between classical and quantum unclear. Ultimately, microscopic *dynamics* and the theory's founding constraints should be the origin of all collective and limiting behaviors.

To discuss the thermal and hydro properties of condensed quantum systems, it would be very useful to have a consistent quantum treatment of classical matter. This would suggest when parallels will be justified and not. Hydrodynamics and elasticity are traditionally classical fields though there has been an encroachment on them by quantum means to get transport and mechanical properties just as there has been a supplanting of classical statistical mechanics by quantum methods. Although some of these calculations have been very successful, others, with a priori just as much reason to succeed, have not and the foundations of quantum statistical mechanics is far more ad hoc and conceptually vague than its classical counterpart. Indeed, many of the exciting advances in statistical mechanics in recent years [35][67] have been limited to classical cases with no path to finding a quantum version.

The theory of measurement is another example where such a unified treatment would be valuable and make the case that such intuition is valid. Such claims and proposals now provokes a great aversion on the part of physicists. After years of philosophy heavy discussions and posturing that seemed to produce no new predictions many are, if not true positivists, more inclined to work with existing formalism than risk getting drawn down an unproductive avenue or engage in arguments that seem more about words than physics.

The quantum theory of measurement is typically done by way of the Born interpretation, a measurement ansatz where a "measurement device" is associated with a linear self-adjoint operator that projects out a spectrum of possible measurements and their probabilities in a measurement "event" [42][133][24]. Despite having no fundamental way to explain why certain devices are measurement devices and what their spectrum of action should be, this has been the most economical and enduring approach to the problem.

Frustration with the current theory of quantum measurement goes back to Schrödinger himself who said that if he knew what they were going to do with his wavefunction, he never would have written it down [66]. When quantum and classical worlds seemed so vastly separated by scales, a positivist attitude seemed justified. Strangely, it was argued that nothing more was to be asked. This notion was a kind of life goal for Bohr and became broadly accepted. Of course, this separation of scales was destined to be temporary and, more than any argument about determinism, ontology, epistemology..., eventually we will need a unified description of classical matter in the same language of the microscopic. As an example, the action of a given measurement device should be determined by its microscopic nature. We should not have to require classical + quantum descriptions + a "by-fiat" assignment of the quantum measurement action of a given classical object. Ultimately we would like to replace "interpretation" with direct implication.

In the first few chapters, we take the point of view that all matter (of fixed particle number) is a wavefunction and well governed by the Schrödinger equation. By applying the basic constraints of classical rigid bodies to a wavefunction we derive quantum description for a solid body than includes a set of many body excitations clearly identifiable with phonons thus allowing a direct wavefunction description of, while not phonons themselves, the solid in an excited state corresponding to phonon occupancy. This represents a departure from the usual second quantized description. As a by-product we find that solid bodies (and therefore much of what we call classical matter) are actually somewhat far from true eigenstates of the Hamiltonian describing them even if they are cooled to absolute zero. They do however have the property of very long lifetimes (according purely to Schrödinger dynamics). As a side effect of this description we demonstrate that a "many worldsy" sort of measurement theory follows immediately from their interaction with delocalized particles. The large masses of these macroscopic objects creates an effective long lasting partition of the space that can be indexed by the incident wavefunction. Unlike most approaches where the wavefunction "collapses" (inducing locality problems, concerns about conserved quantities and back reactions), in this case the macroscopic world is "sliced" into temporal foliations by their interaction with delocalized bodies. The many body wavefunction continues to exist but these indexed slices cease to interact on human time scales thus leading to a kind branching of paths for the observers. Interestingly, this gives a completely local description of measurement that also allows for noninertial and otherwise dynamic measurement devices, situations that a complete theory should address but, for which, no obvious linear self-adjoint operator (LSAO) exists [24].

In the case of classical statistical mechanics, the problem of the Gibbs correct counting of states is well known and considered resolved by the particle symmetries in quantum mechanics [127]. The use of ensembles introduces more subtle problems. The use of phase space using the canonical momenta for N particles gives a conservation law for the probability by Liouville's

theorem. Once the energy of the system is fixed the system is constrained to a 6N-1 dimensional hypersurface. These states on this surface are delta functions that compose our ensemble. If the system is ergodic, the time average equals the space average, this is sometimes used to justify the unweighted sum over such states to derive our thermodynamic microcanonical averages. Ergodicity is not generally true [1] though Boltzmann was careful not to let his theory of gases depend on this [16] Even when ergodicity does hold, there is the problem that the time for an orbit to sample a representative fraction of the phase space is typically far longer than the time we observe a system to obtain information on its thermodynamic variables. A better perspective is probably to forget about ensembles and focus on the "typical elements" of the space that already possess values we obtain from such averaging in almost all instants on its orbit. When we show that such elements dominate the constant energy hypersuface we have the desired thermodynamic results.

Energy is not the only conserved quantity of motion. Generally, each of these further partition the hypersuface into lower dimensional subspaces. Angular momentum is typically ignored. As long as the quantities we probe don't depend on this, we can count ourselves as lucky in carrying out such rude ensemble calculations. The study of self bound systems introduces the possibility of nonextensive thermodynamic quantities [129]. Violations of the local density approximation for gases introduces such concerns. Some of these gases can be given large angular momenta and "nonlocal" effects ranging over the scale height of the gases would suggest extensivity fails. (Nonlocality arises in quantum many body systems explicitly in Hartree-Fock, implicitly in Gross-Pitaevskii, and other such approximations because we try to fit "3D boots on 3N-D feet." We will discuss this more later.) Equilibration and the arrow of time are not resolved by such a model but it does show that if one starts with a typical state then it moves to a state of higher or equal entropy and one recovers thermodynamics and hydrodynamics [41] the vast majority of the time (at least "for a while").

Whatever problems classical statistical mechanics has, quantum statistical mechanics' problems are much worse. The microcanonical quantum ensemble is based on collecting all the eigenstates "sufficiently close" to a given energy E_0 and assigning a number $\Omega(E_0)$ to it[1]. This is reminiscent of the classical case but, in the classical case, our hypersurface really did have to encompass *all* states with the given energy. An attempt has been made to weaken the microcanonical postulate [18] to include all superpositions with fixed energy E_0 and evaluate the most likely distribution. The cardinality of such a set is a power set of the continuum $2^{\mathcal{C}}$. Summing over such large sets is notoriously hard (as attempts to make Feynman path integrals rigorous demonstrate).

We formally get around these problems by introducing the density matrix and the master equation. The basic object is a "mixed state" which corresponds to a kind of ensemble of

[1]This vaguely defined criterion is not much help where states start getting thin and irregular in their density.

"pure states," i.e. wavefunctions, generally eigenstates. As above, the angular momentum of the states in a given potential is also conserved. This should partition our equations further (but this seems to rarely or never be done). Despite many years of trying [36] no one has been able to truly derive quantum statistical mechanics from the master equation. Even though the true eigenstates of many body functions can contain long range correlation effects, the state of the art is to ignore this and define parcels and assign local meaning to these results in a classical hydrodynamics.

We observe that classical (condensed) matter possesses well define position, shape, orientation and internal atomic structure. It should not be surprising that, typically, no many body wavefunctions possess these properties. This is one sense in which the "classical limit" is not just obtained by taking large N or large mass. Similarly we will see that thermodynamic states are not statistically typical when the full range of possible wavefunctions of given energy are considered. As such, thermodynamics does not arise as a consequence of merely having large N and large energy. This is a central consideration when considering what aspects of classical physics, specifically thermodynamics, hydrodynamics and implicit assumptions in the local density approximation, can be applied to the cold atomic gases being studied today. Despite these challenges and buoyed by some compelling results on solids, we apply classical kinematic constraints of hydrodynamics to gases to derive plausible conditions on typical wavefunctions and derive constraints on when classical thermal and hydrodynamic behavior occurs. This will suggest where to look for a "thermal-quantum" transition in ultracold gases.

In the first part of this paper we will review some aspects of quantum solutions rather carefully. Next we will propose a set of wavefunctions for solids and liquids that are actually, very far from eigenstates but persist in such condition for very long times. These are the special subset of wavefunctions that exhibit the usual kinematic freedom of classical bodies as 3D objects with Newtonian dynamics. From will demonstrate a measurement theory, in a proper limit, identical the Born ansatz. Extending this we will find a theory of measurement that holds for moving (noninertial) deforming measurement devices that can be changing in chemical/crystallographic nature, measurement efficiency and even relativistic.

It turns out to be essential to investigate fluidity together with thermal equilibrium from a purely wavefunction based perspective. The delocalization rate of atoms is simply too fast for a classical kinetic model to be valid, regardless of the success of the relations derived. Our strategy is modeled off the previous approach to solids, write down the simplest possible wavefunctions with the observe kinematic freedom. The success in the description of solids suggests some liberty is allowable to investigate gases, which, surprisingly, turn out to be much more complicated. For gases built directly from wavefunctions, there are numerous considerations. Gases fluidity and thermal motion are inseparably linked so one has to tackle both simultaneously unlike the elastic motion of a solid which can be largely treated independently from its

thermal response. We are ultimately interested in the interpretation of ultracold gases in traps. How well described by thermo and hydro are they? Could the stand on the edge of transitions from truly quantum systems that can continuously transform to classical behavior? What is the nature of the damping we observe and how does it relate to our standard paradigm built on the Kubo relations? Will two fluid behavior be observable in a richer form that the appearance of visible vortices and will it shed light on why such a model works so well for Helium below its critical temperature?

There are some very successful hydrodynamic approaches to the small mode oscillations of gas clouds in traps[37]. This suggests that it is at least worth considering a thermodynamic description of these systems. Because, at the unitary limit, there is no length scale we can form from parameters of the system (other than the very small effective range and actual short range potential width) it can be argued that such a set of thermodynamic descriptors must be scale invariant. In this spirit one can measure the period and the damping rates or changes in a cloud during free expansion and extract a viscosity. Various symmetry arguments [120] [135] suggest that the bulk viscosity is zero and only shear viscosity remains. Furthermore, holographic duals from string theory [103] have given bounds on the ratio of viscosity to entropy density η/s and a survey of all known liquids seem to respect this. The closest approaches to the bound are found both in the extremely high energy RHIC experiments and the the ultracold fermion trap expansion and oscillation experiments.

John Thomas' group [8] has done some trap expansion experiments that we will use as comparison with results from scale invariant thermodynamics combined with classical hydro. The agreement with the inviscid motion is very good indicating that the collective constraints on the motion at unitarity are very strong. It will be shown that the results from expansion from a rotating cloud give a relatively weak signal to extract the viscosity and that trap oscillation experiments are much better. This is not entirely surprising. Expansion is a kind of "one shot" even whereas oscillations can be observed for extended periods of time.

The case of quantum fluctuations is a compelling subject and recently we have acquired data from ultracold gases through beam interference [47] [89]. Quantum fluctuations from hydrodynamic modes has a successful history in predicting diffusive light scattering [6] and predicting critical phenomena [60]. It has become popular to view liquids as the long distance limit of an effective field theory. Viscosity and other transport coefficients are then computed from Kubo formulas that give stresses from these coupled modes. An interesting angle of these problems is that the particular form of the hydrodynamic equations used writes the nonlinear convective term as a stress. This is truly a "pseudo-stress" and many derived moment and energies derived from it are also "pseudo" quantities. There are still arguments about the role of such stresses in determining real forces on materials however it does give a definite bound on the role of fluctuations in determining viscosity including a scale at which hydro "breaks." Specifically,

when the form of the evolution can no longer be expressed as a gradient expansion in the form of a modified Navier-Stokes equation. This turns out to be at very low order. The powerful controls we have on ultracold gases suggest that confinement to reduce the fluctuations could be an interesting probe of this effect.

1.4 Outline

This thesis is structured as follows. In Ch. 2 we discuss the case of molecules and solids. In particular, we investigate how the kinematic degrees of freedom we see in classical bodies are at odds with that of atoms and molecules. Beyond the metastable details of particular nuclear states, atomic bond arrangements and finite thermal excitation, the existence of well defined shape and orientation imply that the condensed matter we encounter in nature (including ourselves) must correspond to far-from-eigenstate wavefunctions with long lasting features. This leads to specific wavefunctions for the solids with phonon excitations and constrains the kinds of discrete symmetry statements we can make in some unsuspected ways. Ch. 3 demonstrates the usual measurement theory follows in a deterministic fashion from the interaction of such states with delocalized states. These sections serve to show that the single wavefunction approach to evolution can arise naturally and deserves consideration in the case of ultracold gases. Side results on quasiparticles, specifically phonons, and the distinction of pseudomomentum and true momentum are relevant for linear response theory approaches to deriving true forces on fluids in terms of their interactions.

The origin of thermodynamics and the meaning of canonical averages has been a long standing problem. In many cases, the computational methods have been very successful yet most serious books on quantum statistical mechanics admit somewhere that the foundations of the subject are ad hoc or lacking. Since thermodynamic and hydrodynamic approaches are so important for ultracold gases, in Ch. 4 we derive the conditions necessary for thermal equilibrium and the canonical averages to hold for a single wavefunction approach (in contrast to an ensemble or "mixed" state). In Ch. 5 we give corresponding conditions on a gas to give and propagate states that can correspond to classical hydro of gases. This gives a fluid dynamic sister contribution to contrast with the solid state in Ch. 2. The contrast between these states has implications for the role of vorticity and why it is so different in condensed gases versus high temperature states. Ultimately, we make the case for persistent athermal properties in some ultracold gas states here.

In the next section of this thesis, we introduce some hydrodynamic approaches to computing the shear viscosity of unitary gases. This necessitates we introduce some definitions for dimensions which we do based on the free fermion gases in Ch. 6. In Ch. 7, based on the paper by Schäfer and Chafin [116], we demonstrate how thermodynamics in the scale invariant unitary

case greatly constrains hydrodynamic motion and allows us to extract bounds on the viscosity from experiments on free expansion and trap oscillation.

In Ch.8 we examine the role of fluctuations on the shear viscosity in the case of two and three dimensional fermionic gases. These observations are based on the paper "Hydrodynamic fluctuations and the minimum shear viscosity of the dilute Fermi gas at unitarity" [31] and the paper "Scale breaking and fluid dynamics in a dilute two-dimensional Fermi gas" [30]. Fluctuations are shown to lead to a minimum in the ratio of shear viscosity to entropy density, η/s. This bound is not universal but depends on the detailed thermodynamics and breakdown scale of the system. Nonanalytic terms suggest that Burnett order Navier-Stokes corrections may be inconsistent.

Two dimensional systems have gained increasing popularity because of their unique properties including their unusual density of states. As optical traps have made progress in approaching this limit, there has been increased interest in the hydrodynamics and possible appearance of quantum anomalies in such systems. In Ch.**??** we describe the hydrodynamic corrections to the equation of state and the monopole oscillation mode from the virial expansion. Finally, in Ch.9 we discuss implications of these results and outlook for future research.

Chapter 2

Condensed Matter and the Classical Limit

2.1 Molecules and Bonds

Before we consider the case of the wavefunction of a large classical body, we consider the few body case. The two body case is one of the few exactly solvable examples. Separation into relative and center of mass (CM) coordinates $(x_1, x_2) \rightarrow (x_{rel}, X_{cm})$ gives a free translating part with the net mass $M = m_1 + m_2$ and internal motion given by radial oscillations and angular motion of a single particle with reduced mass $\mu = \frac{1}{m_1^{-1}+m_2^{-1}}$.

The nature of the two body potential and particle symmetries enter here by determining the nodal structure of the ground state wavefunction at the origin of the relative coordinates. For the case of a hydrogen atom, the function has no node here and we find that the ground state is unique and angular excitations require the presence of radial ones. This is encompassed in the rule for the angular and magnetic quantum numbers $l < n$ and $|m| \leq l$. If the potential is for a pair of fermions or comes from composite bodies with an effective hard core repulsion then there can be a node in the ground state of ψ_{rel} and angular excitations may be much less expensive than radial ones. This explains why the specific heats of diatomic molecules occupy the angular excitations before the vibrational (or equivalently, radial) modes make a contribution whereas, for the electronic states of a Hydrogenic atom, this is not the case.

Often the consideration of angular and vibrational modes of diatomic molecules, as that of the phonon modes of solids, is done by a quasi-classical consideration with "quantization" of the classical modes done as a final step. This breaks the continuity of the argument and leaves room for doubt as to the consistency of such an analysis from a direct consideration of the total wavefunction of the system. Many students have wondered when to insert such a magical/inspired step and if they really understood the solutions to the Schrödinger equation

after all.

In the spirit of interpreting all the dynamics of a system in terms of its wavefunction, let us approach this differently. The wavefunction of H_2 decomposes into a 3-D center of mass part and a 9-D internal component $\Psi = \psi_{cm}\psi_{int}$. Including the 2^4 component spin basis this gives a set of 16 12-D functions to keep track of. Because the electrons have such small mass compare to the protons we can, in some sense, ignore them with small correction in deriving the energy levels. However, if the center of mass is delocalized to a much greater extent than the radius of the atom, we can have a very large relative discrepancy in the *value* of Ψ at any given point in $\mathbb{R}^{12}$ and the relative size of such an approximation gets worse at larger values of the particle coordinates even though the energy per density changes are small. It turns out that a careful accounting of the center of mass coordinates and large coordinate effects arising from particular small energy changes will be central to later arguments so we will be, prima facie, pedantic about this.

In molecular orbital theory (MO) we often consider the relative coordinate wavefunctions to be those of the electrons. Since the reduce mass corrections are small, this is often accurate enough for such calculations. However, when considering the antisymmetry of the electronic part of the wavefunction this does introduce some error. Ultimately, the antisymmetry must be done over the electrons coordinates not the weighted mix of electron and core coordinates that make up the relative coordinate wavefunctions.

For the present case, let us place our H_2 molecule in a box of length L where $d \ll L$ and $\frac{L}{d} \ll \frac{m_p}{m_p - \mu_H} d$. Here d is a measure the atomic size in the relative coordinates of the atomic cores and μ_H is the reduced mass of the Hydrogen atom. The first approximation makes sure the box is not so small as to radically alter the relative coordinate distance of the free molecule. The second is more subtle. The coefficient $\frac{m_p}{m_p - \mu_H}$ is a large number. We don't want the box to be so large that the total Ψ suffers a large fractional shift in its amplitude at large coordinate values. An s-orbital approximation gives,

$$\Psi = \hat{\mathcal{S}}_e \hat{\mathcal{S}}_p \phi_s(x_1 - (X_1 - X_2)/2)\phi_s(x_2 + (X_1 - X_2)/2)\psi_{rel}(X_1 - X_2)\psi_{cm}(X_1 + X_2) \qquad (2.1)$$

where the lowercase variables are the electron coordinate labels and the uppercase are the protons. Since we assume opposite spins for both these are symmetrized by the operators $\hat{\mathcal{S}}_{e,p}$. $\psi_{rel}(y)$ gives a strongly peaked function at $|y| = d$, the proton separation distance. It is a spherically symmetric function that damps strongly at zero. The electronic contribution looks like a pair of overlapping orbitals that we see in books on molecular orbital theory or band structure. The details of the hidden coordinates are generally obscured by these pictures and models. They inherit the rotational symmetry from ψ_{rel} as we advance through the $y = (X_1 - X_2)$ coordinate subspace. It is a slight inconsistency that we use the reduced mass and

relative coordinates to specify the atomic orbitals but use the entire mass of the the atoms to form the molecular wavefunction. The overlap region shifts the mass density of the electrons in a way not considered here and the the relative coordinates in the orbitals are really only partly electronic and contain small components of proton coordinate contributions.

This begs the question of how do conservation laws relate to symmetries in the case of many body wavefunctions. We generally look at the classical Lagrangian and apply Noether's theorem then assume (or verify independently) the system inherits these symmetries after "second quantization." It would be more satisfying to simply have a Lagrangian for the many body wavefunction to start with and derive these directly. We will leave this (and its surprising complications) for a later section. For now, we notice that for the interacting case and absent the large box we placed around the system, there is free translation along the center of mass coordinate. Rotational symmetry is expressed in the rotation in the proton relative coordinate variable $y = (X_1 - X_2)$ and the relative wavefunction ψ_{rel} gives a narrow width spherical shell. The angular modes are thus easy to excite and their narrow radial spread justifies calculations using the classical moment of inertia in estimating their energy. In the case of allowing a finite mass contribution of the electrons, the rotational freedom would involve simultaneous rotation of different sizes in each of the four coordinates such that the center of mass remains unaffected.

Not making details of the atomic and molecular orbitals explicit in terms of the underlying particle coordinates clear invites a number of paradoxes such as the effects of bulk rotation on a metal or superconductor. Consider the case of a rotating metal or superconductor. According to band theory, as we rotate the solid, the electron band occupancy should become excited to cancel any net current of the cores. This however requires the existence of vortices in the electron cloud. In the case of superconductors, this is particularly expensive and difficult to cancel the field in the interior without many of them to cancel the fields of the previously introduced ones. To resolve this, consider the case of a lone atom being moved at quantized angular velocity over a circular loop of radius R. If the proton is considered to to this motion and the electron moving in a cloud about it then we expect the electron cloud will exhibit a precessing deformation from small contributions of excited angular momentum states. The associated vorticity from these will generally be far into the low amplitude tail of the electronic wavefunction. This small correction to the atomic orbital can then correct the underlying atomic orbitals the make up the band structure leaving no need to make expensive and complicated changes in the band structure (molecular orbital) occupancy.

2.2 Solids

As we combine larger numbers of atoms to build solids we are left with the following questions. Do larger numbers of particles automatically give classical bodies? Do they necessarily lead to

thermodynamically equilibrating states? Here we will investigate the first question and leave the second for later. MO theory and the Bloch model of solids generally involves placing atoms at specific locations (of their center of masses) as delta functions and using energy minimization over the possible atomic orbital combinations to derive the molecular orbitals or band structure. The role of metastability of these various combinations is rarely discussed especially in terms of how these states relates to the *true* eigenstates of the given nuclei and electrons.[1]

On of the more lightly thrown about phrases in introductory quantum mechanics is that "identical particles are indistinguishable." This is often used in conjunction with semi-classical pictures of atoms at specific locations. STM images of a solid surface which show atoms as well defined peaks might seem to contradict this. These atoms can have the same nuclei and atomic structure as their neighbors yet are "distinguished" by their different locations. Indeed the atoms at a surface are different in their electronic structure from those in the bulk of the solid and there are gradations of variations as we move away from the surface and variations introduced by time dependent thermal fluctuations. The essential message of "indistinguishability" is that the many body wavefunction needs to have specific symmetries imposed on it. Such vague language confuses the particle coordinate label and the particle location. This probably arose from the long and confusing arguments regarding complementarity and other exotic early twentieth century attempts to explain quantum mechanics.

In general, there is no well defined "location" and using such language just takes us further from a language built around the persistent reality of a many body wavefunction as the fundamental descriptor of the system. A better phraseology is to say that the coordinates of the wavefunction corresponds to various particle types and spin labels and this wavefunction has various preserved symmetries. In some cases, the wavefunction seems to correspond to a set of sharply defined atomic locations. This is a property we expect of classical condensed matter, especially solids.

Let us consider the ground state of N atoms of an alkali metal. It is natural to expect it to decompose into CM and internal coordinate parts with a two parameter rotational freedom in the internal part: $\Psi = \psi_{cm}(X_{cm})\psi_{int}(x_1^{rel} \dots x_{n-1}^{rel})$ where there is a (passive) transformation $T_{(\theta,\phi)}$ of the $Y_{rel} = \{x_i^{rel}\}$ such that $\psi_{int}(Y_{rel}) = \psi_{int}(T_{(\theta,\phi)}Y_{rel})$. Colloidal condensation of metals gives special polyhedra based on the number of atoms they contain. As this number grows they tend to spherical bodies yet the crystalline structure still destroys rotational symmetry. We expect the one body density matrix of the true ground state to be roughly spherical. Of course, the actual possibilities for solids are highly varied in shape, internal crystalline structure, nanoscale order and orientation. The fact that our observation of solids show a particular

[1]Of course, the states of nuclei are also generally metastable and the role of variable particle number spaces in defining a basis of stationary states is not immediately obvious so we are really just investigating the first layer of such considerations.

shape, position, orientation and microcrystalline structure have both a well defined location and orientation suggests that the center of mass is localized and the rotational and many other internal degrees of freedom are in a highly excited state that allows particle locations to be well defined.

Beyond this, the internal structure is likely in an internal superposition as well. The apparent "ground state" of such a body is often associated with zero temperature but clearly requires many extra nodes corresponding to excitations and many body currents associated with being far from a true eigenstate. When we investigate the primitive excitations of such a body we should to remember that there is this noisy hidden background. The apparent excited eigenstates of these N atoms system will involve nontrivial combinations of the true eigenstates that may include bound and unbound states, ionization of some atoms and states with unclear surface boundaries in the one body density function and so on. Such situations are exactly what we do not see in classical matter. Justifying this gulf in observed behavior in terms of wavefunctions is a task that should be considered of comparable importance to other fundamental problems such as the "arrow of time." Here I will show it is not that hard, In fact, the resolution can be thought of as already implicit in some solid state and transport calculations.

Nowadays, often some notions from decoherence are used to explain away why we don't see superpositions of macroscopic objects. This is ultimately not much more satisfying since it often just seems like another act of modifying language with few (if any) testable consequences. Instead of this we will proceed with a description of the world in terms of wavefunction consistent with our observations the classical world. The large mass of a classically sized body means that the delocalization time for its position and orientation is enormous. (Gases do not suffer such a constraint since the many body wavefunction can evolve freely in each coordinate most of the time.)

This leads us to our first fundamental assumption about the quantum state of classical matter:

Proposition A: Solids and liquids (with the possible exception of Helium) are described by long lived far-from-eigenstate wavefunctions where the atomic locations are well defined. Specifically, the wavefunction is well approximated by an appropriately symmetrized products of delta functions in the atomic coordinate labels and symmetrized products of atomic orbitals in the electron coordinates located about the corresponding atomic orbital locations $\{R_i\}$. The atomic coordinate part we will call Ψ_{core} and the electronic part that has been projected out for a fixed value of the atomic locations at a local maximum is Ψ_e. The appropriately symmetrized product of these we will call Ψ_{class} which is a near approximation to the true wavefunction

descriptor of the system.

$$\Psi_{class} = \hat{\mathcal{S}}_e^f \hat{\mathcal{S}}_a^{f/b} \prod_{j=1}^{N} \psi_0(X_j - R_j) \prod_{k=1}^{N} \phi(x_k - X_j) = \Psi_{core} \Psi_e \tag{2.2}$$

where R_j are the lattice locations of the atoms (including its nonchemically active electron coordinates explicitly), $\psi_0(y)$ is a narrowly peaked function (meaning much narrower than the electron orbitals) indicating its position, $\phi(x)$ is the symmetry adapted electron orbital wavefunctions of the chemically bonding outer electrons. $\hat{\mathcal{S}}_e^f$ is the (anti)symmetrizing operator for the electrons (with coordinates$\{x_i\}$). $\hat{\mathcal{S}}_a^{f/b}$ is the appropriate symmetrization operator for the atomic cores (coordinates $\{X_j\}$) depending on their Fermi or Bose nature.[2] Spin labels have been suppressed but their effects are important in the symmetrization over "particle labels"; specifically exchanges of the coordinate and spin labels of a particle together.

Since we have been discussing the confusing distinction between location and coordinate label this is a good moment to discuss the notion of discrete symmetry of a solids. We know from STM images that we can "see" atoms at precise locations on a solid surface. Above we see that the wavefunction of such a state encodes this in a very nonlocal fashion. Often it is suggested that liquids have a continuous symmetry that is broken in the transition to the discrete symmetry of a solid. Aside from the obvious problem that there are amorphous solids with no discrete symmetries even on very small scales, we see that while there can be a discrete set of symmetries among the lattice sites $(R_1, R_2 \ldots R_N)$ when viewed in $\mathbb{R}^3$ such a symmetry is not evident in the wavefunction Ψ_{class}. The CM is localized and so translations, continuous or discrete, do not map it into itself. We can find a symmetry among the maxima when viewed in $\mathbb{R}^3$ but this is a model dependent statement. If we consider two lattices in $\mathbb{R}^3$ that differ in the number of particles as N and N+1 but otherwise overlap, the corresponding wavefunctions have different numbers of coordinate variables. If we consider discrete translations of Ψ_{class}^N along its CM by one lattice site in all coordinates then take a slice of Ψ_{class}^{N+1} by fixing x_{N+1} we see that we have a correspondence of the functions in that the maxima of Ψ_{class}^N are found among those of Ψ_{class}^{N+1}. In general, it is not possible to give a discrete set of transformations for a wavefunction of a solid that correspond to those of the discrete 3D lattice associated with the core locations.

Liquids have been a difficult phase to explain from a microscopic point of view. Landau has stated [6] that the liquids have a continuous symmetry and therefore the "phonons," as in

[2]Interestingly, this is pretty much the only sort of wavefunction you can write down that has the observed classical properties and degrees of freedom. The innovative part is realizing that it persists for very long times and that we should leave the notion of eigenstates behind. Given that measurement theory and quantum statistical mechanics are built on the notion of eigenstates, this may be a leap. It requires one now reconsider both of these from another point of view as we do next.

the case of Helium, carry a mass flux and that this lets them contribute to the viscosity (as opposed to the quasimomentum of phonons in solids). The inconsistency with this point of view is that such a flux also implies a high diffusion rate as in the case of gases. The diffusion rate of liquids is far too small to justify this opinion. Solids maintain shear stress by deformation of the atomic orbitals. It seems likely that liquids do as well but allow for relaxation and this provides the microscopic mechanism for transfer of forces and dissipation. This should be detectable spectroscopically. Indeed for polymer melts polarization is observed under shear implying a general change in the microscopic order.

This model of solids suggest that liquids (with the possible exception of Helium) have a similar localization property to solids but with an interconnection of potential wells that allows current to travel between nearby maxima. If this is a good model one has to wonder if MD computations are missing an essential quantum feature in the description of liquids. Electron clouds also become thermally excited making the Born-Oppenheimer approach potentially valid only if it is built from a quasistatic change of this excited electronic state. It is unclear what a "continuous translational symmetry" means in such a model. As we saw above, the discrete translational symmetry of a crystal only has meaning among the equilibrium core set $\{R_i\}$ when viewed in $\mathbb{R}^3$. The discrete translations don't have any obvious meaning in terms of the true many body wavefunction.

We are now in a position to give an estimate to how much of an excitation energy must be possessed such a solid block due to its classical state. We can take such a block and cool it to absolute zero but the localization energy still persists. These will induce oscillations and currents in various correlated directions. Certainly there is some metastability in the nuclear components. This will create a high frequency small amplitude we will ignore. Similar consideration goes the chemical structure of the material. The true ground state (modulo those effects) will be rotationally symmetric not just in its shape but in the angular localization of the atoms. We can estimate the first contribution from the surface area of the block. If the energy per bond is E_b we have that the energy contribution is $U_{surf} \sim E_b L^2$ The angular excitation must localize the orientation to well within an atomic radii d. This corresponds an energy of $U_r \sim \frac{\hbar^2}{Md^2}$. This is made up of counter moving rotational modes. Each one gives some radial excitation of the body. Assuming the Young's modulus is Y we have $U_{el} \sim \frac{\hbar^2}{MYd^2L^3}$. These generate oscillations that are present regardless of how far the object is cooled and gives a measure of how far a classical object must be energetically from the true ground state of the system. To "cool" the system further, the atoms must diffuse to a more symmetrical shape and the shape itself must delocalize into a state where the crystal locations are ambiguous. Here it is even more evident that there is no fundamental translation corresponding to the discrete symmetry of crystal as an action on its many body wavefunction.

2.3 Phonons

The description of the low order excitations of solids is typically done by the Debye model of examining the classical (longitudinal) normal modes and quantizing them. The second quantized formulation is often introduced here in analogy with photons. This distinction is that photons are actually elementary particles that introduce their own coordinate labels and so increase the dimensionality of the system. Phonons exist as modifications of the solid 3N-D wavefunction (the "pseudo-ground state") and so we should be able to write down not a wavefunction for them, but describe them as a modification of the lowest energy wavefunction of the solid.

Using our above wavefunction, we expect the atomic peaks to be bound in potential wells that are well approximated by harmonic potentials. Shifting the peak locations gives linear restoring forces corresponding to the normal modes of the classical solid. We have, of course, obscured the low amplitude many body currents hidden by our classical approximation of the wavefunction or, more accurately, our wavefunction description of classical matter. The modes generated by this many body potential well are the "pseudo-eigenstates" of the wavefunction, specifically long lived nearly orthonormal excitations that we suppose dominate the energy of thermal motions. Naturally these correspond to phonons. Consider the one *particular* peak of Ψ_{class} at $\tilde{R}^{(1)} = (X_1 = R_1, X_2 = R_2 \dots X_N = R_N)$ and displace by δx in all directions to obtain the effective many body harmonic potential. Let the 3N-5 directions of the eigenstate of the ith mode be indicated by $k_l^{(i)} = (y_1, y_2 \dots y_{3N-5})^{(i)}$ where $k^{(i)}$ is normalized to one, i indicates the mode type and l the particle coordinate. This gives frequencies ω_i and effective masses m_i. The corresponding eigenfunctions for the nth excitation level is $\psi_{n_i}(x) = f_n(m_i, \omega_i) H_n(\sqrt{\frac{m\omega_i}{\hbar}}x)$. These can be though of as centered about our particular R_i peak and oriented along $k^{(i)}$. Putting these all together to obtain the wavefunction of such a solid with excitation level $\{n_i\} \in \mathbb{N}^{3N-5}$ in each of these 3N-5 modes:

$$\Psi_{class}(\tilde{X}, \tilde{x}) = \hat{\mathcal{S}}_e^f \hat{\mathcal{S}}_a^{f/b} \prod_i^{3N-5} \psi_{n_i} \left(\sum_j (X_j - R_j) k_j^{(i)} \right) \psi_{cm}(X_{cm}) \psi_r(\theta, \phi) \prod_k^N \phi(x_k - X_j) \quad (2.3)$$

where ψ_{cm} is a narrow function. To be consistent with the originally proposed Ψ_{class} we should choose its width to be that of ψ_0. The rotational function ψ_r specifies a particular narrow angle fixing the orientation of the body. These two functions will be narrow but long lasting nearly monochromatic packets if the body is translating or rotating. The peaks are centered so as to fix the last five R_j's. This follows from our expectation that these are gaussian like peaks in each coordinate so hyperspherically symmetric in the atomic core sector of the many body space. The oscillations of the core locations give restoring forces from the shifted atomic orbitals. This arises because the energy of the overlapping ϕ change as a function of relative position of the

cores. Our assumption here is that this is not enough to appreciably change the from of the atomic orbitals used in this approximation.

In nuclear physics there is an analogous problem for highly deformed nuclei. Both mean field and Slater determinant approaches violate the rotational symmetry of the ground state. This can be put back in [98] by introducing rotational symmetry of such a state. For strongly deformed nuclei, this makes a difference in the final energies. For our localization functions ψ_{cm} and ψ_r this makes an extremely small difference in the energy as estimated in Sec. 2.2. However, the state is at best metastable (a pseudo-ground state) arrangement so the energy of this state is actually appreciably far from the true ground state. Furthermore, we shall see that it makes a huge effect on the dynamics of the system as it interacts with delocalized particles and gives a local and satisfying explanation of quantum measurement.

In the usual phonon language we would say that the ith mode has occupancy n_i. Here we see that this corresponds to a particular many body direction having where the wavefunction has n_i oscillation nodes. If we were to excite to higher levels some anharmonicity would show up in the form of these potentials and their general separability would fail. This might be mistaken to mean that a nonlinear interaction is causing phonons to scatter. However, it only means that the many body pseudo-eigenstates now have excitations that don't increase by constant energy steps and the net many body states don't separate. Second quantization is built around such harmonic states so it is hard to glean this geometric intuition from it. Typically there are phonon interactions or other more ad hoc approaches. Some of these may be valid but it would be an advantage to have a geometric description, and its associated improvement in intuition, to suggest which ones. This will be discussed further in Sec. 2.4.

We can compare the widths of the relative ground state ψ_n functions. The widths $w_i \sim (m_i\omega_i)^{-1/2} = (\kappa_i m_i)^{-1/4}$ where κ_i is the effective spring constant of a given mode. Since the spring constant doubles when we half the wavelength of a mode and this reduces by half the amount of mass involved we see the widths are invariant. This gives a consistency check that our ground state function in equ. 2.3 has the same localization as in equ. 2.2. In computing the energy of these excited states we should note that the localization given by ψ_0 was optimized to give a minimum. This implies that we do not need to include a zero point energy contribution per mode. It was already included in the energy. If we do include it, the potential energy must be combined with it to give an identical net energy of the system. This has obvious implications for any theory of the Casimir effect based on phonons.

It is interesting to consider what happens in the case of Fermionic atom cores. These will still localize to give peaks at the many body points given by all permutations of $\tilde{R} = (R_1, R_2 \ldots R_N)$. The space is now divided into a set of nodal cells. In dimensions higher than one, this is typically two or four [29] for the ground state. The peaks now divide into equal sets of positive and negative amplitude but they still have the same decomposition into a set of normal modes.

These give a set of 3N-3 directions that can each be excited to increasing numbers of oscillations. This is the reason that phonons obey Bose statistics when enumerated in second quantization even for fermionic atoms. The actual wavefunction does not represent phonons as anything but nodal bifurcations of the localized peaks corresponding to a classical solid's atomic locations.

Despite formal similarities, phonons are very distinct from actual material particles. As quantized sound modes they transport no mass hence have true momentum density of zero. They are labeled by k-vectors corresponding to the oscillation frequency given by the normal mode decomposition of the many body potential for the long lived localize states at the N! maxima in the $\mathbb{R}^{3N}$ configuration space. There is a long confusion about the distinction between true momentum, pseudo-momentum and crystal momentum [88]. Most solid state books give a brief mention of the distinction between between the latter two but often mislabeling the pseudo-momentum as "true momentum". Enduring confusion persists because of the coupling rules in field theory methods that "conserve (pseudo)momentum" without mentioning that it is pseudo-momentum. A similar situation has occurred in acoustic, plasma physics and the theory of ocean waves. Often in places where some field theory method or a heavy vector calculus treatment of a hydrodynamic system is used. The confusion often begins with the choice to fold in the nonlinear advection term $v \cdot \nabla v$ into the stress term Π_{ij}.

$$\rho \partial_t v + \rho v \cdot \nabla v = -\nabla \cdot \Pi \tag{2.4}$$

$$\partial_t (\rho v) = -\nabla \cdot (\Pi + \rho v \otimes v) = -\nabla \cdot \Pi' \tag{2.5}$$

This is mathematically and dimensionally consistent but is properly a "pseudo-stress" with no microscopic representation as true stress hence of dubious value in deriving true forces on the boundary of or within the medium. It is clearly understood that the group velocity is the relevant quantity to discuss the transport of mass hence specify momentum (since "mass flux"="momentum density" for massive particles except for tiny relativistic corrections) in the semiclassical theory of electrons [7] however in the case of phonons there is no mass transport at all. The situation grows even more confusing for the case of superfluid Helium where the linear part of the dispersion relation is labelled "phonon" and mass is actually transported over significant distances with these modes [71]. In Ch.8 we will be using this to calculate the stresses due to fluctuations. For simplicity we will relabel Π' as Π in these sections.

Inspecting the origin of momentum conservation rules for Feynman diagrams in QED we see that they arise from the Fourier transform of the spatial locality condition on the interaction. Conservation laws alone can dictate conservation of momentum order by order in the Dyson series but not diagram by diagram. Transporting these ideas to condensed matter theory suggests it is a good idea to conserve such pseudomomenta in diagrams as long as the true momenta is conserved as well. This is a bit of a subtle question and we won't pursue it further here.

2.4 Fock Space and Quasiparticles

One can give a many particle description of a quantum system in terms of Fock space. This is generally accomplished by the use of creation and annihilation operators and a formal algebra. Since we are interested in geometric intuition and consistency, we present and explicit model for such actions here. Firstly, for the case of true particles then in the case of quasiparticles corresponding to collective modes.

One can write a many body space representation for spinless bosons as $\Psi = a + b\,\langle\Psi^{(1)}(x_1)| + c\,\langle\Psi^{(2)}(x_1,x_2)|\ldots$ with appropriate symmetries for each wavefunction.[3] In the case of second quantized treatments, the dominant way to treat such systems when particle numbers can change, we are interested in using creation and annihilation operators with respect to a particular one-body basis $\{\psi_i(x)\}$. In this case it is good to write the basis of each N-body function explicitly as a symmetrized product on the basis

$$\{1, \{\psi_i(x_1)\}, \hat{\mathcal{S}}\{\psi_i(x_1)\psi_j(x_2)\}, \hat{\mathcal{S}}\{\psi_i(x_1)\psi_j(x_2)\psi_k(x_3)\}\ldots\} = \{1, \psi_i^{(1)}, \psi_{ij}^{(2)}, \psi_{ijk}^{(3)}\ldots\} \tag{2.6}$$

where $i \leq j \leq k\ldots$(and all other such $\psi_{ijk\ldots}$ are taken to be zero).[4] A general object is then representable as

$$\Psi = \sum_{N=0}^{\infty}\sum_{i_k=1}^{N} b_{i_1,i_2\ldots i_N}^{(N)}\psi_{i_1,i_2\ldots i_N}^{(N)} \tag{2.7}$$

A creation operator $\hat{a}_s^\dagger$ can then act on Ψ in this representation by acting on the coefficients. From this example the most natural definition would be to define the map

$$\hat{a}_s^\dagger : b_{i_1,i_2\ldots i_N}^{(N)} \rightarrow \begin{cases} b_{P(i_1,i_2\ldots i_N,s)}^{(N+1)} & \text{if } N > 0 \\ 0 & \text{if } N < 0 \end{cases} \tag{2.8}$$

where P induces the above partial ordering among indices and the map gives the shift of the values of the coefficients in the expansion. This operator is well-defined since it is one-to-one. The corresponding annihilation operator would be

$$\hat{a}_s : b_{i_1,i_2\ldots i_N}^{(N)} \rightarrow \begin{cases} b_{i_1\ldots\hat{s}\ldots i_N}^{(N-1)} & \text{if } s \in \{i_k\} \\ 0 & \text{if } s \notin \{i_k\} \end{cases} \tag{2.9}$$

and the $\hat{s}$ indicates that (one of) the $i_j = s$ label(s) has been omitted. In practice these operators are defined with extra coefficients that are functions of the "occupancy" of the state, specifically

[3] We are included a "vacuum state" constant value here. When we consider phonons, we will revisit this.

[4] Typically, the coefficient sets are limited in such expansion as a consequence of symmetry. Here we have restricted the basis set instead so that any other coefficients not satisfying this index constraint have no effect.

the number of s-indices present in the coefficient. Let n_s be the number of such indices in the $\psi^{(N)}_{ijk\ldots}$ coefficient $b^{(N)}_{ijk\ldots}$. By letting

$$\hat{a}^\dagger_s \to \sqrt{n_s+1}\;\hat{a}^\dagger_s \tag{2.10}$$

$$\hat{a}_s \to \sqrt{n_s}\;\hat{a}_s \tag{2.11}$$

we can get the commutation relations $[\hat{a}_s, \hat{a}^\dagger_t] = \delta_{s,t}$ and the identity for the number operator for the occupancy $n_s = \hat{a}^\dagger_s \hat{a}_s$. In the case of fermions we can construct a similar basis with introduction of spin labels and restriction on occupancy due to antisymmetry. The manifest representation of creation and annihilation operators then gives a set of anticommutation relations, as familiar in all quantum textbooks.

Typically calculations of this sort are done strictly formally. In the case of fixed N-body quantum mechanics in an external potential, this can be shown to be equivalent to the usual many body Schrödinger equation evolution [119]. The downside of this approach, aside from its formality, is how to describe this reality in a manifestly basis independent fashion? One can transform to other one-body basis sets in an obvious manner but this still not completely general. In principle one could use two-body bases but a truly geometric discussion would be more along the lines of the Schrödinger equation itself where there is no decomposition in terms of a basis and explicit manipulation of coefficients arises in the description. In the case of real particles, it is not immediately clear how to proceed but in the case of collective modes (phonons) we will show the situation is a little better.

In the case of phonon "creation" and "destruction," note that this does not change the number of coordinate variables at all. Specifically, if the system is described by N coordinate labels at one time, $\Psi^{(N)}(x_1, x_2 \ldots x_N)$, it is so at all times. To describe the action of these operators on one of the basis functions

$$\Psi_{core}(\tilde{X};\{n_i\}) = \hat{\mathcal{S}}^{f/b} \prod_i^{3N-5} \psi_{n_i}\left(\sum_j (X_j - R_j)k^{(i)}_j\right)\psi_{cm}(X_{cm})\psi_r(\theta,\phi) = \hat{\mathcal{S}}^{f/b}\Phi(\tilde{X};\{n_i\}) \tag{2.12}$$

we need a way to shift the occupancy of a particular mode. We can think of $\Phi(\tilde{X};\{n_i\})$ as the local function of a solid with phonon occupancy n_i about the many body location specified by the lattice positions in their "standard order": $\{R_1, R_2 \ldots R_N\}$. Seeking a kernel for Φ alone to raise the occupancy of the the $k^{(s)}$ phonon from n_s to $n_s + 1$

$$\tilde{K}^{(\Phi)}_{n_s,n_s+1}(\tilde{X},\tilde{X}') = K_{n_s,n_s+1}((X_j - R_j)k^{(s)}_j, (X'_j - R_j)k^{(s)}_j)T(\{(X_j - R_j)k^{(i)}_j\},\{(X'_j - R_j)k^{(i)}_j\}) \tag{2.13}$$

where $T(\tilde{X}_\perp, \tilde{X'}_\perp)$ is a transverse 2(3N-3)-D function (so uses all $i \neq s$) that maps all (N-1)-fold products of phonon oscillations (and the five CM and angular localization functions) into themselves.[5] $\tilde{K}^{(\Phi)}_{n,n+1}$ is chosen so that

$$\int d\tilde{X'} \tilde{K}^{(\Phi)}_{n_s,n_s+1}(\tilde{X}, \tilde{X'}) \Phi(\tilde{X}; \{n_i\}) = \Phi(\tilde{X}; \{n_1 \dots n_s + 1 \dots n_N\}) \tag{2.14}$$

Since these peaks are very weakly overlapping, even for high phonon occupancy, we can define a kernel

$$\tilde{K}_{n_s,n_s+1}(\tilde{X}, \tilde{X'}) = \hat{\mathcal{S}}^b \tilde{K}^{(\Phi)}_{n_s,n_s+1}(\tilde{X}, \tilde{X'}) \tag{2.15}$$

that performs the same action on $\Psi_{core}(\tilde{X}; \{n_i\})$. The corresponding form of the creation and annihilation operators are:

$$\hat{a}^\dagger_s = \sqrt{n_s + 1} \int d\tilde{X'} \tilde{K}_{n_s,n_s+1}(\tilde{X}, \tilde{X'}) \tag{2.16}$$

$$\hat{a}_s = \sqrt{n_s} \int d\tilde{X'} \tilde{K}_{n_s,n_s-1}(\tilde{X}, \tilde{X'}) \tag{2.17}$$

where it is understood that a function $\Psi(\tilde{X'})$ stands to the right inside the integral. Note here that the operators are only defined for integers $n_s > 0$. We can define the action of $\hat{a}_s$ on occupancies $n_s = 0$ (i.e. the ground state) to be zero. This completes the operators definition and ensures the usual commutation relations. Unfortunately, the operators require a function of well define n_s on the RHS so it is not suitable to give a manifestly basis-independent description for any Hamiltonian built from such operators. It is possible that the kernel could be modified to be invariant for all pairs of consecutive integer indices but the coefficient out front spoils any possibility of such a construction. If we abandon this coefficient, as in our initial guess above, we lose nontrivial commutation relations but might obtain a basis invariant form of the equations of motion that map onto the usual second quantized approach.

The question of locality is still somewhat vexing. For the many body Schrödinger equation, locality is manifest and the natural basis for second quantization for such a description is the δ-function set. In terms of the collective modes, the operators are integrals so quite nonlocal. To understand if locality is really preserved we should consider the way that these operators couple modes together and what is the microscopic origin of these rules. To do so, we should consider the kinds of models used that cause phonon interactions. Heat transport and electron-phonon interactions are often framed in the momentum representation. As in the case of QED, the spatial locality of the interaction fixes (pseudo)-momentum conserving relations among the

[5] $K_{n,n+1}$ here really only needs one subscript since we are not defining it for all subscripts in K_{ij}. The pair is just a reminder of the action.

diagrams.

Acoustic phonons are often the canonical example of quasiparticles. Some quasiparticles, like electrons, can carry mass so real momentum as well. The discussion of "dressed electrons" from this point of view would get rather lengthy but we can now suggest what sort of many body systems are amenable to a quasiparticle treatment. In the one particle case, we can turn up a potential and observe the changes in the energy levels. Typically there are avoidances but some symmetries allow (generally transverse) crossings to occur. This allows one to map the original $|k\rangle$ labels of the free eigenstates to the ones of those with interactions.

In the many particle case, interactions can be viewed as complicated sort of potential. The free body states $\langle k_1, k_2 \dots k_N|$ map, as above, to new interacting states. However, we still would like to use the one-particle picture as much as possible. Generally, the interactions destroy the symmetrized product form of the eigenstates so we need to know how to give meaning to a state $|k\rangle$ with such strong interactions (and when it has any meaning at all). Based on the generally desired properties of quasiparticles, additivity, we can suggest that the low energy many body eigenstates be of the form:

$$\Psi_{n_1,n_2,\dots n_N}(\tilde{X}) = \hat{\mathcal{S}}^{f/b} \int d\tilde{u} \prod_i f_{n_i}(u_i) F(\tilde{X}, u_1, u_2 \dots u_N) \tag{2.18}$$

The coordinates $u_i(\tilde{X})$ give a tailored set of coordinates to orient to the optimal independent low energy oscillations of the ground state. For phonons $u_i = (X_j - R_j)k_j^{(i)}$. The kernel F acts similarly to a Jastrow correction by introducing potentially strong N-body changes to the ground state while the f_n functions give the oscillations along these optimal directions. To the extent that such a wavefunction holds, we can think of the system as made up of quasiparticles. Notice that we have not included a CM or angular localization function. Classical bodies will require this but we are also interested in systems like gases, ultracold gases, and electron systems where such a localization may not be present. In the absence of such localization, this is now a set of true low energy eigenstates.

In the case of a solid, when it heats to the point that is starts to suffer a net expansion (so the core locations shift) or anharmonicity arises in each of the optimal many body directions, this picture starts to fail. Thermal conductivity models incorporate such changes while retaining the phonon picture by introducing classical kinetic notions such as "mean free path" and "collision time" and by introducing coupling between phonons. The first set of notions is troubling because the phonons are intrinsically nonlocal objects that don't form packets in any obvious way.[6] The

[6]The closest approximation to a phonon packet is probably as follows. Consider a connected subset of the core locations $\tilde{R}' \subset \tilde{R}$ and define a corresponding basis of phonon oscillation functions corresponding to these. The resulting set of states can be expanded as functions on $\tilde{X}$ by including localization functions in the unused directions. These must then be expressible on the original phonon basis $\psi_{n_i}(\tilde{X})$. The resulting collection of modes are initially localized in space and restricted to the frequency set corresponding to the smaller volume.

second is troubling because, anharmonicity just indicates that our harmonic approximation of the modes is no longer valid. These models have met with some success though there is certainly continued debate about their success and validity. Hopefully, this perspective can shed light on the validity of green's function methods and how to best modify them in such situations.

2.5 Newtonian Limit

The task of deriving classical mechanics from quantum mechanics has seemed intractable for many reasons. Ehrenfest offered a naive result for a localized packet and showed that given and arbitrary external electromagnetic field with gradients small compared to the packet localization one recovers the classical trajectory. The larger the mass of the object, the longer the packet stays localized and the result is convincing. For large mass objects, like all objects we experience through our senses, this seems plausible, at least for the CM coordinates. One problem is that there is no reason that nature has to provide us with only localized large mass bodies much less ones with well defined shape and internal structure. Additional complications like the "Schrödinger's cat" and "Wigner's friend" paradoxes [66] leave us with macroscopic superpositions that seem quite unlike the observed natural world.

By assuming that all macroscopic matter starts in the state described by Assumption A, we have a chance of getting such a limit and we will see shortly that it can be greatly expanded. We have no immediate reason for starting with such a state based on assumptions about the state of the early universe, only that it gives the proper kinematic features over long times. As a first step in such a "Quantum-Classical unification" we should at least show that a rigid body, as we described by Ψ_{class}, moves freely according to Newton's laws. Ehrenfest's Theorem demonstrates the center of mass motion moves properly. The rotational motion part is more subtle. Rotation of electrons about atoms is irrotational and introduces radial oscillation and the characteristic non-rigid body rotation. These are wavefunctions as well so rotation requires singular vorticity. However, this can be outside the primary support of the body. For a solid, internal deformations are energetically expensive. The localization in the primary angular direction means there are large regions of low amplitude for vorticity to occupy unlike for the true rotationally symmetric ground state.[7]

This implies that rigid body rotation follows by conservation of angular momentum and that all deformations of this function for a solid have high energy cost. We can compare the kinetic energy of a rotating body to its binding energy. $\frac{K}{B} \sim \frac{mv^2}{u}$ where m is the mass of a particle and u is the energy per bond. In any angular momentum conserving scenario we expect deviations to have to overwhelm the binding energy. This is approximately when the edge of the

[7]Ultracold gases in spherical traps have an energy cost for vorticity penetration and the low energy excited states are, accordingly, propagating irrotational surface waves with singular vorticity near the surface.

body approaches the speed of sound. A similar argument explains why the internal structure is so slightly affected by rotation. Centrifugal expansion can occur but the local relative positions of the cores remains largely unchanged. In the true ground state and nearby eigenstates, such core locations are not well defined.

Chapter 3

Measurement: Quantum-Classical Interactions

3.1 Overview

The quantum theory of measurement, generally via the Born interpretation, consists of a quantum system to be measured, a macroscopic object that is classical and some experimentally determined property of it that measures a quantum state of the system. The most basic of quantum measurements is that of position. Measurements are presumed to correspond to a linear self-adjoint operator. A canonical example is that of a delocalized atom, electron or photon incident on a screen. $\rho(x) = \psi^*(x)\psi(x)$ gives the probability density that a the particle "collapses" at x.

Some shortcomings of this point of view are as follows. If the beam has cylindrical symmetry perpendicular to the screen this gives a unique result, however, one can certainly construct wavefunctions of a single particle that are much more varied. For example, consider a wavefunction broken up into two spatially separated packets traveling at different velocities and directed at different areas of the screen. The time of the the events must be part of what we "measure" and these we don't expect to occur at the same time. Indeed the packet length can be much longer than any measured "collapse time" and the measurement device can sometimes accelerate and move faster than the wavefunction itself.

We can construct correlated incident systems of N particles. The above criterion tells us nothing about the expected probability of results in correlated measurements or if measurement devices can be constructed that look specifically at linear operators of two body systems. Certainly, there has been much work on hidden variables [45] [13] that do look at correlated measurements but these require a way to apply our measurement devices into the larger dimensional space described by these functions. As such, this is properly an extension of the original

Born interpretation. Certainly we should be able to take different measurements like the position of one particle and momentum of another. In principle the granularity scale of measurement should be something that can be modified as well. (An example could be a lattice of cold atom traps with large delocalization.) Having a more intrinsic theory of measurement could suggest a broader range of questions and macroscopic interactions with delocalized bodies.

The microscopic details of a body should say something about what is "measures." The efficiency of the body to make a measurement versus reflect, allow transmission or otherwise interact with the body should also be something we can derive. We already apply quantum ideas to describe microscopic properties of condensed matter. It seems overly pessimistic to accept the positivist limitations on our ability to further apply quantum ideas to get a complete description of bulk matter. The velocity of delocalized particles can be quite low and their packets quite extended. We have the freedom to change location of the measurement device as it interacts with the particle. This can be done in a noninertial fashion. It can accelerate, rotate, even deform and change its chemical and electrical properties mid-measurement. Somehow, the results of such experiments should be expressible in our theory. Uncollected portions of the wavefunction can be altered by external fields during a later pass at it. For continuous sources, it is often unclear how to think of the beam of particles emerging from it. For example, are these correlated? How large is the wavepacket for each one? If one uses a "chopper" to partition the beam with a unit mass, does this correspond to one particle or partial combinations of several particles where the rest of their amplitude has been averted?

All these concepts suggest that there is a kind of "incompleteness" to quantum mechanics as it currently stands. This is not the incompleteness suggested by Einstein, Podolsky and Rosen [45] where hidden variables rescue determinism and locality. Rather, it is a incompleteness in doing the basic job of giving a full description of what we can measure even given a probabilistic interpretation. Relativistic concerns are well known for the measurement problem. The Newton-Wigner operator [66] is a (failed) attempt to extend the position measurement operator to the relativistic domain. More generally, the instantaneous and delocalized nature of measurement seems hopelessly at odds with relativity.

One can even argue that the basic Born interpretation is often not consistently applied in the cases where it is used. The measurement operator $\hat{X}$ is a 3D operator that acts instantaneously everywhere. (Presumably the rigid measurement device specifies a particular reference frame.) In practice we make 2D measurements on screens or measure paths in cloud chambers or, their modern successors, semiconductor and wire arrays. These give paths that could be viewed as a sequence of position measurements with lost time information or as momentum measurements. The momentum eigenstates are properly delocalized in space so do not give a quasi-1D path. Maybe the best interpretation would be to consider these as continuous measurement sequences that measure position in the transverse direction and momentum in the longitudinal direction.

Of course, the very notion of "transverse" is dependent on the choice of longitudinal one so these are not really independent measurements. Regardless of such ambiguity, physicists have found ways to apply these rules to pull out useful and accurate data and relate it to expressions in the theory.

3.2 Surface Position Measurement

It was our supposition that quantum measurement is the result of a small delocalized or otherwise nonclassical body interacting with condensed matter, typically solids. For a first special case let us consider our special case of a solid Ψ_{class} with an extended flat surface normal to the direction of propagation of an incident particle. We choose it at rest and investigate the action of an incident delocalized atom (distinct in type than that of the solid) that will bind chemically to its surface. The oscillation energy density of the packet ψ is assumed never great enough to penetrate the surface and the support of its width is less than that of the surface layer of atoms at the time of contact. Furthermore, that the center of mass, angular and shape changing spreading rates of our solid body are much smaller than the temporal variations in energy, charge, momentum, etc. density of the incident particle wave. (This is almost always satisfied.) Chemical changes during binding are also assumed to occur rapidly compared to any oscillation time of such quantities and ψ has slow spatial variations in these quantities on the granularity scale (atom size) of the body.

At $t = 0$ we can describe this as a product function $\Psi_{class}(\{x_i\}, \{X_j\})\psi_{inc}(x)$.[1] When the wave interacts with the surface we generally assume it adsorbs to single site. The conservation laws of center of mass motion seem to be violated by this event. If it were not, there would need to be a rapid impulse to shift the measurement device to correct for it. Other conserved quantities have similar problems. Everett [48] proposed a kinds of many worlds interpretation that has the potential to solve this and was a favorite among many of the old guard looking for an "interpretation" of the wavefunction. Instead of a radical transformation of the observed system, the universe, instead, obliges to bifurcate itself into the plethora of possible outcomes. We will see that something similar arises here in that the the space is partitioned into a distinct number of spaces determined by the granularity scale of the detector at every measurement event. However, the key is just an implication of our particular subset of wavefunctions that describe macroscopic objects.

For the moment, let the incident packet be a very narrow sheet that meets all points of the surface at the same time t_1 as in Fig. 3.1. The wavefunction forms bound states at each point

[1] The x coordinate describes the CM location of the incident ψ. The X_j and x_i coordinates are the core CM and electron coordinates of the body. The electron coordinates of the incident ψ have been suppressed.

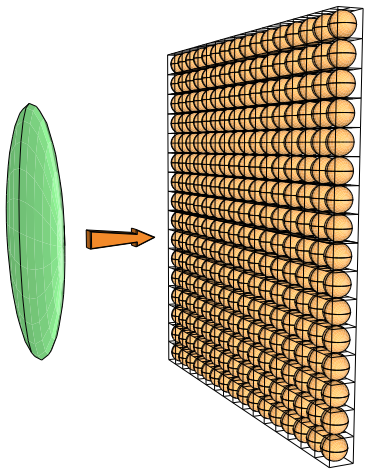

Figure 3.1: A particle with a broad narrow CM packet is incident on a surface. The orange spheres evoke a sense of the electron cloud size although we are concerned here primarily with the localization of the cores (which are much more tightly localized). The green ellipsoid indicates the dominant support of the incident packet and the orange arrow, the net direction of motion.

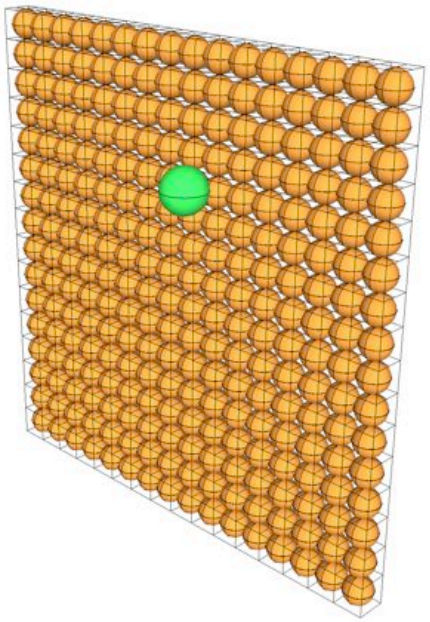

Figure 3.2: The resulting state of the system in a slice where one location is selected.

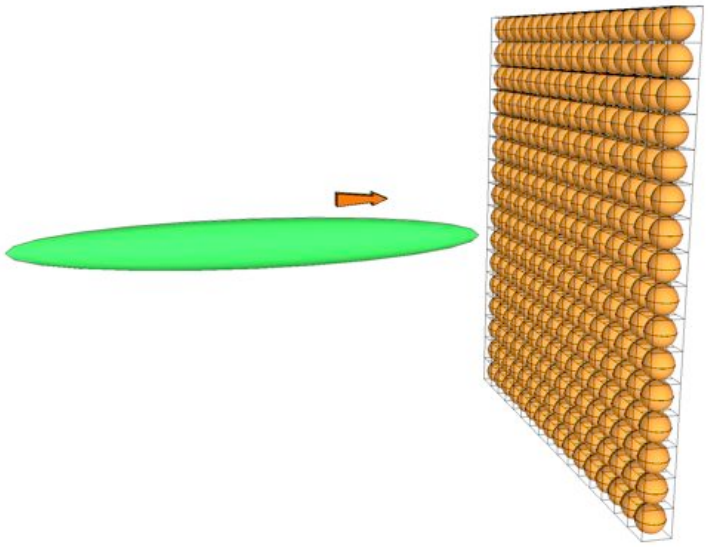

Figure 3.3: A particle with a narrow CM packet that remains incident at the same location on the surface but that has amplitude arriving over an extended period of time.

and gives a new function (up to thermal oscillations and radiation loss contributions)

$$\Psi'(x,\{x_i\},\{X_j\},t_1) = \hat{\mathcal{S}}\sum_s \psi(R^{(s)},t_1)[b(x-R^{(s)})\Psi^*_{class}(\{x_i\},\{X_j\},k)] \tag{3.1}$$

where the bracketed fraction is the wavefunction with localization at a site and the left factor is the weighting factor that now parameterizes the state. The local linear and angular momentum and energy on the granularity scale is transferred to the each corresponding site on the now *excited* medium Ψ^* that includes the acoustic recoil and localized heating of the adsorption.[2] $R^{(s)}$ indicates the set of N_s surface binding sites of the solid. The energy cost of localizing the incident wave on the granularity scale to the narrow packet $b(x)$ is given by the binding energy. We see that $\psi(x,t_1)$ acts as a parameterization for the set of N_s solids with bound surface atom in the N+1 dimensional space (spin and other labels are suppressed). The result valid for all

[2]Since adsorption is always accompanied by photon emission, we should properly include higher photon number spaces, hence a nonrelativistic limit of the physics described by QED. The temporal slicing granularity scale is then naturally the lifetime of the excited states. Unfortunately, this extension of these ideas is rather complicated and requires a future discussion.

times is

$$\Psi(x,\{x_i\},\{X_j\},t) = \begin{cases} \hat{\mathcal{S}}\psi(x,t)\cdot\Psi_{class}(x,\{x_i\},\{X_j\},t), & t<t_1 \\ \hat{\mathcal{S}}\sum_s \psi(R^{(s)},t_1)[b(x-R^{(s)})\Psi^*_{class}(\{x_i\},\{X_j\},t)], & t>t_1 \end{cases} \tag{3.2}$$

The original $\psi(x)$ values play the role of introducing phase shifts and a weighting amplitude among similar copies of the original macroscopic body.

We can now appeal to the strongly localized classical aspect of the original states. Since the delocalization times of the solid are very long we can view the space have having been effectively "sliced" into N_s copies that evolve as independent classical bodies one example of which is in Fig. 3.2. For an observer or recording device riding along with the system, this generates the usual $\psi^*(x,t_1)\psi(x,t_1)$ probability distribution over many such events. This situation will continue until the classical nature of our solid starts to fade, for example, when we have imparted so many delocalized bodies relative to the total mass of the measurement device that it has inherited a net center of mass delocalization from them. Essential to this argument is that the CM localization of the solid is enough so that the slices from neighboring adsorption events do not overlap. We define a "slice" to be a wavefunction describing the macroscopic body with an adsorbed particle at a specific site that occurred at a particular time t'.

Next we consider a very narrow but elongated incident ψ packet traveling in a straight line (to the right along the x axis) with very little transverse spreading as in Fig. 3.3. This strikes the same point $R_k^{(s)}$ but does so over an extended period of time from $[t_0,t_1]$. For simplicity, let us assume the surface is located at $x=0$ The set is now parameterized by $\psi(R_k^{(s)},t)$ where the value of s determining the site is only one fixed value and t is the time to get the value of ψ at that location. (We will integrate over the time of overlap.) We already expect the final state to be a sum of terms like $\hat{\mathcal{S}}[\psi(R^{(s)},t')b(x-R^{(s)})\Psi^*_{class}(\{x_i\},\{X_j\},t',t)]$ but its internal dynamics will record differently when the event took place.[3] This makes one worry that we will have strong superposition among these different slices. Even a very small difference in the final *internal* configuration (from acoustic recoil and heating) with time with respect to of a single coordinate label is enough to destroy long term overlap if the localized peak width is narrower than it. For now we consider this to be a constraint on the initial data.

[3]The notation for Ψ^*_{class} now includes both the current time, t, and the time of the adsorption, t', since this time of internal dynamic response to adsorption is now variable.

This leads us to conjecture the solution is

$$\Psi = \begin{cases} \hat{\mathcal{S}}\psi(x,t) \cdot \Psi_{class}(x,\{x_i\},\{X_j\},t) & t < t_1 \\ \hat{\mathcal{S}}\psi(x<0,t) \cdot \Psi_{class}(x,\{x_i\},\{X_j\},t) + & \\ \hat{\mathcal{S}} \int_{t_0}^{t} dt' [j_\perp(R^{(s)},t') e^{i\phi(R^{(s)},t')} b(x-R^{(s)}) \Psi^*_{class}(\{x_i\},\{X_j\},t';t)] & t_1 < t < t_2 \\ \hat{\mathcal{S}} \int_{t_0}^{t1} dt' [j_\perp(R^{(s)},t') e^{i\phi(R^{(s)},t')} b(x-R^{(s)}) \Psi^*_{class}(\{x_i\},\{X_j\},t';t)] & t_2 < t \end{cases} \tag{3.3}$$

where $j_\perp(x,t)$ is the flux of $\psi(x,t)$ inwards and perpendicular to the surface and $\phi(x,t)$ is its phase. (This flux is $j = -\frac{\hbar}{m}\Im\psi^*\nabla\psi$ if the flux is normal to the surface *and* the surface is at rest.) This ensures proper normalization of the function over space. The function $b(x)$ is a normalized bump function describing the localization of the adsorbed particle. This solution gives an intermediate product state with the remaining free part of the wavefunction and the screen with the previous adsorbed history.

Now let us consider a more general $\psi(x,t)$. The previous limits on its oscillation rate still apply but now we allow it to be more generally distributed in space. The solid body is now allowed to have an irregular curved surface S and the body is allowed to move freely and deform so long as the density of adsorbing sites on its surface does not change. Let the surface sites be denoted by the points $R^{(s)}(t)$ with outwards surface normals $n^{(s)}(t)$. To compute the sliced classical solid wavefunction we track the incident flux and phase of ψ to the surface within the granularity sweep of each site. Essentially, the surface captures all the amplitude it sweeps across and at each such event the system is sliced into a noninterfering history. We must now include the possibility that the unadsorbed parts of ψ can be altered in its evolution by the previous motions of the body and its adsorption history. This is a significant complication. Furthermore, the wavefunction incident on our measurement device may be moving rather slowly so that our device can move relatively quickly and so alter the interference of the transmitted portions that other portions of the device can measure later. A specific example is shown in Fig. 3.4.

Our notation is getting rather cumbersome. Let us now adopt the following shorthand for our macroscopic body. $\Psi_{class}(R^{(s)}(t), n^{(s)}(t); t', t)$ gives the evolving block under the external and internal motions. The surface sites and normals are retained but all other coordinates are suppressed. To describe the total system at any time we are looking for solutions that are a sum of noninterfering adsorbed states with different histories that are then in a product with the remaining free part of ψ. Such a state looks like a sum of terms like

$$\Psi_{pre} = \psi(x,t)\Psi_{class}(R^{(s)}(t), n^{(s)}(t); t) \tag{3.4}$$

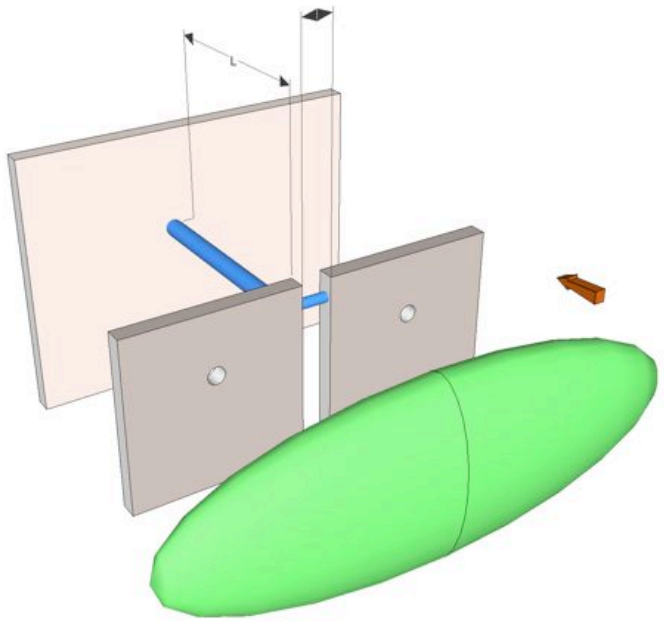

Figure 3.4: A measurement device which has holes to allow partial transmission and interference. The separation of the holes and distance to the farther measuring portions of the device can change in time faster than the characteristic speeds of the wavefunction itself.

and

$$\Psi_{post}(s',t') = \rho(R^{(s')},t')e^{i\phi(R^{(s')},t')}b(x-R^{(s')}(t))\Psi^*_{class}(R^{(s)}(t),n^{(s)}(t);t,t') \tag{3.5}$$

where the ρ and ϕ factors are a function of the value of $\psi(x,t)$ at the location and instant where contact with the solid occurred. The index s' is the site where adsorption has occurred and s is a generic site index. The notation Ψ_{pre} indicates a pre-adsorption history and $\Psi_{post}(s',t')$ indicates a post-adsorption history that occurred at site $R^{(s')}$ at time t'. The $\tilde{X}$, x and t parameters are suppressed. Our total wavefunction at any time is $\Psi = \Psi_{pre} + \Psi_{post}$.

These results are complicated by the fact that the moving measurement device can cast a "shadow" across the incident ψ and introduce new gradients at regions of strongly changing support due to the binding of amplitude to the body. Energy, momentum and the like must all be conserved in this process so these gradients must be paid for from an enhanced binding energy where such tangential or rapidly oscillating motions of ψ and surface motion occur. For a specific example, the surface could have a hole through which ψ can pass. It can then pick up lateral motions just as a light beam will but the strong curvature induced near the wall must come from the binding energy at the edges. This means that we cannot simply evolve the surface sites through the path of ψ and ignore changes in ψ that may occur as a result since these may affect later measurements for other slices. A distressing consequence is that we cannot evolve Ψ_{pre} independently of the Ψ_{post} fields where events have already occurred even though Ψ_{pre} remains in the form of a well defined symmetrized product.

The separation of the wavefunction into long separated slices suggests we update Proposition A to allow for such harmless superpositions.

Proposition B: The classical state of (condensed) matter can contain slicing over multiple delocalized coordinates as long as the delocalization rate of each "classical component" is too slow and the gradients between them too slight to give significant currents over observable time scales.

This allows us to consider classical matter with wavefunctions of the form

$$\Psi = \sum_i^N \Psi^i_{class} \tag{3.6}$$

where each Ψ^i_{class} is a classical component with well defined shape, center of mass localization, translation, rotation and sufficiently distinct internal structure so that no significant overlap occurs among the other components for long times. In the case of nonequilibrium solids and liquids, we will allow different internal flow fields and temperature gradients. These must be all independently evolving for long times.

Using this definition of classical matter and its dictionary-like translation to a quantum

description we now suggest a completed measurement hypothesis.

Measurement Hypothesis: At the point and time of contact of a delocalized particle with a classical component of condensed matter, the body becomes sliced into a set of independently evolving components indexed by the phase of the wavefunction at the moment of contact. This persists for long times due to the large mass of the bound system. The local energy, momentum and other conserved quantities of the particle are locally deposited in the sliced body at that time and evolve in an effectively classical fashion from then on. The remaining parts of the wavefunction exist in superposition with the unaltered body as a product function. The slicing may introduce local curvature in the unadsorbed part of the wavefunction and the price for this comes from the local binding energy. Energy, momentum, angular momentum, spin, and center of mass motion are not conserved in a given slice but norm, mass and charge are.

This hypothesis is built on the property of classical matter that allows all measurements to be derived from local processes in space and time. This is independent of the awareness of any sentient observer. This might be surprising given the variety of measurement operations we generally think about. In the case of a helicity separated photon or a Stern-Gerlach spin separated charge particle we see that the action of measurement is a local space time action. Calorimeters measure the energy deposited from such an action. Velocity measurements are often taken from wire array data which gives a transversely localized particle path with some curvature. This seems to be a sequence of localization events that condense slowly compared to the rate the particle passes. Cloud chamber experiments always involve a surrounding solid material that the particle passes in or out of.[4] Note that this measurement hypothesis is testable both experimentally *and* theoretically by direct investigation of the Schrödinger equation. This sets it apart from other approaches with the possible exception of decoherence which itself has yet to resolve basic questions.

This hypothesis seems a little nonspecific. We ultimately need an extension of the Schrödinger equation of motion for ψ and classical ones for the macroscopic body (which may include pre-programmed changes in response to adsorption events or actions of a sentient being) which then well describe the motion of the net system from the true many body Schrödinger equation. We make explicit the hypothesis with the following rules.

1. Ψ_{pre} evolves according the Schrödinger equation for ψ and Newton's laws for the body subject to sink terms at the surface of the body due to normal currents there. This ensures no ψ amplitude exists in the interior of the macroscopic body. (The evolution *at* the surface is to use derivatives in the external local half-space so no discontinuities exist.)

[4]Tracks in cloud chambers have been knows to exhibit lateral spreading consistent with delocalization. This suggests that either before or after the particle entered the chamber, a slicing event occurred. We will later see that gases are intrinsically delocalized objects that do not produce a granularity scale or natural slow partitioning for measurement.

2. Ψ_{post} states evolve in a Newtonian fashion with a fixed relative phase amplitude and weight defined by the $j_\perp$ flux and phase at the surface at each time t' in the past.

In the case that the binding energy density of adsorption is much greater than the kinetic energy density of the incident ψ this seems like a reasonable set of assumptions since the energy conservation constraint does not need to force a local change in free ψ evolution from neighboring collapse events.

Let us consider the implications of our measurement theory. It certainly does give the original Born interpretation result in the case of a steady beam with a static flat screen for a measurement device when evolution does not continue to the extent that our slices start to overlap. No operator for the general position measurement problem seems to exist. The evolution of the incident particle wavefunction will not always be independent of the history of the device that measures it.

We can now compare what we might expect from a "collapse of the wavefunction" point of view. The rapid transfer of mass over large distances has not only causality but energy problems. Presumably, this would have to come from somewhere. The net shift in the center of mass motion requires a back reaction on the part of the measurement device. None of these effects have been detected. Most importantly, the collapse interpretation requires an operator exist to describe the result of measurement from the collapse. As we noted above, the history dependence of the device should affect the "uncollapsed" portion of the incident wave and there can be energy imparted to this wavefunction from the binding energy to it as well. These give distinct features that can distinguish these models experimentally. It seems odd that purely Schrödinger evolution of a many particle system should reproduce the standard interpretation in typical cases but cause some more dynamic ones to be so different.

3.3 Other Examples

3.3.1 Accelerating Surfaces

The temporal aspect of measurement is not clear in the usual quantum formalism. We can elucidate it with a simple 1D case. Consider an advancing broad packet, corresponding to a single particle, of amplitude A of length L and traveling with velocity v_g in the x-direction. Let a measurement device, in this case a large flat surface perpendicular to x be at rest at the origin and at time t_1 undergo a large impulse that moves it rightwards at velocity $v \gg v_g$. The probability that the particle is adsorbed is the integral of the amplitude squared over the time the wave and the surface intersect. If a measurement occurs it is recorded at a time $t < t_1$ and any further measurement of it later at some point $x_1 > 0$ by another device will be at a time that is $t' \geq x_1/v_g$.

When the surface is jerked away from the support of the incident wavefunction, it leaves an abrupt step that could be shorter than the typical wavelength λ_ψ. Such a situation invariably leads to broad distribution of frequencies and backwards traveling waves. Since this step seems to be present even for the case of a fixed surface, it suggests there may be limits on the absorptive efficiency of any surface as a function of the granularity scale and wavelength of the incident packet. The energy to create the step can only come from the binding energy of the adsorbing particle so gives another way for the Ψ_{post} history to alter the remaining Ψ_{pre} evolution and a potentially measurable deviation from the presumed perfect independence of these histories implicit in the Born interpretation.

3.3.2 Velocity Measurement

Consider the motion a packet normally incident on two parallel thin material plates that leave detectable heat or structural changes as a particle transiently binds then continues on. In this case, the particle is localized but the momentum and energy absorption by the system is considered to be small compared to its net energy. The transverse motion is constrained by the event and we have a sliced set of evolving beams after the first surface. The transverse localization in each slice costs energy and this must come from somewhere and the only candidates are from the longitudinal kinetic motion and the internal energy of the plates. Furthermore, the event leaves a time signature so also localizes longitudinally. This sets bounds on the minimal Δv of the packet and possibly the width of the transverse localization. Assuming this is still small, the packets will evolve from each site at a well defined t and a spread in v. These spread to reach the second plate with a corresponding spread in arrival time according to its time in transit. The final many body wavefunction is a sliced set from the first location and then a further slicing of each from interaction with the second one.

3.4 Uncertainty Relations

The role of the uncertainly relations has been argued with no great resolution though they have practical value in placing bounds on experimental results or allowed initial data. In a deterministic sense, $\sigma_x\sigma_p$ constraints are nothing more than a statement relating packet width to frequency. Landau has been quoted as saying "There is evidently no such limitation-I can measure the energy, and look at my watch; then I know both the energy and the time!" [99] Bohr and Rosenfeld [15] have given a long discussion on the meaning $\sigma_E\sigma_t$ constraints. In a theory that assumes the system is a wave at all times, the relevance of such relations is not clear. It might be more productive to look at details surrounding the measurement process (since this model gives the specifics to do so) and investigate the detailed reshaping of packets

and associated transfer of conserved quantities between measurement device and field. This will no doubt give many inequalities tailored to the particular configuration at hand.

As far as the energy of the energy-time relation, the natural place to look for meaning is in the Fourier transform of the time coordinate since this is how the position-momentum relation is derived. Localizing the temporal oscillations of a packet in time with fixed x is problematic because it violates energy conservation. Such a localization at a point requires lateral energy flux in the spatial directions. If we localize a particle in space without a potential we have a similar problem with momentum flux. To get a stationary analog, we need to turn up a potential uniformly over all space that drives down the oscillations of the packet at $t = \pm\infty$. The extent to which we get a set of localization in time of our oscillatory region is bounded by the uncertainty in the frequency by $\sigma_t \sigma_\omega \geq \frac{1}{2}$. This frequency can be related to the *kinetic* energy as $\sigma_t \sigma_{KE} \geq \frac{\hbar}{2}$. We should note that this is only possible for massive particles and the oscillation frequency ω we assign to it in the Schrödinger equation has already hidden the mc^2 contribution present in the Dirac solutions.

3.5 Decoherence

Decoherence is a proposed many body wavefunction process of creating the appearance of collapse[118]. The off-diagonal elements of the density matrix are assumed to vanish under natural evolution. It has been objected by John Bell on the grounds that resolve problems "for all practical purposes" [66] but leave oscillations present that could be uncovered through an expensive and time consuming measurement. The notion of eigenstate is still explicit in its formulation so seems quite far removed from our picture here of particular class of wavefunctions corresponding to classical objects. The "collapse time" a measure of the time for the off-diagonal components of the density matrix to vanish. In our described measurement process such a notion clearly has no meaning as will be elaborated below. Another way to see that these two pictures are not equivalent is in the observation that the quantum probabilities don't always follow the usual projector description as noted in the examples.

An essential difference between the method discussed in this paper and decoherence is the role of the eigenstate and that classical matter only has the right kinematic features when it is very far from the eigenstates of the actual Hamiltonians. Interestingly, the kind of specialized Hamiltonians we construct in condensed matter physics for particular crystal structures, in some sense, incorporates this as they implicitly assume well defined atomic locations. It has been overlooked that the solutions of these Hamiltonians are different from the true ones in profound ways. In understanding thermal equilibrium and transport, the true eigenstate basis will turn out to be similarly irrelevant but also point to a new way to interpret quantum statistical ensembles without the usual contradictions and ad hoc nature.

3.6 Origins of the Initial Data

So far we have no idea how the initial data suggested by Proposition B arises. We can consider an "Ehrenfest-gas" of localized clusters at most experimental densities. This moves briefly in a classical fashion but rapidly delocalizes over distances far greater than the interparticle separation. Furthermore, this process is independent of the thermal energy of the initial system. For this reason, the classical description of thermodynamics and hydrodynamics we arrive at from a kinetic theory of bouncing billiard balls seems completely irrelevant. That the numerical results we obtain do an excellent job of modeling most aspects of high temperature gases, seems almost like a red herring or, at best, a hint towards some similarity between the dynamics of a "typical" delocalized many body wavefunction at high enough energy and the classical problem.

We are not going to address thermodynamic equilibrium here in depth from this point of view, but to comment that such a condition is problematic for a genuine quantum system where the particular superpositions of eigenstates for an isolated system are preserved for all time. However, this sort of situation is exactly the initial data from which our sun and planets, hence all available condensed matter presumably arose.

In a strongly delocalized gas, condensation involves ejecting energy in the form of radiation and ejected particles to allow the forming matter to attain a lower energy state. The discussion presented here does not include radiation, since the particle number is assumed fixed so we are limited in this respect. In the case of a forming dust particle, we see that a forming pair has no well defined orientation. Further adsorption leads to a superposition of many shapes and binding site choices. As these clusters grow, rebounding particles that leave the system provide more low mass parameters to slice the systems and keep the growing macroscopic superpositions increasingly isolated. This provide a qualitative picture of the origins of the state but clearly leave much room for further analysis. Interestingly, nucleation theory [137] is still in very unsatisfactory state giving another reason why such a more specific picture of quantum and classical transitions is germane.

3.7 Further Complications

Schrödinger cat type arguments involve the alteration of classical behavior in response to a quantum measurement. We can certainly do this with our moving measurement device above. The important distinction is that the shadow effects on the incident ψ depend only on the history of the device up until a selection event is made. Everything after that has no effect on the later adsorption events.

The particle adsorption does not really create the slicing of the system. The measurement device is already sliced into copies indexed the the values of the incident wavefunction $\psi(x)$. The

adsorption event simply causes the identical copies to exhibit different behaviors. Decoherence approaches are concerned with the time for the collapse to occur. For our description, no such notion arises. There are however other timescales. For example, the time for the binding to occur, typically measurable by the length of radiation losses. Also the local elastic changes that radiate out from the site of adsorption and equilibrate at the speed of sound over a number of crossing times of the body. For relativistic measurement devices this is unchanged. However, it is presumed that there is some equilibration over the totality of the measurement device before the events occur. In the case of a gas there is no collective binding that generates a set of localized sites for this to occur. For a condensing solid or a flowing liquid, the partitioning of the space into a well defined set of slices that would be consistent with Proposition B may not have arisen. In laboratory work this may not generally arise, except for the case of strongly isolated mesoscopic solids that might arise in future trapped gas and diamagnetic levitation work, but it may be a concern for astrophysical systems and nucleation.

Macroscopic superpositions such as "Schrödinger's cat" produce no paradoxical effect because we have been very specific in the sort of wavefunctions to correspond to the system. We can see that the energy changes with and without the superposition are very small. The measurement induces long lasting partitions of observer histories with the observed probabilities for static devices. If we consider more general and naive macroscopic superpositions such favorable conditions do not hold. Consider a block with core locations at $\tilde{R}$ and a slightly shifted or rotated lattice $\tilde{R}'$. If we now make a naive superposition of the cores as $\Psi_{class} + \alpha\Psi'_{class}$ we have some cores that will in general be much closer than the interatomic separation and others sitting between interstitial sites. When we construct the corresponding electron orbitals that form the bonds to hold the lattice together the energy per bond is increased by an amount on the order of the deepest bound electron energy per electron. Such a solid is certainly not stable and the energy contributions per atom are much greater than orbital binding energy.

The superselection properties of quantum mechanics have never had a clear resolution. Symmetry breaking depends on it but why nature chooses one option is never clear. Consider the case of a single domain magnetic grain isolated in space to which we had or subtract heat. When we cool below the Curie temperature it must select a direction to magnetize. The superposition of both up and down spin solutions is permissible based on Schrödinger evolution yet we don't observe these (though ferromagnetic transitions in ultracold gases may be a place to look). When the magnetic field of the body interacts with the external world and its own atoms it polarizes spins and alters electron orbits through paramagnetic and diamagnetic effects. It seems that the property of Ψ_{class} to slice into functions that evolve independent of each other forces observers to observe living in a world where only one of the two options occurs. Reheating above T_c seems like it would lead to interference and a "revival" of interaction among the alternative slices to interfere and create unexplainable changes or forces to the observers

and even a conflict in the memory of a recording device. The magnitude of internal structural changes in such a system seems crucial in determining if this occurs. Phase revival has been seen in bose gases[39]. If we can condense such gases into solids while preserving their isolation and delocalization, this might be an ideal testbed to study the process of superselection. The presence of superselection is more ubiquitous than often noted. The famed "Mexican hat" potential associated with symmetry breaking does not fix a given value. Specific systems of importance that exhibit superselection are the quantum blockade, the selection of a particular supercurrent in superconductors, superfluid vortices in liquid He, and the quantum Hall effect.

The metastable nature of the classical states we describe introduce a natural arrow of time to the system. Long before we encounter Poincare cycle like behavior we should confront the long time limits that compromise the classical nature of the solids and observers that comprise it. This can occur just but allowing time to evolve but iterative measurements will enhance it. The slicing of our many body wavefunction cannot go on indefinitely. Eventually delocalization causes these to interfere. Delocalization of these classical states undermines the very notion of a body with well defined shape, orientation and even particle number. In the theory of quantum information, information itself is recognized as a physical quantity. General wavefunctions lose the ability to durably store information in a binary fashion and thus to manipulate it in a repeatable manner. The long time limit seems to have problems bigger than the Poincare cycle and the arrow of time. It loses these essential properties on which life and consciousness themselves seem to depend.

Chapter 4

Thermalization

4.1 Conceptual Problems

Thermalization is most natural as a classical notion. It implies that observable history dependent effects are obliterated over time so that a system with fixed energy (and other conserved quantities) tends to states that are apparently equivalent. This seems to violate the time reversibility of the fundamental equations of motion. Usually this is phrased in terms of the "microscopic" equations. In the classical case this is resolvable. Larger scale motions and less stable small scale ones are generally short lived over the longest time scales [68]. This does not mean they cannot return arbitrarily close to their original state. In fact, for isolated systems of fixed size, the Poincare cycle implies they must and extensions of this result show they must do so with arbitrarily long arithmetic progressions [102]. However, the long time behavior is dominated, in almost all cases, by global uniformity of motion and a local particular velocity distribution that is well attained by averaging over short time scales of the system. If there is a conceptual problem, it is how such initial data arose that led to such an apparently unidirectional time. The anthropomorphic principle gives a suitable resolution. If there were no such gradients present, there would be nothing to power living beings to observe it.

Quantum systems are more troubling for a number of reasons. It is standard to invoke a kind of loose standard to quantum arguments that allows a convenient mixing in of classical notions. When forced to be more specific about this, there are numerous problems. If we wish to think of quantum effects as driving the "microscopic" equations, we have the situation that quantum effects can manifest on large scales as in the case of superfluidity and superconductivity. In the case of ultracold gases, we will show there can be other large scale quantum effects that do not vanish as well. In the previous chapters, we saw reason to not exclude macroscopic superpositions of a certain class. This makes it unclear if we can expect our observations to settle down into an apparent uniformity and consistency of motion with initial larger scale variations vanishing into

unobservable smaller scale ones. More frustrating is that quantum dynamics never change the eigenstate distribution of a given state so the origin of "equilibration" is even more mysterious.

Classical gases have the property of thermalization. This is most easy to see in the case of a gas where a system with a spatial energy and momentum distribution that is "uniform" in some spatial average over mean free path size parcels equilibrates to the Maxwell-Boltzmann distribution; usually in just a few collision times. Analyses of this state can be from the classical kinetics [16] of billiard-like motions to more abstract formulations in terms of phase space distributions, ergodicity or the partition function [127]. The former treatment is the most direct, though much more demanding. It has the virtue of being a *dynamic* approach rather than a kinematic one based on more abstract notions (that we would ultimately need to validate by dynamic means) and therefore include information on fluctuations and transient relaxation. It is easily seen that the delocalization rate of gas particles at usual densities causes the wavefunction spreading to rapidly exceed the interparticle separation. This weakens the conceptual link of this model with a realistic gas that we expect to be described by a wavefunction. We will pursue this when we discuss hydrodynamics.

Phase space is well defined for the classical case as any set of N particles can be represented as a point in 6N-D phase space. Allowing for some uncertainty in the initial data, we may define a weighted volume in this space and evolve it accordingly. Liouville's theorem guarantees the volumes of parcel are preserved and so suggests that the canonical momentum gives the natural measure on this space. Most physical Hamiltonians give strong stretching and folding of this volume in the manner of a Smale Horseshoe map[1]. In many cases this mapping is ergodic; specifically the time average at each point tends to be uniform in phase space. This lead to the temptation to use such phase space averages to give thermodynamic averages. However, not all systems display ergodicity and, even for the ones that do, the sampling time to fill out the phase space to a given level of global uniformity is generally far greater than any observation time of the system. Boltzmann understood that ergodicity was a poor foundation for statistical averages and was determined not to involve ergodicity in the definition of thermal equilibrium values. The long lasting confusion that ergodicity was essential can be traced to an early and well read article by the the evidently confused P. and T. Ehrenfest [16]. Additionally, there are other conservation laws to preserve. This demonstrates to us that to discuss thermal states we really need a "typical" element of our system that gives the averaged thermodynamic quantities as nearly-always holding conditions of the system rather than the sum over an ensemble (though we expect there to be generally no difference in the resulting values).

In quantum mechanics, the partition function and thermodynamic averages have greater problems and a long frustrating history. The Boltzmann factor is so strongly validated by experiment that theory must offer an explanation. However, the justification in quantum treatments of statistical mechanics is even worse than in the classical case. One root of the problem

is that quantum systems do not "equilibrate." Eigenstates and finite superpositions have predictable stationary or periodic behavior. Infinite state superpositions are not generally periodic but still maintain a fixed ratio of occupancy. If "equilibration" depends on arriving at a special subset of distributions of states, this never happens.

The microcanonical ensemble [127][80] is of fundamental importance since it is the starting point to later generate the more practical canonical and grand canonical ones. To form the microcanonical ensemble one takes a sum over the *eigenstates* of energy E_i within some δE spread and, for large enough particle number N, constructs a quasicontinuum of such states with the number of such states as $\Omega(E) \equiv e^{S(E)}$. Weakly coupling with an another much larger such system allows the subsystem's eigenstates to remain near eigenstates with long lasting validity and products of such functions give good approximations to the net system's eigenstates. The exponential growth of the density of states and an enumeration argument shows that the most likely ones are from a sharply peaked distribution where the energy per particle in both the system+reservoir and the system individually is $\epsilon = E_{Net}/N$. Defining the temperature as $T^{-1} = dS/dE$ for this closed system[1] we arrive at the "probability" of a state with energy E_i in this distribution of as $p_i \sim e^{-E_i/T}$. Combining this decreasing probability with the exponentially increasing number of states $\Omega(E)$ gives back our sharply peaked distribution for our system about $E = N_{sys}\epsilon$.

Of course, there is no reason to assume that the system is in an eigenstate and there are many superpositions that have net energy E that do not come from the narrow band of many body eigenstates near this value. Since any weighted combination of eigenstates are allowed and this never changes, it is hard to see how this "probability" has any meaning as a likelihood from an equilibration. We can imaging scenarios where we randomly turn on and off coupling to the reservoir or otherwise perturb the system to try to bring this situation about but classical systems seem to reach equilibration in isolation. A famous method for treating quantum equilibration by coupling to a "bath" of harmonic oscillators is the Caldeira-Leggett model [25] yet each of these seems like just a more elaborate contrivance to obtain the Boltzmann factor we know is somehow important.

Energy is not the only conserved quantity in physics even though it is the one that plays the singular role in almost all statistical mechanical calculations. Galilean translations alone give ten global invariants. A rotationally invariant potential gives angular momentum conservation. In the classical case, we can just impose this as another subfoliation of our fixed energy surfaces in phase space. (It is interesting that this is typically ignored for net $L = 0$ systems yet we still tend to get correct results.) Nonrotationally invariant systems can give nonzero time averaged L conservation for many solutions as in the case of the vertical pendulum so this is a concern for thermodynamics even when rotational invariance fails. In the quantum case, it is unclear

[1] Volume, net energy and particle number are fixed and T is explicitly a function of them.

what to do. Do we restrict our microcanonical ensemble to only consider eigenstates with the desired angular momentum? Do we bias the weights in the distribution in some yet unspecified way? Instead of the ensemble, should we just look at the totality of possible wavefunctions with fixed L and E and average desired quantities? If so, will this agree with the microcanonical result as $L \to 0$? The canonical ensemble does provide an ansatz for handling this with the thermodynamic average, specifically $\langle \, | \, Q - L\omega \, | \, \rangle$, but this seems like one more bit of subject lore to be remembered rather than explained.

There is no natural analog of phase space in quantum mechanics. Classical systems are described by position and momentum but quantum ones are described by vectors in Hilbert space or, more humbly, smooth bounded wavefunctions where the value at each point[2] is a complex value. There have been arguments using a vague partitioning of the (p^{3N}, q^{3N}) phase space via the uncertainty relation. Some of these have led to useful results but it is unclear how to make these precise and why they should be meaningful.

The canonical ensemble introduces "mixed" states that do not correspond to any eigenstate of the system [133]. Such objects are inconsistent with the evolution of a single wavefunction. One can attempt to justify such collections by assuming these other states simply represent some uncertainty in our knowledge as observers outside the system. In this case, it is hard to see why the equilibration and averages should ultimately depend on them and why further measurements should not restrict the set to a more refined subset of such a distribution. If one believes the many body quantum objects we study in cold gas traps are truly just evolving wavefunctions, it is hard to see how one could justify using the canonical or grand canonical ensemble for results beyond what would automatically hold by consistency with the microcanonical one. Furthermore, why should such objects even be limited to such a narrow range of energy eigenstates in its construction and how does introducing angular momentum to the initial data alter this?

In the case of typical macroscopic objects, we have come to expect some sort of disconnect between the worlds of quantum and classical dynamics. As such, we get more comfortable with using quantum reasoning to determine microscopic properties that map on to the macroscopically classical physics. In the case of effective field theory and green's function approaches to transport in hydrodynamics, we assume that classical hydro holds and then introduce linear response theory to compute the relevant parameters in the equations. In a sense we have assumed our way almost to the conclusion and derived the missing values. From such a picture, it is not such a great step to then introduce some additional baggage of the mixed states. However, for our cold gas traps we are more directly confronted with the inconsistency. A trap is with one particle is clearly a pure state. So is one with two, three and so on. At what particle number do we transition to a mixed state? Is this Bayesian uncertainty in our knowledge a result of

[2]Here we allow "point" to be both a position in coordinate and spin space.

large N? coupling to the outside world? Is it just a harmless tool that works because of sharply peaked distributions?

The difference between quantum and classical statistical mechanics can be summed up this way. A classical gas at fixed energy will almost always be in a state that is locally reasonably described as thermal. An isolated quantum gas is in whatever distribution of eigenstates it starts in and this never changes. Classical gases rapidly tend to a well defined hydrodynamic flow but in the quantum case, the space of configurations is so much larger that, as in the case of solids above, a well defined velocity profile $v(x)$ seems like a rather special subset of them. The evolution of such a general state will be considered when we discuss hydrodynamics.

In the spirit of seeking subset of wavefunctions for classical matter that corresponds to "thermal" states we will begin by giving a criterion for the "thermodynamic limit." Traditionally, this is the $N \to \infty$ limit. For trapped gases and small clusters, this seems overly restrictive since some sort of equilibration can occur for them for very modestly sized N. Furthermore, we will show that there is both experimental and theoretical reasons to believe that isolated cold atomic clouds can persist in very far from what we would consider a thermal state. These can have exotic momentum distributions and lack the properties of self-thermalization and thermalization with other bodies they are made to interact with.

There has been recent work utilizing the properties of very high dimensional spheres (Levy's theorem) [105] to show that in the high dimensionality of a many body system, the thermal distribution is overwhelmingly favored. This is kinematic argument and gives no notion of how such states would be arrived at. Other methods to attempt to justify the thermodynamic dominance of the microcanonical states generally involve some Hilbert space measure [18] [55] and a coupling to an external pure state universe. External coupling is known not to be important for equilibration and, moreover, there is no immediately obviously physical measure on this space. Such a natural measure could only be defined by the dynamics of the system in choosing it in equilibration, not the mathematical aesthetics of a theorist. These methods typically don't include any other conserved quantities but energy that the system must conserve. Ultimately, we would like dynamic understanding of equilibration that incorporates all of them.

We argue that wavefunctions of systems that start off sufficiently "broadband," not made of a very small ΔE spread or number of energy eigenstates and for which the expected standing *and* dynamic fluctuation wavelengths are much smaller than the interparticle separation, tend to long time stable distributions of local current flux balanced systems. This is generally independent of the details of the energy distribution of the superposition and gives a new way to assign meaning to the "ensemble averages" in terms of a typical *single* wavefunction. Local dynamics of such a wavefunction near the scattering centers naturally leads to equipartition and gives a reason for the success of classical kinetic results of thermodynamics. Since the particular eigenstate distribution of such states can be hugely varied, we are seeking a kind of universality

in the behavior of currents that almost always dominates in such cases. For this reason we anticipate that large enough subregions of these functions will posses the same fluctuations and energetic distributions as a "typical" or "thermal" wavefunction that will have its eigenstate distribution built from the canonical probability distribution. Such a state will be a convenient tool to extract thermodynamic data, fluctuations and let us give a concrete justification of the canonical average itself.

The "thermal wavelength," $\lambda_{th} = \frac{\hbar}{2\pi m k_B T}$ is a basic parameter used the thermodynamic discussions of quantum systems. The arguments using this are typically vague but this parameter does give a unique length scale in terms of the temperature. We will be primarily interested in wavefunctions far from eigenstates that approach a kind of local regularity in their behavior independent of the particular distribution of eigenstates they are constructed from. For fermions with an energy per particle $\epsilon \lesssim E_F$ we have a lot of curvature to the wavefunction we don't want to consider as "thermal." The traveling component of the waves associated with local currents is the part that we are concerned with. In some cases there may be states with too little energy above the ground state to give what we consider thermal, specifically a local kind of universality independent of the initial data.

It is convenient to have a term to describe the kinds of wavelengths that appear in the currents in both of these cases. Assuming some dominant local frequency exists at a point, we can express λ_{typ} in terms of the local current $\tilde{J} = -\hbar\rho\frac{1}{m_i}\nabla_i\Phi$ where tilde's indicate a many body (3N component) vector and Φ is the phase of the many body wavefunction. In a region with nearly constant potential height, the nonzero current part of the oscillations have wavelength (along the x_i coordinate direction) $\lambda_{typ}^{(i)} = 2\pi/|\nabla_i\Phi|$. The updated "thermodynamic limit" for quantum systems will then be $N \to \infty$ *and* $\lambda_{typ} \ll d_{mfp}$ where λ_{typ} will correspond to the thermal wavelength in the limit of high energy ($E \gg E_F$ or $E \gg E_{gs}$ for fermionic and bosonic atoms respectively).[3]

For later reference, we extend the above notion more precisely and notice that the kinetic energy of a wavefunction can be decomposed uniquely into standing and traveling wave components. This is convenient when we wish to discuss the kinetic energy that arises from vorticity (hence angular momentum) and currents from thermal motion independently of the, sometimes dominant, standing wave component especially at very low energies. For the one-body case, $\Psi = A(x)e^{i\phi(x)}$. The kinetic energy density of the wavefunction decomposes as $\mathcal{E} = \frac{\hbar^2}{2m}A^2(-A''/A + \phi'^2) = \mathcal{E}_s + \mathcal{E}_j$ for the static and current components. This obviously generalizes for many body wavefunctions. We thus have a local decomposition of energy density

[3]The thermal state of metal band electrons seems like it would be a counterexample since the thermal oscillations in wavelength can be much longer than the mfp. However, the net effect will still usually be governed by these atomic wavelengths since the net wavefunction is a function of cores and electrons and the cores typically give much shorter wavelength. The case of ultracold fermionic gases is different since the cores themselves typically have very short wavelength.

$E = E_s + E_j + U$. Extensions of virial results are possible. For example, classical gases have $U \approx 0$ and $E_s = E_j$. Eigenstates (with Dirichlet boundary conditions) in potentials without rotational symmetry give $E_j = 0$. The energy of solids are dominated by U. If we let ΔU be the difference in potential energy over the ground state, harmonic solids also have $E_j + \Delta E_s = \Delta U$, by the usual virial theorem.

4.2 Typical Thermal States

Let us consider some first guesses at a typical thermal wavefunction and see why they don't work. The microcanonical distribution suggests that we choose a wavefunction from the span of eigenstates sufficiently close to E_0. If we make this width narrow enough we eliminate all temporal fluctuations. Spatial correlations will generally persist and this is what is generally referred to as the quantum fluctuations of a system. Temporal fluctuations are often treated by imposing stochastic forces but, presumably, a good approximation to the actual wavefunction would let us read these off directly. Since we know that temporal fluctuations are an important part of thermodynamics, we do not use the microcanonical ensemble as our starting point.

The next logical choice is to try the canonical distribution as a guide. Noting that $P(E) = Cg(E)e^{-\beta E}$ where $g(E)$ is the (many body) density of states, we try a trial wavefunction

$$\Psi = \sum_k g(E_k) e^{-\beta E_k} e^{i\theta(E_k)} \Psi(E_k) e^{iE_k t/\hbar} \tag{4.1}$$

There is quasicontinuum of energy levels and we choose one representative from each level E_k with a random phase specified by $\theta(E_k)$. It is not clear how well defined this definition is since we can keep refining our δE separation of levels until the quasicontinuum approximation fails and eventually we include every such state. Spatial coordinates are suppressed but the time evolution is explicitly included. Two major problems exist with this wavefunction. First it is unclear how a system ever arrives at it under (reversible) Schrödinger evolution. Second, some of the "representative" states of each energy level can be highly anisotropic both in their 3D projections and in their many body directions e.g. the high angular momentum eigenstates and the strongly interacting ultracold gas ground state. Experience with high temperature gases tells us that isotropy is favored and correlations disappear. (In terms of a wavefunction this would imply it averages to be isotropic on scales larger than the mean free path[4] when rotated about hyperangular directions.) It is probably true that a random wavefunction from the space

[4]The meaning of "mean free path" in the quantum case should be clarified. For the case of short wavelengths compared to the particle cross sections, we have geometric scattering and the meaning is obvious. This is primarily the case where we argue thermalization occurs. For phonons, which don't have an easy packet construction, as argued earlier, so the collision time is a better measure. It can be defined by the time our quasiparticle picture maintains its product function like validity.

spanned by this energy width δE has these properties. However, the previous reasons make it clear we should work harder at finding what a typical thermal wavefunction should look like. Let us begin with a proposition that describes what equilibration means for a wavefunction.

Equilibration Condition : The scattering rates of many body currents at each frequency from scattering centers about the two body diagonals along each single body coordinate direction must balance. Specifically,

$$\left\langle \left| \frac{1}{m_i} \Im \nabla_{x_i} \Psi(\tilde{X}) \right|_{x_i \approx x_j} \right| \right\rangle = \left\langle \left| \frac{1}{m_j} \Im \nabla_{x_j} \Psi(\tilde{X}) \right|_{x_i \approx x_j} \right| \right\rangle \tag{4.2}$$

where these are time averages over time scales typical of the local oscillation periods and spin labels have been suppressed. The region of consideration around $x_j = x_i$ is the zone where incident flux is changing due to the scatterers. For this energy scale, we are concerned with the region near the classical turning point of the two-body potential out to the region where the potential makes small changes for such kinetic motion.[5]

If we think in terms of momentum flux balance this gives $\langle \rho m v \cdot v \rangle = 2\mathcal{K}$ along each coordinate evaluated near the two body diagonals. Here v is the velocity of the currents $v = j/\rho$ along each one-body coordinate direction. At higher energies we expect oppositely moving traveling waves to have no correlation and potential energy contributions to vanish so that half of the kinetic energy is in the form of such fluxes. This shows that we should have the same kinetic energy contribution for gases along each coordinate direction. This condition does not depend on the particles having the same masses.

A very simple picture of the equilibrated state we envision as a fine scale excitation over the ground state of the system where the oscillations' wavelength is much finer that the curvature of the potentials and ground state wavefunction. Because of this, we expect it to "fill in" regions of lower potential energy function $\mathcal{U}(\tilde{X})$ much like water fills in a basin. The kinetic energy density is

$$\mathcal{K}(\tilde{X}) = \begin{cases} E - \mathcal{U}(\tilde{X}), & \text{if } \mathcal{U}(\tilde{X}) < E \\ 0, & \text{otherwise} \end{cases} \tag{4.3}$$

subject to the condition that

$$\int dX^N [E - \mathcal{U}(\tilde{X})] \Theta(E - \mathcal{U}(\tilde{X})) = E_{thermal} \tag{4.4}$$

that implicitly defines E. This is reasonable as long as the vast majority of the the amplitude is not in the low KE density region where the function tails off. For phonons we have a set of very anisotropic wells corresponding to orthogonal directions in $\mathbb{R}^{3N-5}$. When we get excited

[5]This makes the Coulomb potential and any other potential where the range may extend larger than the interparticle separation a poor candidate for this model and further consideration in those cases is important.

occupancy in all directions the material tends to melt [108]. For realistic solids we expect that the lowest phonon modes will have high occupancy and this tails off to near zero occupancy for a finite fraction of states. The thermal wavefunction we can expect to satisfy the high frequency equilibration condition in terms of the two-body diagonals of the normal coordinates: $u^{(i)}(\tilde{X})$ but not for the low occupancy states. This means that this simple picture is only valuable for a solid when the vast majority of the thermal energy is in such high occupancy modes.

We can not specialize our equilibration condition to describe situations where we expect the collection to have thermal meaning:

Equilibrated Thermal State: A wavefunction where there are a combination of both time varying currents and standing waves with typical wavelengths over a broad distribution that are much smaller than the scatterers and the mean free path, $\lambda_{typ} << \sigma^{1/2}, \lambda_{mfp}$, and the local oscillation distribution of the many body wavefunction is stable for long times over short time averages.[6]

To continue, we consider that the kinds of matter we most associate with classical behavior are solids and gases. (Liquids are still a subject of much debate.) In the former case the oscillations are phonons. In the latter, they are mostly unobstructed long range motions of individual particle waves. These both give nearly free motions in terms of these respective bases. Instead of giving an exact representation of the wavefunction on the true eigenbasis, we will utilize this property and describe it on the corresponding basis for this nearly-free approximation (NFA).[7] Specifically, for gases, we use a basis of free waves and for solids, we use a basis of phonons. It is not clear if this is a completely general approach. When excitations get large enough, as when temperature is large enough to cause appreciable expansion of the material and change in its elastic properties, the state is still built of many body eigenfunctions but they not decompose into products of the phonons as in the case of the low energy states. Our motivation here is that, for such high frequency states, geometric scattering tends to locally dominate and so that such an NFA basis gives a good local picture of the wavefunction away from the two-body diagonal scattering regions. It is such a basis that we presume always exists and will give meaning to the otherwise hard-to-justify ensemble averages and macroscopic thermodynamic quantities.

[6]The case of electrons in a solid is slightly deceptive. It seems that, at typical temperatures, these wavelengths are often rather long compared to the atomic, electron-electron separation or electron mean free path. The decomposition of electron and core parts is artificial. There is really only one wavefunction for the combination of them. The typically short thermal wavelengths of the heavy cores determine the scale for both over time. This distinguishes electrons in solids from fermionic gases where no such background of heavier objects exists. The effects of this on thermalization will be discussed.

[7]It is important to not use the true basis set for this description because we can start with an enormous distribution of energy eigenstates still attain a "thermal state." The energy distribution in this basis will never change in isolation. We use the NFA basis in this global fashion but are really only interested in it as a good local description of the wavefunction away from the two-body diagonals. This is certainly not constant as the wavefunction evolves. To the extent that the system allows a viable 3D description, the evolving expression on this basis describes the microscopic current oscillations to give a more physical approach to stochastic thermal motions.

As a specific case, let us attempt to encode the (free and spinless) MB gas into a trial thermal wavefunction. Given the constant energy sphere in N-body momentum space we know that typical many body wavevectors $\tilde{k} = \{k_1, k_2, \dots k_N\} \in \mathbb{R}^{3N}$ satisfy the MB distribution in its one body components. We can construct a trial wavefunction

$$\Psi = \hat{\mathcal{S}} \prod_{j=1}^{N} (e^{ik_j \cdot x_j}) \tag{4.5}$$

Since this is an eigenstate, it has no temporal oscillations so is not suitable for our purposes. Neither does it have the expected MB statistical distribution.

Using the one body kinetic result as motivation, let us consider a general Boltzmann weighted sum on a free gas basis. Let $\psi_k = e^{ik \cdot x}$ be the one body free states with energy $E_k = \frac{\hbar^2 k^2}{2m}$. (The volume normalization is chosen π^3 for simplicity).

$$\Psi = \hat{\mathcal{S}} \prod_{l=1}^{N} (\sum_{k \in \mathbb{Z}^3} \psi_k(x_l) e^{-\beta E_k}) = \sum_{\tilde{k} \in \mathbb{Z}^{3N}} e^{i\tilde{k} \cdot \tilde{X}} e^{-\beta \frac{\hbar^2}{2m} \tilde{k}^2} = \sum_{\tilde{k} \in \mathbb{Z}^{3N}} e^{(i \cdot \tilde{X} - \frac{\hbar^2 \beta}{2m} \tilde{k}) \cdot \tilde{k}} \tag{4.6}$$

This latter wavefunction has (desirable) oscillatory time dependence, since it is not an energy eigenstate, but also possesses phase correlation at $t = 0$ that are undesirable. To eliminate the artificial phase correlations we choose a set of random phases $\theta(\tilde{k})$ and define our trial thermal wavefunction as

$$\Psi_{th} = \hat{\mathcal{S}} \sum_{\tilde{k} \in \mathbb{Z}^{3N}} e^{(i \cdot \tilde{X} - \frac{\hbar^2 \beta}{2m} \tilde{k}) \cdot \tilde{k}} e^{i\theta(\tilde{k})} \tag{4.7}$$

where the phases are random up to the symmetry conditions implied by bosonic or fermionic symmetry. (Spin labels have been suppressed in this discussion.)

As evidence for equilibration among wavefunctions that tend to such a local description, consider the *interacting* dilute gas. A distribution of high frequency random oscillations produce currents that interact with the hard core scattering centers in the manner of geometric optics. In the two body CM frame, these centers gives the same dynamics as packets with energy and momentum conservation; the same dynamics that generate the classical MB distribution for hard spheres then apply here. The big difference is in the delocalization of the many body wavefunction so that is cannot be thought of as a set of billiard balls on the microscopic scale. Ultimately, even at such high frequencies, we know that there are eigenstates and superpositions that do not give us anything like MB or hydrodynamic behavior. From a Green's function point of view, these are cases with constructive scatting interference. The supposition here is that, at least for thermodynamics, this is rather unusual and energy distributes itself rather uniformly

over space and with a range of frequencies given by equ. 4.7. We have presumed a unique local equilibrium distribution and this should be investigated further but, as in the classical case, expect it to be so.

The conditions on the smallness of the wavelength versus the scatter sizes and separation extends this reasoning to the case of solids with phonons as discussed above. In the case of liquids, the localized peaks presumably delocalize into a percolating structure that replace the lattice of well defined locations; some of the phonon modes being replaced by traveling modes that transport mass and allow greater penetration of vorticity. The "necks" in the percolating structure could provide for scattering losses from asymmetry in the density buildup about them and the shape of these altered by electron bond strain. This removes the need for aperiodicity to produced scattering which is important since we showed in Ch.2.2 that that notion of periodicity in a crystalline solid has no intrinsic meaning among transformations of the wavefunction corresponding to it.[8]

4.3 Transitive Equilibrium

So far we have not define the parameter β which we anticipate will be related to the reciprocal of temperature. The most basic feature of temperature is its transitive nature; equilibration of a body A with a body B and equilibration of B with C implies A is also in thermal equilibrium with C. We can check to see if two such thermal wavefunctions with the same value of β give a similar state.

$$\hat{\mathcal{S}}\Psi_{th}\Psi'_{th} = \hat{\mathcal{S}} \sum_{\tilde{k}\in\mathbb{Z}^{3N}} e^{(i\cdot\tilde{X}-\frac{\hbar^2\beta}{2m}\tilde{k})\cdot\tilde{k}} e^{i\theta(\tilde{k})} \sum_{\tilde{k}'\in\mathbb{Z}^{3M}} e^{(i\cdot\tilde{X}'-\frac{\hbar^2\beta}{2m}\tilde{k}')\cdot\tilde{k}'} e^{i\theta(\tilde{k}')} \tag{4.8}$$

$$= \sum_{\tilde{k}''\in\mathbb{Z}^{3(N+M)}} e^{(i\cdot\tilde{X}''-\frac{\hbar^2\beta}{2m}\tilde{k}'')\cdot\tilde{k}''} e^{i\theta(\tilde{k})} e^{i\theta(\tilde{k}')} \tag{4.9}$$

Where $\tilde{k}'' = (\tilde{k}', \tilde{k})$ and similarly for $\tilde{X}''$. Assuming that the action of scattering mixes the phases sufficiently, this NFA basis representation of Ψ_{th} gives an equilibration for two uniform density interposed gases. From this we can define thermometry based on equilibrium with a particular chosen standard gas.

[8] This is often overlooked because the electron part of the wavefunction for a solid with fixed cores is typically what is written down. This function does have discrete translational symmetry. However this part has only a limited role in determining the fluidity of a liquid.

4.4 Thermodynamics

The case of homogenous state thermodynamics is of limited interest but really all that we are in a position to now discuss. Inhomogeneous stationary cases like heat transport and dynamic cases like sound waves and hydrodynamics generally require the validity of a 3D description so that we can apply the Navier-Stokes equations and chemical potentials. When such a description holds and the extent to which it applies in the case of ultracold gases will be the subject of the next section.

The homogeneous case gives a starting point to try to assign meaning to the ensemble averages and thermodynamic variables. Pressure, temperature and entropy can all be defined in terms of the NFA basis. For an interacting gas this gives the free gas pressure which is correct microscopically. The two body interactions alter the net pressure on the edges of the trap by excluding regions from contact with the support of the wavefunction and replacing them with potential terms. Entropy and temperature have similar microscopic meanings. The larger scale values don't have an immediately obvious connection with the true density of states of the system. For this reason we investigate these in terms of the true eigenstates of the system.

Our initial trial wavefunction of equ. 4.1 was built on the NFA basis not using the true many body eigenstates. The thermal equilibration condition leads to local configurations well described by this but obtaining the macroscopic averages requires us to do better. We know that the NFA basis with the thermalization property led to a dominant contribution from a narrow distribution of states. For similar reasons we assume the same is true on larger scales where the true basis gives a better description. It is important to remember that the net wavefunction is in the same eigenstate distribution it started in. The scales we are talking about are much larger than the mean free path but much smaller than the total system size.

We extend equ. 4.1 for the quasicontinuum to a typical state of the form

$$\Psi_{th} = \int dE g(E) e^{-\beta E} e^{i\theta(E)} \Psi(E) e^{iEt/\hbar} \tag{4.10}$$

where $\Psi(E)$ is a suitably isotropic and random element of the constant E sphere. When the distribution is strongly peaked, the hyperarea, $\mathcal{A}(\Psi_{th})$, of the dominant energy surface is all we need to characterize the state for this purpose. In terms of this we can define the entropy as $S = k_B^{-1} \ln \mathcal{A}(\Psi_{th})$ temperature $\beta = (k_B T)^{-1} = \partial \ln \mathcal{A} / \partial E$ which lead to the usual thermodynamic relations and canonical averages without requiring the use of mixed states or any type of "ensemble." Introducing additional constraints on angular momentum and other conserved quantities is important when computing results for macroscopic matter. These are always well defined here although it is not immediately clear how to best do this and if history independent results must follow. The most natural guess would be to restrict each of the $\Psi(E)$ to be a

most probably choice with the restricted angular momentum. This certainly deserves more consideration but is probably an involved topic on its own.

Chapter 5

Hydrodynamics

5.1 Convection and Vorticity in Solids

In Ch. 2 discussed the kinematic constraints of a solid and the nature of microscopic (longitudinal phonon) excitations. The equations of motion of a wavefunction are always linear but the motions of fluids and even acoustic waves in solids contains nonlinear advective terms. It is illuminating to examine how this and the classical pressure and stress arise in the solid case briefly first before examining the fluid case. The location and mobility of vorticity is an important topic in fluid dynamics but here we will argue it is also very important for a comparison of classical hydrodynamics with angular momentum and quantum systems ranging from ultracold bosonic and fermionic gases to superfluid Helium.

We conventionally think of sound waves as particular linear combinations of phonons. The weakness in this argument is that the core displacements in the phonon are assumed to be small changes in their equilibrium positions. For larger solid with long wave sound of even modest amplitude, the displacements can be many atomic spacings. There is no reason to doubt that such excitations can be built on eigenstates of the system but it is not clear that they can be made from one-body excitations in the quasiparticle limit of such modes with long lifetimes. In this case, by "lifetime" we mean that duration of time that the solid can be well represented in the form

$$\Psi(\tilde{X})^{(N)} \approx \hat{\mathcal{S}}^{f/b} \int d\tilde{X'}_{\perp} du F(\tilde{X}; \tilde{X}'_{\perp}, u) \Psi(\tilde{X'}_{\perp})^{(N-1)} f(u) \tag{5.1}$$

where F is a kernel that includes two-body and higher corrections near the ground state and $\tilde{X}'_{\perp}$ gives the 3N-3 coordinate space perpendicular to u.

The classical equation for solid motion is the Navier-Stokes (N-S) equations with strong

local restoring stresses

$$\rho\partial_t v + \rho v \cdot \nabla v = -\nabla \cdot \Pi \tag{5.2}$$

$$\partial_t \rho = -\nabla \cdot (\rho v) \tag{5.3}$$

where the internal stress tensor Π provides energy and momentum conservation and provides restoring forces. (Following convention we have used $\rho = nm$ here as the mass rather than the particle density.) More accurate treatments include thermodynamic changes from local compression and their effects on temperature. For gases this gives a large contribution to the speed of sound but for our discussion of solids we neglect it.

As a first example consider the wavefunction of a solid, Ψ_{class}, consisting of N distinct atoms on a lattice as in equ.2.2 but without the symmetry constraints on the core locations. This corresponds to a single localized peak in $\mathbb{R}^{3N}$ space corresponding to the lattice sites $\tilde{R} = \{R_1 \dots R_N\}$. If we perform a displacement of the cores while preserving their localization we obtain a new set of lattice sites $\tilde{R}' = \{R'_1 \dots R'_N\}$. We can map this into a 3D density function $\rho(x) = m \langle R_i \rangle$ where $\langle R_i \rangle$ is the volume averaged density of the cores on a scale much larger than their separation. By using the local velocity of the cores and the bond energy density we can define v and Π to derive equ. 5.2. This follows from the lagrangian form of the Schrödinger equation since these are long lasting qualitative states and in this limit we obtain the classical lagrangian. Since N-S are a nonlinear equations we expect that the corresponding evolution in terms of an eigenstate expansion must probe regimes of the many body eigenstate spectrum beyond any linear quasiparticle picture. It also implies that such a regime always exists in any system that gives classical N-S behavior.

Now let us consider the simplest case of vorticity and solids: rotation. A classical body undergoes rigid body rotation with velocity field $v = r\omega$ where r is the distance from the axis of rotation. This velocity field has the virtue of having the lowest kinetic energy of any velocity flow field with a fixed angular momentum. Quantum systems with large amounts of angular momentum like superfluid Helium exhibit an Abrikosov vortex lattice [106] that give this as an averaged velocity field. This suggests that we might expect a solid to have such a hidden lattice of rotation somehow hidden in its corresponding many body wavefunction Ψ_{class} however we will see that this can be very far from the truth. We saw in Ch. 3 that being specific about the kinds of wavefunctions that specify classical matter removed the apparent problem with macroscopic superpositions by giving low energy long lasting partitions of the observers evolution and that naive superpositions created huge energy barriers that lead to unphysical states. Here we will see that the way vorticity can enter the wavefunction of such a classical body generates very little energy change unlike the usual quantum fluid examples we are familiar with.

Let us continue with our example of distinct particles in the solid as above. The state of

this system is represented by a single peak at $\tilde{R}$ that now evolves according to the classical orbits $\dot{R}_i(t) = \omega \times R_i(t)$. This generates a 1D loop in $\mathbb{R}^{3N}$. This loop induces a 2D surface but, in such a high dimensional space, it has no unique normal to orient a vortex line about the center. We can, nevertheless, choose any one of many vortex lines through the middle it with a (typically huge) winding number that generates the orbit in a period about the loop of $T = 2\pi/\omega$. The vortex cuts through the low amplitude tail of the wavefunction so has very little energy contribution to the system. Furthermore, there are many such vortices that can generate the same behavior. In fact, many vortices could be used as long as they generate the uniform orbital motion around the 2D loop. If we now allow the atoms that make up the body to be identical (or just as problematically, allow them to be composed of the same type of constituent fundamental baryons and leptons) we now symmetrize and generate a set of $N!$ peaks and the same multiplicity of new vortex lines. In a solid there are many low amplitude regions between the cores so it is energetically favorable for them to fish their way through these percolating "interstitial" gaps.

Now consider a cubic solid that has undergone a shear deformation and is released at $t = 0$. The net angular momentum of the solid is zero but the motion is now a combination of shear and rotation so that relative motions induce opposing vorticity that is created and destroyed over time. We can still use the above method to track the core locations and make statements about the kinds of vorticity distributions allowable. In particular, the constant density of the material implies that vorticity only passes in and out of the surface rather than being created. This means that we can expect apparently singular domains of vorticity at the edges of the body in the low amplitude tails of the wavefunction.

Even though it seems like there is no net vorticity, the presence of opposing vorticity have dynamical effects are are important especially in classical fluid dynamics. The enstrophy is defined as the measure of the square of the vorticity. For a constant density fluid, this has kinetic energy contributions. However, for our solid, it seems that the low amplitude regions of the wavefunction induced by the strong binding forces that induce relative localization and motion constraints among the cores are so much more important than any vorticity contribution to the kinetic energy that vorticity is simply created, destroyed and moved about as needed with little effect on the classical motions. Gases will not have such features and the role of vorticity here will be different.

5.2 Classical Gases

The distinction between classical gases and familiar quantum gas cases is central to the upcoming discussion on thermalization and the validity of hydrodynamics for ultracold gases. For this reason we will enumerate some of the differences in the observed behaviors and what

corresponding differences the many body wavefunction describing each must exhibit.

Consider an isolated 1 kg solid. The delocalization of an atom versus that of the CM is related by $\sqrt{N}\delta X_a = \delta X_{CM}$. Assuming each atom is localized to $\delta X_a \approx 10^{-11}$m we have the CM localized to $\delta x_{cm} \approx 10$ m. The delocalization rate of the CM is therefore $v_{del} \sim 10^{-33}$ m/s.[1] In contrast, the delocalization rate of a lone atom with the same initial localization is $v_{del} \sim 10^4$ m/s. Thus, while the atoms of a solid maintain the picture of being classical very well, the gas leaves the category of "classical" rapidly and expands into a very delocalized object where strong correlations are necessary to avoid the large overlap energies we obtained earlier from "naive superpositions." The kinetic oscillations will still dominate the gas as they are much more energetic than the curvature of delocalization. In one sense, this is heartening, if the gas were to stay very localized then it would cast doubt on the relevance of the entropy values derived from the Sakur-Tetrode equation. In another sense, it is distressing because it makes it hard to justify the 3D parcel assumptions we generally use to build thermodynamics and hydrodynamics. Being so energetic in the relative coordinate directions suggests that there is very little energy cost to generating vortices that enter the support of the wavefunction.

We can make a first estimate this by using the thermal wavelength to bound the size of norm exclusion about a vortex core. In the low temperature bose gas case the correlation length specifies the damping of the order parameter about a vortex [106]. Here the vorticity does not experience the same tendency to correlate over all particles but for our estimate here we want the density to truly get driven to zero when we symmetrize so we assume an N-fold vortex product. Such a "vortex line" of length d generates a volume exclusion of $\sim \lambda_{th}^2 d$. The local energy cost for this is very little kinetically since the local oscillation curvature of the attenuation about the vortex is comparable to the thermal curvature it replaces. The density change must be compensated for in the overall compression of the gas so, assuming each vortex[2] gives angular momentum $N\hbar$, we have a net hidden quantum contribution to the thermodynamic energy of $\Delta E \approx P(\lambda_{th}^2 d)(L/N\hbar)$ where d is a measure of the extent of the cloud and L is its net angular momentum. From this we conclude that $\Delta E \ll E = \frac{3}{2}k_B T$ when the rotational period of the cloud, Ω, satisfies $\frac{k_B T}{\hbar} \gg \Omega$. (If we have residual quantum enstrophy this gives another increase in the energy correction.) For a room temperature object this gives $10^{12} \gg \Omega$. It is evident that only very small and tightly bound objects can ever obtain such a rate of rotation. When $\Omega \sim k_B T$, which occurs for $T \sim 10^{-8}$ for KHz frequencies, the quantum correction to the thermal energy of the system becomes comparable to classical thermal one which is when visible coherent vortices dominate the motion instead of rigid body rotation. In both cases the angular momentum is due to vortices in the cloud but in the high energy case there is no favored

[1] It is surprising that the CM is not extremely well localized based on this assumption but the kinematics of large bodies can be unaffected by it. Placing two such bodies adjacent to each other encounters no overlap or restrictions from it since the interactions come from the lack of localization in each individual coordinate label.

[2] We will reexamine this assumption more carefully in Sec. 5.4.

coherence of them so that angular momentum must increase in $\sim N\hbar$ steps rather than just $\hbar$ steps.

In principle we will see there is no quantum limits on the actual size of vorticity due to possibilities for superpositions but there is always a "vorticity penetration cost" that dominates in the lower energy states where the ground state curvature is large relative to excitations. How vorticity appears in higher energy wavefunctions to give classical hydrodynamics is the central topic of the next sections.

The effect of collisions of gas atoms with solid walls is known to be profound. It was observed in the 1880's that the viscous flow of gases in narrow tubes can only be explained if there is a nonspecular reflection of gas particles at a solid surface [68]. The results are consistent with adsorption and reemission of gas particles as thermalized with the surface. A delocalized gas molecule undergoing an effective measurement by the surface would effectively be part of the phonon structure of the solid at the end of it. Ejection follows from the state of the surface being unable to bind the molecule even at rest rather that from a conservation of momentum at the surface. A highly correlated history of collisions induces some constraint on its history in that slice. Whether this is a strong enough effect to induce a well defined 3D hydrodynamic gas flow in each slice is an important question and a possible future test for this model.

In the absence of such solid material, the gas will continue expanding to even much larger distances to create a wavefunction that has little in common with the classical billiard ball picture of a gas. The distinction is so strong that it is hard to see how calculations based on this model can be considered to make any statement about the system. It turns out that things are not that bad but only after a more serious consideration of the system based on its actual state as a wavefunction. Thermal properties seem to agree, however, the resurrection of classical hydrodynamics is rather complicated. We follow our example with solids and write down the simplest plausible many body wavefunction consistent with classical hydrodynamics and discuss some conditions under which it would evolve according to the hydrodynamic limit.

5.3 Quantum Gases

The experimental quantum fluids are superfluid ^{4}He, ^{3}He and ultracold gases. There are other examples of experimental quantum systems like superconducting electrons and exciton-polariton condensates that can exhibit migration but neither exhibit the clear fluidity of hydrodynamic systems. The telltale features of superfluid behavior are irrotational motion, specifically the presence of vortices, a lack of viscosity and two-fluid behavior. In the case of Helium, the two-fluid model has been well verified [106]. Damping has been measured in particular configurations like the oscillating plate Andronikashvilli experiment and the case of vibrating wires. It is often stated that these experiments measure viscosity. Damping can be calculated by the phonon and

roton scattering model of Landau and Khalatnikov [71] however viscosity is more than just a measure of damping. It is defined by the N-S equations and places very particular constraints on how vorticity can move and enter the fluid. In the constant density fluid, the vorticity transport theorem [12] implies vorticity is advected and can only enter or leave through the boundaries. In Sec. 5.8 we will examine the possibilities than nonequilibrium history dependent behavior is persisting and what small effects might be evident in the cloud shape from them including a tendency to keep vorticity out of the higher density regions.

The two-fluid model describes a fluid as having a normal and superfluid component where the superfluid part has no viscosity. As $T \to 0$ the normal component vanishes yet these damping processes persist and the critical velocity in small tubes remains finite. The damping of flow in larger tubes and flow rates what phenomenologically explained by Landau due to quasiparticle excitations. This explanation is largely no longer believed as pictures of superfluid turbulence have become more clear. Thus the case of superfluid Helium seems to still have some mysteries despite the successes of the two-fluid model and there is no fundamental understanding of how the two-fluid model arises.

These considerations are important because ultracold bosonic gases have exhibited long lasting vortices. This suggests superfluidity and that a two-fluid model might apply to them however, these vortices often decay leaving one to wonder what is happening to the angular momentum they possess. The possible existence of quantum limit on viscosity [96] is a pressing problem and has attracted much theoretical and experimental attention with the study of these gases playing a central role. For this to be a valid approach, thermodynamics and hydrodynamics should provide a well defined description of them.

The most simple and successful treatment strongly repulsive bosons at low energy is the Gross-Pitaevskii (GP). The simplest treatment of GP is to assume that the many body wavefunction is a simple product $\Psi = \prod_i^N \psi(x_i)$. Variational methods then give the evolution equation

$$i\hbar\partial_t\psi(x,t) = \left(-\frac{\hbar^2}{2m}\nabla^2 + V(r) + \frac{4\pi\hbar^2 a_s}{m}|\psi(x,t)|^2\right)\psi(x,t) \tag{5.4}$$

where the last term which could be summarized as the interaction strength "g" is written in terms of the two-body scattering length a_s and the normalization has been chosen $\int |\psi|^2 dx = N$. With this normalization ψ is usually called the order parameter and labeled Φ_{GP}. It is distressing to have a nonlinear equation appear but the price of forcing a product function solution. A more realistic function would have the form

$$\Psi(\tilde{X}') = \int d\tilde{X} F(\tilde{X}', \tilde{X}) \prod_i^N \psi(x_i) \tag{5.5}$$

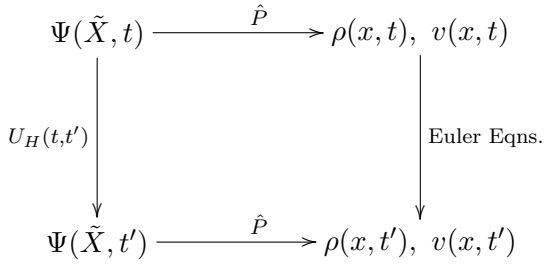

Figure 5.1: For a near ground state of an interacting Bose gas the kinds of adiabatic deformations and release in a trap and the stiffness of such a wavefunction implies near commutativity of the diagram. In contrast, a noninteracting gas makes this exact since the induced many-body currents cannot transfer energy to its transverse directions.

The interaction strength is really a measure of the interaction contribution at the near contact potential and the kinetic energy induced by the curvature as summed up in the kernel $F(\tilde{X}', \tilde{X})$. This is important since the true interaction between particles is often attractive. We can obtain effectively repulsive effects by having the system in an excited branch of the two body potential's spectrum.

Being in a low energy state suggests that the wavefunction is strongly limited in the motion it can exhibit. If we have a cloud in a spherical harmonic trap and make small quasi-static deformations of it through a one-parameter set of quadrupolar deformations, we can obtain a set of wavefunctions $\Psi(\tilde{X};\alpha)$ where α gives the deformation. A deformation that is then released in the spherical trap can then evolve over this set to a good approximation so long as $E_j \ll E_s$ for all time. This gives a solution $\Psi(\tilde{X};\alpha(t))$. The many body Ψ can be described in terms of a limited set of variables like the one-body density $\rho(x)$, a one-coordinate projection $\psi(x) = \psi(x_1) = \Psi((\tilde{X})|_{x_2=c_2 \ldots x_N=c_N})$, the best fit product expansion as in equ. 5.5, or even the single parameter α. Any equation of motion in terms of these variables must eventually fail since the Ψ has current terms and so is not going to stay well describable by such a limited class of function forever. Since the Schrödinger equation can be written as a hydrodynamic equation with a quantum pressure term it is not surprising that we can get a linearized Euler equation for the dynamics in terms of $\psi(x)$ induced $\rho(x), v(x)$ valid for some finite time. This is expressed in Fig. 5.1. The extent to which such a situation holds for more general gases the subject of the following sections.

Another approach to such abbreviated "order parameters" to describe Ψ is to look at it along a particular subslice. For bosons we could use the value of Ψ near the many body diagonal $x_1 = x_2 = \ldots x_N = x$. The function must near vanish there due to interactions but we can look at an ϵ displacement from it $\psi_d(x) = \Psi(x + \epsilon, \ldots x + \epsilon)$. This is also possible for a fermionic

wavefunction as long as we don't evaluate it on a node $\psi_d^{(f)}(x) = \Psi(x, x+\epsilon_1, x+\epsilon_2, \ldots x+\epsilon_N)$ where $\epsilon_i \neq \epsilon_j$ for all $i \neq j$. This can be made unique by choosing the many body directions that give the largest local amplitude. Of course, such an approach is most interesting if we can give an equation of motion valid for reasonably long times in terms of it or relate it to some measurable quantity. For large deformations or time changing potentials or interactions, it will often be the case that such a description is not meaningful since the evolution of Ψ will access many more degrees of freedom on much shorter time scales.

In the favor of such an approach for bosons is that the GP equation for ultracold bosonic gases gives excellent static description of cloud densities. Dynamically, it has given qualitative and sometimes quantitative descriptions of such clouds [39]. In the case of small oscillations of boson and fermion clouds near unitarity, the hydrodynamic approximations for static cloud shapes works very well and predicts the small oscillation periods quite accurately at least for the lowest modes [123]. This is rather profound. A classical gas as a set of billiard balls defines mean free path, collision times, cross sections and the like in a very intuitive manner. The quantum case, as we have seen, allows rapid delocalization of localize packets into a cloud where correlation effects can dominate. Even in the high temperature regime it is not clear that we should get Navier-Stokes evolution and that the huge cardinality of degrees of freedom in a general many body wavefunction should condense to the very limited set corresponding to a cloud with well defined temperature, velocity, density etc. that are purely 3D variables. Microscopically we expect that this is a single wavefunction with a well defined phase moving with only singular sources of vorticity. We know a wavefunction can exhibit perfect stationary or periodic motions at any energy by producing linear combinations of eigenstates, yet hydro and thermodynamics give a vastly restricted class of motions. To date there has been no derivation of classical hydrodynamics from a wavefunction based approach. It is not even obvious how to choose appropriate initial data for such a description.

Shortly, we will give a proposed explanation for N-S behavior as a suitable limit for high temperature gases and a non-hydrodynamic explanation for why and when the linearized N-S equations should give a valid description for oscillatory modes in bosonic gases. Damping of these modes provides an additional challenge usually tackled through linear response theory and the Kubo formula. These can be thought of as scattering based approaches. For a fixed external potential and interaction strength, the system could also be considered as expanded on a basis of eigenfunctions. This should give a consistency check on linear response theory since the end results must be consistent. The Kubo formula for dissipative response has been very successful yet there are longstanding serious doubts about the validity of its derivation [70]. No conclusive resolution of these problems have been obtained. Linear response theory is generally applied to get response functions and transport coefficients. In the case of hydrodynamics, a N-S model with possible gradient expansion is assumed and the coefficients are derived. Classically,

higher order expansions tend to have convergence problems [36]. The Kubo approach generates fractional order expansion coefficients that cannot be mapped onto any gradient expansion. Fractional differential equations might hold some promise for resolving this but tend to introduce many unfavorable behaviors on their own. Generally, this situation is described as the case when hydro "breaks." However, the aspect of this problem that is generally ignored is when the N-S expansion is even valid at lower order for such gases. For it to be so, important correlation properties must hold and persist. This would then be a specific model to give an eigenstate based consistency check on the linear response approach.

5.4 Angular Momentum and Vorticity

In quantum mechanics we learn that angular momentum is quantized in units of $\hbar$. This is evident from eigenstates of the Hydrogen atom. Photons don't have a wavefunction and classical electromagnetic waves exhibit a kind of "angular momentum paradox" due to the fact that classical spiraling wave solutions seem to posses zero angular momentum. However, for photons, we use second quantized solutions with angular momentum given by the helicity of the wave derived from the operator rules [119]. In the case of superfluids we append the superfluid phase rule $v_s = -\frac{\hbar}{m}\nabla\phi$ to the two fluid model and verify integral increases in angular momentum corresponding to all particles in the superfluid fraction contributing $\hbar$.

For a general wavefunction, is it clear that angular momentum requires a current hence an advancing phase (so $E_j \neq 0$). Topologically, this implies there are 3N-1 D hyperlines where the phase evolves about with diverging velocity near them, the amplitude of the wavefunction must vanish there. Thus, angular momentum necessitates the presence of vorticity.

Angular momentum is always determined about a fixed base point. In the study of rigid bodies, the parallel-axis theorem tells us we can compute the angular momentum of a system about their CM and then the bulk motion of these bodies about the base point. For a general wavefunction let us consider the implications of shifting the base point on the angular momentum of the system.

For an Abrikosov vortex lattice in strongly interacting bosonic systems, the collection of vortices rotate like a rigid body and the velocity advances, when averaged over scales larger than the coherence length, to that of rigid body rotation. Consider a wavefunction with uniform support in a cylinder of radius R, height H and attenuation at $r_0 \approx 0$. The density is $\rho = (\pi H(R^2 - r_0^2))^{-1}$. If we have a single vortex line down the central axis the velocity field is $v(r) = v_s\frac{R}{r}$ where v_s is the velocity at the surface then the angular momentum is $L = \int dm(r)v(r)r = \int(m\rho H\ 2\pi r dr)(v_s)r$. Since this field corresponds to a wavefunction $v_s = n\frac{\hbar}{mr}$ where n is the winding number so we have $L = n\hbar$. The kinetic energy is $K = n^2\frac{\hbar^2}{m(R^2-r_0^2)}\ln(\frac{R}{r_0})$ which tends to the classical result for a ring as $r_0 \to R$. The logarithmic trend vanishes in the limit of

many closely packed vortices but for dilute vortex fractions such considerations are important. Thermodynamic quantities are generally extensive in the size of the sample. Angular momentum is not but the ratio of it and rotational kinetic energy for a solid are nicely related by $K/L = \frac{\Omega}{2}$. For our irrotational rotating cylinder the ratio is $K/L \approx \frac{n\hbar}{mR^2} \ln(\frac{R}{r_0})$ which demonstrates that, for lone vortices, there are persistent nonextensive contributions.

If we displace the vortex from the center of our cylinder (moving the attenuation radius with it) so that the phase pattern remains uniform, both the angular momentum and kinetic energy are altered. To measure the angular momentum we must make a choice between still using the center of the cylinder and using the new center of the vortex. If we keep the base point at the center of our distribution and displace the vortex radially then the angular momentum of the system drops to zero as the vortex moves to infinity. If we, alternately, keep our base point at the vortex center then the angular momentum decreases similarly. As the vortex leaves the support of the density and approaches large distances, the cloud picks up a net motion about the vortex center. In neither case is angular momentum (nor linear momentum) conserved. Since the vortices are topological objects that can combine with vortices of opposite helicity but, otherwise must enter an leave the support intact, changes in the angular momentum must occur by changes in their curvature and orientation, the local phase gradients that wrap around them or the density of the norm. Naive shifts in vortex structures are generally forbidden by angular momentum conservation.

Regardless of what what base point we choose, the kinetic energy is, of course, the same which reminds us that the ratio of K/L generally won't have any coordinate invariant meaning. The angular momentum per vortex is now no longer $\hbar$. How can this be? The state is clearly not an eigenstate since there is now a transverse velocity field at the boundary. The angular momentum was never really a localized quantity. We only associated it to the vortex since it has an obvious and precise location. The phase fronts do not need to be uniform as in the cylindrically symmetric case. General superpositions are allowed so that the many body vortices can give $L < N\hbar$. These all make evident that intuition we have gleaned from superfluids or symmetrical quantum eigenstates are prone to lead us astray. The interesting questions are how classical and superfluid motion arise from such a general wavefunction. It is now clear that we must now be more careful in assuming that there is a simple relation of the form $L = N_{vor}\hbar$ where N_{vor} it the number of vortices in the sample. If a uniform lattice exists with vortex separation distance given by d, there is a smoothed flow that gives rigid body rotation as is evident by computing the circulation about symmetrically nested circles.

We are now in a position to compute deviations from the rigid body result. For a uniform density rotating disk $L = \int d\theta \int \rho\ r\ dr(vr)$ where $\rho = M/\pi R^2$ and $v = \Omega r$ so $L_{class} = \frac{1}{2}M\Omega R^2$. If we consider our vortices are made of nested rings at radii r_k spaced by d, the circulation in the integral is altered since $vr = \Omega r_k^2$ for $dk = r_k < r < r_{k+1} = d(k+1)$. The resulting angular

momentum is

$$L = \int (r\ dr) d\theta \rho\ (v\ r) \tag{5.6}$$

where the approximation $v = \Omega r_i \frac{r_i}{r}$ between every pair (r_i, r_{i+1}) gives the *exact* circulation along every closed loop in this interval. The resulting integral becomes

$$L = 2\frac{M\Omega}{R^2} d^4 \sum_j^s j^3 \tag{5.7}$$

$$\approx \frac{1}{2} M\Omega^2 d^2 \left(s^2 - 2s\right) \tag{5.8}$$

where $s = R/d$. Neglecting density changes from attenuation near the vortices, the classical result is excessive by $\Delta L \approx 2\frac{d}{R} L_{class}$. Similar corrections exist for kinetic energy that is actually in excess of the classical result. Notice that this correction is only small because of the large number of vortices. A few widely separated vortices give energies that are not even independent of the size of the system.

The case of interacting (repulsive) bosonic gases are the most dramatic in terms of angular momentum because these gases can exhibit visible vortices and vortex lattices like we see in superfluid Helium. This is the opposite limit of a high temperature gas since the thermal oscillations are now small compared to the ground state curvature. This leads us to expect the kinetic and potential energy cost of introducing vorticity will be much larger hence give different behavior. In the noninteracting case, we can have a product of individually evolving one-particle functions that each have arbitrary vortex structures. The role of interactions is to force the many body wavefunction to cause these structures to correlate so that these give a visible density drop in the one body density function $\rho(x)$. Using one-particle language we would say that every particle shares in the same vorticity structure. If the vortex is at the center, this corresponds to $L = N\hbar$ where N is the total number of particles. If we model two body interactions with a set of Jastrow-like corrections the function looks like

$$\Psi(\tilde{X}') = \int d\tilde{X} F(\tilde{X}', \tilde{X}) \prod_i^N \psi(x_i) \tag{5.9}$$

where $\psi(x)$ encodes the phase and vorticity structure and $F(\tilde{X}', \tilde{X})$ gives the curvature due to the interactions.

The repulsive interaction is greatest at the two-body diagonals. If the vortex structure was built from a set of functions that did not have vorticity at all the same points we could still symmetrize it but the cores would not be falling on these repulsive diagonals. If we used only

$n < N$ of the particles in the system then a fraction of the N^2 diagonals would not intersect with these diagonals. Even if this was only $\sim N^{-1}$ particles there are still $\sim N$ diagonals with amplitude not vanishing except for the damping action of the kernel F. We have implicitly considered each vortex to have winding number $n = 1$ (often the most stable case) but, in this "one-body" picture of the many body vortex, we also have to consider the "occupancy" of these vortices. Implicit in the two-fluid model is the the superfluid component has "full" occupancy and, for ultracold bose gases, the stable states do as well. This observation tells us that it is more accurate, for superfluids, to describe the vortices of having full occupancy rather than quantized angular momentum since we saw that shifting these vortices relative to the fluid surface changes it when we leave the base point fixed.[3] A better understanding of this might lead to a non-phenomenological description of the two-fluid model in terms of the specific dynamics of a many body wavefunction.

As we noted above, displacing the vortex from the center of an axially symmetric cloud, reduces the angular momentum of the system. The coherence effect seems to be more a statement of the orientation of the many body vortices due to the interactions than one of angular momentum quantization itself. This begs the question of what happens as the cloud relaxes as this vortex shifts or if less than such an optimal amount of angular momentum is initially imparted.

If the angular momentum is low enough of a cloud in an axially symmetric trap, we can get surface waves which correspond to vorticity at infinity or at finite distances in the low amplitude tails of the distribution. These vortices don't suffer the same vortex penetration costs. Such surface waves are familiar in both bosonic and fermionic clouds. What is unclear is what happens to it as these oscillations seem to settle down. The angular momentum must be preserved. In a classical gas, we expect the final state to give rigid body rotation as predicted by viscous N-S evolution. In the case of interacting bosons, this seems to require vortices to penetrate the whole cloud uniformly like a vortex lattice or to be "uncorrelated" in the sense above. This gives large kinetic energy contributions without the corresponding decrease in interaction energy. An energetiically more favorable situation would by to allow some angular decorrelation in the picture of one-body states in equ. 5.9. If we use the one-body functions $\psi(x_i; \theta_i(t))$ as elliptically deformed rotating states where $\theta_i(t)$ indicates the angle of the major axis of the ith function then a final state such wavefunction is

$$\Psi(\tilde{X}') = \hat{\mathcal{S}} \int d\tilde{X} F^{\star}(\tilde{X}', \tilde{X}) \prod_{i}^{N} \psi(x_i; \theta_i(t)) \tag{5.10}$$

[3]We will soon see that high temperature gases tend to a coarse grained irrotational product function to reduce scattering. Vorticity is less expensive for these gases and the higher velocities are short range so not necessarily so constrained. For strongly interacting gases, similar scattering effects may explain why vorticity does get so restricted.

The choice of $\theta_k(t) = k\frac{2\pi}{N} + \Omega t$ gives an axially symmetric one-body density function for Ψ that retains the angular momentum of the state with $\dot{\theta}_k(t) = \Omega$ for all k. ($F^\star$ indicates that the kernel we use to include correlations may be somewhat different than the one used for the true ground state.) There is a reduction in the interaction energy at the surface due to reduced interaction energy. This provides a distinct picture than the GP equation for angular momentum to exist and ultimately enter the bulk of the cloud in more observable form. Since the overlap of the one particle wavefunctions gives the interaction energy. The decorrelation of these semi-major axes reduces the repulsive interaction so that the cloud radius will contract compared with the simple rotation of the one body functions.

Due to interaction effects and the possibility of hidden phase gradients it would be convenient to have a measure of the number of one body wavefunctions that overlap. We can quantify the "number density" in this model in a fashion other than the usual GP order parameter and independent of the one-body density function $n(x)$. Let

$$\mathcal{N}(x) = \frac{\sum_i^N |\psi_i(x)|^2}{|\psi_{max}(x)|^2} \tag{5.11}$$

where $\psi_{max}(x)$ specifies the index in the sum of equ. 5.10 that gives the largest norm at x. An alternate definition that is model and basis independent is

$$\tilde{\mathcal{N}}(x) = \begin{cases} N \cdot f_N \left(\frac{\int d\tilde{X} |\Psi(x_1 ... x_k ... x_N)| \sqrt{\rho(x_1)\rho(x_2)...\rho(x_N)}\delta(x-x_1)}{\rho(x)} \right) & \text{if } \rho(x) \neq 0 \\ 0 & \text{if } \rho(x) = 0 \end{cases} \tag{5.12}$$

$f_N(y)$ is a function that sends $y = 1 \to 1$ so that product functions give $\tilde{\mathcal{N}}(x) = N$ for values of x where $\rho \neq 0$ and $f \to \frac{1}{N}$ for functions corresponding to well defined locations at different points. For example, if we used a function $|\Psi|^2 = \hat{\mathcal{S}} \sum_j^N \delta(x_j - d\,j)$ then $\mathcal{N}(x) = 1$ at $x = d\,j$ for all integers $0 < j \leq N$ and zero elsewhere. In the case of a product function, of identical functions $\mathcal{N}(x) = N$ everywhere. These functions measure the the extent of spatial correlations. Greater correlations allow hidden irrotational motion that can hide angular momentum from one-body functions like $\rho(x)$ or the GP order parameter $\Phi_{GP}(x)$. If $\mathcal{N}(x) = 1$ everywhere the GP solution is expected to be accurate. A local value of $\mathcal{N}(x) < 1$ indicates that a distribution of phase gradients can correspond to that location so gives a kind of bifurcation of the order parameter allowing an apparent rotational component to the velocity field driving fluxes of $\rho(x)$. This suggests an alternate approach to higher corrections to the GP model but we won't pursue this further here. Ultimately, we would like a measure that tells us when the vortex penetration cost is small enough to allow internal vorticity versus leaving angular momentum in surface oscillations about the surface.

5.5 Hydrodynamic Kinematics

Just as we worked to establish a set of plausible initial data for the wavefunction of a solid classical body that was consistent with the usual phonon and solid state electron orbital calculations, we would like to give some plausible subclass of wavefunctions that correspond to a gas that is thermalized and hydrodynamic. In the case of the Gross-Pitaevskii equation for a condensed bosonic gas, we often consider the order to parameter to be a scaled copy of a single particle wavefunction and all the particles to be "in the same state" as in Sec. 5.3. This is a manifestly single body descriptions of the situation. It is not manifestly clear this makes sense. After all, the "g" that describes the interaction strength (usually in terms of the scattering length) typically is a subtle combination of both potential energy of the interactions and kinetic energy of the wavefunction oscillations about the two-body diagonals so not the same "g" that governs the strength of the contact potential. One can derive a static version of the GP equation from the result of LHY [81] or Bogoliubov [14] theory by applying mean field theory. Extensions of this to time dependence, especially with higher order corrections, as in the case of Bogoliubov-Hartree-Fock theory, introduce unphysical gaps in the energy spectrum or violate conservation laws [139]. Despite these efforts, experiment seems to show that the case of very low T bosonic systems are very correlated systems, rigid enough that they only require a single order parameter for their description. Persistent vortices can occur and hence these gases are often dubbed superfluid, often leading to the inference that the two fluid model is applicable. It is certainly true that any bosonic or fermionic cloud at arbitrarily large internal energy, can possess internal vorticity. The distinction is that these will not generally give depressions in the one-body density function $\rho(x)$ and that the angular momentum may not be $N\hbar$.

What about the high temperature limit? What enforces such a limiting rigidity on the system so that hydrodynamic variables are relevant. In the case of contact potentials, Werner has come to the conclusion that most eigenstates at high energy are noninteracting [134]. This is of little help for seeking how generally and fast a hydrodynamic state is established. In the noninteracting case we can assign every atom a wavefunction corresponding to a different flow. Furthermore, we can superimpose these. The questions we can ask are: Do most such states tend to "equilibrate" to a hydrodynamic state? Does only a special subset of wavefunctions correspond to the kinds of flows we observe, perhaps by starting from equilibrium and then initially driven by classical 3D objects and forces with their associated kinematic constraints? As in the case of thermodynamics, must any gas wavefunction tend to a recognizable hydrodynamic state on its way towards long term equilibration?

Specifically we can ask when the diagram in Fig. 5.2 commutes. Here we have assumed that $\rho(x)$ is the one body density function defined by integrating out $N-1$ of the coordinates of the many-body density. The definition of $v(x)$ is chosen to satisfy the one-body conservation

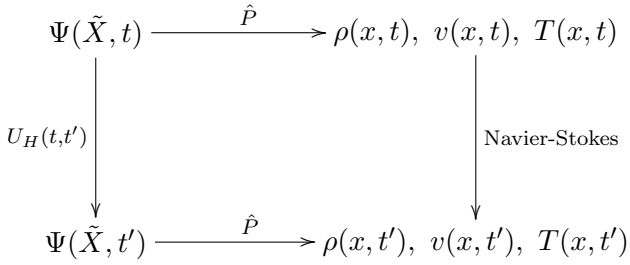

Figure 5.2: Mapping of a general many body wavefunction onto classical hydrodynamic variables by one particle averages. It is unclear when this diagram commutes.

law, $\partial_t \rho = -\nabla \cdot (\rho v)$. This will, in general, lead to a displeasing nonlocal definition via the Helmholtz theorem that is not simply related to the phase of Ψ and may contain rotational components, so not correspond to any one-body wavefunction. The generation of $\rho(x)$ is ultimately a nonlocal action as well but it has the merit of being simpler. The variable T, of course, does not have general meaning even for classical systems. If we can define a generally smoothed density and velocity profile we can interpret the rest of the excitation energy as thermal. By the ansatz $(\text{const}) \cdot k_B T = E_{th}$ we can define such a variable that is consistent with the very high temperature thermalized case.

Discussions of the GP equation often utilize that one way to think of it is as the product of many one-body wavefunctions (with some Jastrow-like correction that is not rapidly changing as the function evolves). If this reasoning is also valid for the wavefunction of a gas in the range of higher temperatures then we would instead have to consider the commutation of actions as in Fig. 5.1 where we assume that dynamics enforce a coarse grained view of

$$\Psi(\tilde{X}) \approx \prod_i^N \psi(x_i) \tag{5.13}$$

The map P is assumed to give $\rho = |\psi|^2$ and $v = \nabla\varphi$ where φ is the local phase of ψ. We are hoping a general Ψ will tend to such a state after some period of relaxation. It is clear there will be many that do not since arbitrary energy eigenstates exist as do few state superpositions of them. The wavefunction of classical gases we expect does not have so much "stiffness" that constrains its possible motion yet there must be some dynamical effect of interactions akin to those that drive thermalization to produce long range order implied by equ. 5.13.

The above picture is appealing at some level but if we seek to derive N-S from this we immediately encounter two problems. First, the thermal motion must be hidden in the fine scale motions of Ψ that are not part of the macroscopic flow. Secondly, vorticity exists in classical flows but appears only in a singular fashion in wavefunctions. Furthermore, we can

have very small vorticity densities in fluids, densities that are much lower than a single quantum vortex would give if granularly spread out on the same scale as the interparticle separation. We will need to update our above mapping $\hat{P}$, specifically its typical inverses, to consider such more general flows.

Given a $\rho(x), v(x)$ we can extract $|\psi| = \sqrt{\rho}$ and irrotational part for the phase $v = -\frac{\hbar}{m}\nabla\varphi$ by the Helmholtz theorem. The rotational part of $v^{(r)} = v + \frac{\hbar}{m}\nabla\varphi$ must correspond to the coarse grained average of 3N-1 dimensional vortex lines. Self consistency dictates these can never end but must go to infinity or close in loops. Fortunately, the identity $\nabla \cdot \nabla \times v = 0$ ensures that this can be satisfied. We may have to consider the low density wavefunction tails outside the support of our classical distribution of matter to do this but we consider this small scale to be resolvable and just a limitation of our best classical description versus a hindrance to a solution. We insert these vortex line function in the product function fashion if equ. 5.13, however, we do not assume there will be N of them.

Gas Hydrodynamic Wavefunction (GHW):
Our trial wavefunction corresponding to a classical hydrodynamic flow $\rho(x), v(x)$ is:

$$\Psi = \hat{\mathcal{S}}_{\{x_j\}} \prod_i^N \psi_i(x_i) \tag{5.14}$$

where $\mathcal{S}$ is the appropriate symmetrization operator over the coordinate labels and $\psi_i = \psi_0 + \psi_i^{(r)}$ is a sum of our best fit irrotational ψ and a similar ψ with a vortex curve and a damping of near it defined by some characteristic length ξ. We have no immediate ansatz to assign winding numbers so we assume that typically the phase advanced by 2π around each. The net effect of all these is to generate the observe vorticity in $v^{(r)}$. A first guess for the characteristic length ξ would be the thermal wavelength. However, we have only incorporated bulk flow and density information into our trial wavefunction. To incorporate thermal information, we note that, in this "geometric" local scattering limit, a Maxwell-Boltzmann distribution is necessary if the current arrives is fluctuating parcels much smaller than the mfp. This lets us define a local distribution of small scale oscillations such that $\psi_T(x) \approx \int e^{i\phi_E} e^{ik_T(E)x} dE$ where $k_T(E)$ is taken from the classical M-B distribution and $e^{i\phi_E}$ is a set of random phases. There is a natural cutoff for the integral so that $k(E) > \lambda_{mfp}$. Our final trial "typical" wavefunctions are labelled $\Psi(\rho(x), v(x), T(x))$ is as in eqn. 5.14 where each $\psi_i(x)$ now incorporates the irrotational and rotational flows as before, $\xi = \lambda_{th}$, and $T(x)$ is embedded in the fine oscillatory structure of each. Furthermore, we randomize the final product phases as in eqn. 4.7.

Although this is hardly a trivial mapping, it seems to be the simplest way to create a plausible typical Ψ corresponding to a classical flowing gas. The evolution of this then needs to be shown consistent with N-S for long times which implicitly includes the persistence of the wavefunction in such a form. Conversely, we want to know that given almost any sufficiently energetic Ψ contained in a volume that it will tend to evolve to such a more limited class of typical thermal and hydrodynamic wavefunctions for long times.

In this trial (GHW) picture notice that the vorticity enters in a very different way than proposed for a rotating solid in Sec. 5.1. The vorticity now penetrates the support of the wavefunction in an unavoidable way and we have favored products of one-body vortices; a condition that deserves future scrutiny. Despite its limitations it does have an advantage over the quantum Boltzmann equation. The derivation of such master equations have occupied tremendous journal space and yet they still seem far from realizing their promise of providing a sound basis for statistical mechanics [131]. In terms of a justification for hydrodynamics, the use of such an equation would be a delicate proposition. The complex part of the wavefunction is encoded in the off-diagonal components of the density matrix ρ_{ij}. These also encode *all* the angular momentum information of the gas. If we don't keep very carful track of these

components this will not be conserved. The attenuated features of the wavefunction norm that exists at the locations of singular vorticity and its mobility is also rather delicate and it is not clear how such information would be mined from the density matrix. N-S hydrodynamics is generally viewed as a statement of energy and momentum conservation and is often derived as such [33]. For a quantum based treatment, it seems advantageous to utilize such conserved and topological quantities as its foundation. We will pursue this as a derivation of the N-S equations from consideration of the wavefunction.

Given the extreme delocalization of realistic gases it is hard to see how the classical billiard ball picture of gases has much of anything to say about gases that are given by many body wavefunctions. The utility of simple picture of classical kinetics has endured a long time and its results are consistent with experiment of high temperature gases however, if the delocalization time of a gas is so short, why should it be relevant? We had some success at a plausible explanation of thermal behavior for a broad class of wavefunctions but the derivation of N-S from such equations looks even more onerous. What can we say about the high energy limit to suggest that such a coarse grained ($n/|\nabla n|,\ |v|/|\nabla v| \gg n^{-1/3}$) product exists?

The free body wavefunction is not constrained and maintains broad long range kinematic freedom. Assuming the typical wavelengths are small compared to $n^{-1/3}$, the interacting case can be thought of of as having $\sim N^2$ scattering 3N-3 dimensional rays that emanate from the origin acting the currents of the 3N dimensional wavefunction. The vast number of these suggests that, when the oscillating wavelengths are long and their currents are small they will tend to move parallel to them. This however, is exactly what we expect for a wavefunction whose phase is a product function $\Phi(\tilde{X}) \approx \prod \varphi_i(x_i)$ since the scattering from the center at $x_j \approx x_k$ is only from transverse components to the many body current $\tilde{J}$ in the (x_j, x_k) subspace. Let us seek a more general global phase in 3N-D to accomplish this. Fix the phase on a one body projection $\phi(x) = \Phi|_{x_2,\ldots x_N}$, and seek symmetry preserving deformations that preserve this and give no transverse fluxes at the scattering centers. Seek a first order deformation of $\Phi = \prod_i \phi(x_i)$ of the form

$$\Phi' = \hat{\mathcal{S}} \prod_i (\phi(x_i) + \epsilon_i \zeta_i(x_i)) \tag{5.15}$$

where all the ζ_i functions are linearly independent of ϕ and not all proportional to each other. We are interested in a solution in the span of this basis that obeys the $\sim N^2$ transverse flux conditions. To get a general solution valid on the scale of our coarse graining $n^{-1/3}$ we need a set of $\{\zeta_i\}$ with oscillations on this scale. This places a bound on the oscillation scale by which we can alter our product function approximation that is finer than we associate with the bulk flow properties our gas.

There are examples where hydrodynamics "breaks," specifically, when no gradient expan-

sion can be accurate. This can nullify the problems of convergence of higher expansions from Chapman-Enskog theory [32] [36] by making them irrelevant but it does leave some uncertainty as to how to correct the evolution. One can further ask if there is a time when thermodynamics itself "breaks." For example, if a gas is in a trap where $|V|/|\nabla V| \lesssim \lambda_{mfp}$ the local velocity distribution may become so distorted and the Knudsen number ($Kn = \lambda_{mfp}/L$) so large that a local definition of thermodynamic variables is not valuable. If one has a rapidly expanding gas where the radial velocity approaches or exceeds the thermal velocity of the thermal waves or the outwards mean free path diverges, equilibration itself become quenched. The currents simply have no time to reach the scattering regions about the two-body diagonals to exchange hyperradial with hyperangular motion. This suggests that bulk expansion of a fluid may introduce some special problems and corrections that are not of a classical nature. One could similarly label this situation as being one where the "classicality" of the gas (as exhibited by equ. 5.14) fails. As an example, consider high frequency sound of a packet with width $d < n^{-1/3}$. In classical kinetics such a density fluctuation makes no sense. However, such high frequency contributions are completely allowed in a wavefunction. On these scales the expansion is governed by unequilibrated motion or the quantum pressure. Such contributions might provide a physical way to extend the hydrodynamic gradient expansions without convergence problems.

There are many persistent oscillatory high energy states that are not similar to product functions on any scale. For the case of contact potentials this is demonstrated with the hyperradial expansion flows in Castin and Werner [135]. Given a square integrable wavefunction with discrete symmetry about exchanges of coordinate labels in a harmonic trap, many periodic solutions can be observed even for states that are very far from symmetrized products. The contact potentials give an exceptional simplicity to the problem that mirrors the free case gas but with boundary conditions at the two-body diagonals.[4] However, for any system made from spherically symmetric two-body potentials we can equivalently consider this to be just an elaborate external potential with a discrete symmetry under coordinate pair exchanges. This immediately implies that any wavefunction with similar symmetry will undergo hyperradial expansion that leaves this symmetry preserved. As such there is no "damping" that drives this energy to hyperangular motions that would allow the one body density function $\rho(x)$ to relax and so interpret the evolution as governed by the N-S equations. These counterexamples shows that the hydrodynamic limit must be somewhat subtle. The harmonic potential is very special in that it is the only one that gives hyperspherically symmetric isopotentials. For gases that start from equilibrium, don't endure extreme expansions and are perturbed by forces that have

[4]Werner [134] in his thesis noted that for contact interactions, at higher energies, almost all states are "noninteracting." My opinion is that the limit of a contact potential has eliminated the very process of thermalization. The finite width of the potentials and the shorter wavelength of the fluctuation's oscillations is what gives the lateral changes in motion that cause equilibration. Similarly, in the case of classical kinetic configurations, they equilibrate in 2D and higher but fail in 1D.

the 3D nature of classical matter we will see that N-S gives a believable evolution for GHW initial data.

5.6 Navier-Stokes Equations

Ideally we would like to know how a general energetic wavefunction settles down to something we would recognize as thermodynamic with a well defined 3D notion of density, velocity and temperature. Even in the classical case, this has been a huge undertaking. A well accepted treatment of the Boltzmann equation was only recently derived [41]. Therefore we accept a more modest set of goals. Given the GHW approximation we need to know 1. why such a function tends to arise and 2. why it persists. The previous section discussed the favorability and durability of the the high temperature coarse grained product equ. 5.14. The evolution of such a state thus amounts to finding the evolution of $\rho(x)$, $v(x)$ and $T(x)$. Since the density is low we know that the currents from the fluctuations carry true momentum and transport mass. This makes them suitable for deriving real forces and stresses on the system. The vorticity penetration cost is considered to be negligible so that it can be transported and created in any locally conserved manner necessary to preserve the other conservation laws.

The velocity field $v(x)$ is assumed to have small gradients on the scale of the mean free path $|v|/|\nabla v| \ll \lambda_{mfp}$ and the currents from the thermal velocity transport mass much faster than velocity v changes. This can be expressed in terms of the collision time $\tau = \lambda_{mfp}/v_{th}$ as $v_{th} \gg \dot{v}\tau$. Since the evolution equations will determine $\dot{v}$, this is a self consistency condition.

The internal stress of a given flow is given by the pressure P that measures the rate of reflected momentum in a parcel several mean free paths or larger. The shear stress is due to the transfer of momentum across mfp sized regions that then average momenta nonlocally. Since this always results in a decrease in macroscopic kinetic energy this results in internal heating. Based on previous arguments, MB statistics for the currents hold so the net stress is identical, to this order, with the classical kinetic arguments $\Pi_{ij} = -P\delta_{ij} - 2\eta(v_{ij} - \frac{1}{3}\nabla \cdot v)$ where P and η are determined by the internal distribution or the thermal velocity and density of the gas [68].

Using that these 3D dynamic variables stay well defined for such conditions we can impose momentum conservation to immediately derive [33]

$$\rho(\partial_t v + v \cdot \nabla v) = \nabla \cdot \Pi \tag{5.16}$$

Together with the conservation of mass condition. $\partial_t \rho + \nabla \cdot (\rho v) = 0$, we have the usual Navier-Stokes equations.

This does not seem very impressive. Essentially, we have done a lot of work to show that the usual hydrodynamic equations hold, at one point, invoking parts of the usual classical

kinetic arguments. A virtue of this is that it reminds us that old arguments with, later revealed, unphysical starting points can still give correct results. At least as importantly, it gives us a new starting point for looking for higher order corrections. The usual Chapman-Enskog expansion has serious and long standing problems [36]. Despite this much labor has been put into deriving corrections from classical virial expansions and molecular dynamics (MD) simulations. A typical wavefunction approach reveals that higher order corrections can have nonclassical variations that include small scale quantum pressure driven waves and variations from the GHW form. Inspired by equ. 5.15 and the bifurcation of the order parameter near the edges of condensed bose gases in equ. 5.10 we might seek corrections of the form

$$\Psi' = \hat{\mathcal{S}} \prod_i (\psi_i(x_i) + \epsilon_i \zeta_i(x_i)) \tag{5.17}$$

where vorticity is distributed among the, otherwise identical, ψ_i and there are a distribution of small irrotational and vorticity corrections included by the ζ_i functions. This wavefunction approach suggests that we might be better off modifying the Chapman-Enskog expansion by allowing a multiplicity of ρ, v, T variables at each point. The classical kinetic approach is limited to the effect of deformed local velocity distributions and their fluctuations. A quantum approach allows for the simultaneous superposition of such variations.

In this discussion we have been primarily interested in the two extremes of high temperature ("classical") and low internal energy (unavoidably quantum) to lend support for the notion that a single wavefunction approach has credibility. Now we move on to the implications of this idea for ultracold gases and history dependent effects that imply thermodynamic and hydrodynamic treatments are overreaching.

5.7 Equilibrium Limit in Gaussian Traps

We have already seen that there are some difficulties in deriving N-S for gases described by wavefunctions at energies that would ostensibly be "classical" even for large particle number. The problems arise from finding a class of functions that can be adequately mapped onto the usual hydrodynamic variables $(\rho(x), v(x), T(x))$ and showing this mapping remains valid under propagation by the Schrödinger equation and that N-S equations give a good coarse grained description in terms of them. However there is a more basic equilibrium problem that is very germane to the types of experiments we do with ultracold traps in gaussian shaped laser traps.

Consider the case of N classical (billiard-like) particles in such a well. The potential for such a trap can be well approximated by $V(r) = V_0(1 - e^{-a^2/r^2})$ where r is the single particle radial coordinate and the net potential is the many body sum of these. If the mean free path is small compared to potential gradients, $\lambda_{mfp}(x) \ll V/|\nabla V|$, we expect MB statistics to be well

reproduced locally. The trap depth is V_0 and the thermal energy per particle is $E_{th} = \frac{3}{2}k_BT$. If $V_0 \gg E_{th}$ we can expect an exponential-like damping in the density with height. However, the MB distribution always has some probability of particles near the edges of the trap (where some *outwards* free paths diverge) have escape energy. This gives losses, assuming ergodicity, that will continue until the remaining particles have less net energy than the energy for a single particle to escape $N_r E'_{th} \lesssim V_0$. Since the energy lost by each escaping particle is $E > E_{th}(t)$, we see that the large N case gives almost all particles ejected and the remaining ones having almost zero energy. Similar losses must exist for self bound gravitational bodies like the sun although with very long lifetimes. However, in the case of gaussian traps, the forces are much more localized and the escape times much shorter.

In contrast, a many body wavefunction localized in the trap by cooling must be primarily composed of components that are truly bound states. Unbound components ($E > 0$) will leak out with characteristic time $\tau \sim \hbar/E$. This leaves the only important loss processes as three body recombination and heating from external sources which are independent and somewhat controllable. The contrast between these two situations is not directly one of hydrodynamic or thermodynamic behavior but of the necessary existence of an enduring bound state in one case and the practical absence of one in the other.

5.8 Ultracold Gases

In the case of ultracold bosons, we have already seen that the energy cost of a vortex penetrating the support of the wavefunction can be prohibitive and that surface waves generated by external vorticity can be favorable. This is especially true for the case of interacting bosons where strong curvature near the two body diagonals makes further attenuation of the amplitude there more expensive and the current's energy, E_j, must increase to avoid these centers. The decorrelation of such surface waves as in equ. 5.10 leads to a state where even the pure irrotational motion cannot be well defined by the classical hydrodynamic variables. These examples give clearly nonhydrodynamic behavior.

The temperature of such gases using the microcanonical ensemble would we derived by many-body eigenstates near a given energy E_0. Many-body superpositions give currents and fluctuations. A gas that is evaporatively cooled by reducing the trap depth allows these fluctuations or higher frequencies to exit the gas. This causes not just the average energy, $\langle E \rangle$ to decrease but also the spread in the energy, ΔE, of the component eigenstates that make up the state. Magnetic field sweeps alter the interaction of the particles and helps keep the hyperradial directions populated with energy for further evaporation. Since superpositions give time dependent fluctuations and these always attain local energies greater than the mean $\langle E \rangle$,

this drives the energy spread to zero faster than the mean energy itself.[5]

For these reasons, it seems fair to assign an evaporatively cooled cloud a well defined temperature. When $\Delta E/\langle E\rangle \approx 0$ the microcanonical definition of temperature suggests we assign $T^{-1} = dS/d\langle E\rangle$ where S is the logarithm of the number of states in window about $\langle E\rangle$. However, this does not mean that such a state has any power to equilibrate other clouds or objects to such a state. If we combine two clouds with the same particle number at different such temperatures corresponding to E_1 and E_2, we end up with a cloud with energy $E_1 + E_2$ but $\Delta E \sim |E_1 - E_2|$.[6]

Now let us compare with the result of a less gentle transformation of the wavefunction. If we make slow enough changes in the potential and interactions the Gell-Mann Lowe theorem guarantees we stay in the same distribution of states we started with and can quasi-statically return to the original state by such a process [101]. A common way of heating such systems is by abrupt trap release and recapture [126]. This can be done in a large step or through many small ones. The distinguishing feature is that the potential is stepwise rather than smoothly evolving so it cannot remove kinetic energy from the wavefunction. The different paths describing these two methods of changing the internal energy, evaporative cooling and discontinuous trap release, are illustrated in Fig. 5.3. To compare these different paths the final number of particles in the trap must be the same. Evaporative cooling changes this so the details of the path must ensure this. More subtly, the evaporation may involve highly correlated currents and we don't know the history of the ejected amplitude. If it all adsorbs to the wall we can expect a slicing of the system in to parts with well defined particle number in the trap. If the particle number of the trap is ambiguous, $\Delta N \neq 0$, we have another level of complication that we will not address here.

If thermodynamic equilibrium is obtained we would expect all observables of the system to be independent of the history of its preparation as in Fig. 5.8. The observables of a cloud in a spherical trap include its radius R and details of its density $\rho(x)$. The velocity is not directly observable but vortex motion can be detected by characteristic density variations and sometimes by careful interference of the matter waves. Momentum distributions are calculated from free expansion of the cloud. The density function $\rho(x,t)$ can be observed and we can measure depth averaged values of $\dot{\rho}$. Perpendicular measurements typically allow an accurate assessment of $\dot{\rho}$ at every point. If this was a product function we could extract v from the Helmholtz theorem

[5] One can ask why such a process leads to a well define number of particles N in the trap since the evaporative flux is continuous and generally correlated. The adsorption of these particles on the walls of the container provide one mechanism to slice the system into such superselected states. If the evaporated particle flux was collected in another trap this would not be the case.

[6] For a thermalized state we expect fluctuations to make up a large part of the kinetic energy so that $E_j \sim E_s$ or $\Delta E \gtrsim \langle E\rangle$ where local oscillations vary much faster than external potential, so such combinations might lead to thermalization. For $T(x)$ to be locally defined by the the nearly free Hamiltonian we still need a kind of coarse product function structure to the system which is not always obviously true.

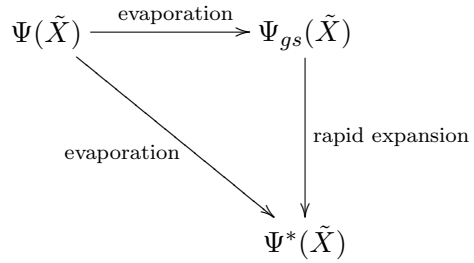

Figure 5.3: The wavefunction for a gas evaporatively cooled to finite thermal E_{th} versus cooled to the ground state then heated by abrupt release to reach the same thermal energy. The diagram does not commute.

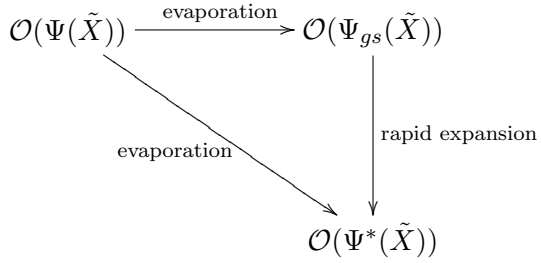

Figure 5.4: Some observables of a many body wavefunction e.g. the cloud radius, may commute under this action if they are only a function of the net energy.

assuming a local conservation law. The resulting many body momentum distribution is then easily found from that of a single state and the multiplicity of copies of it. If the interaction was slowly turned off before the expansion and the system was initially in the ground state, this would be accurate. In general, it is not entirely clear that a one-body velocity function $v(x)$ is well defined. For it to be meaningful, we would expect a local hydrodynamic set of equations to close as a function of v and information derived from $\rho(x)$. For the general many-body wavefunction a histogram of $\Re\Psi^\star\tilde{\nabla}^2\Psi$ gives a well defined measure of the distribution of kinetic energy but it is unclear how this relates to something we can measure. We also are often more concerned with one-body kinetic contributions $\Re\Psi^\star\nabla^2_{x_k}\Psi$ but for interacting or highly correlated functions it is also not clear how to extract the distribution of these values from data either. Presumably, scattering experiments could yield some velocity information but I am unaware of if this is an idea that has fruitfully progressed. Other measurable quantities are fluctuations [89] [47], three body recombination rates and tunneling rates from a trap.

For a narrow ΔE state (near eigenstate) above the grounds state, $E_j/E_s \to 0$. This tells us that the tunneling rates from a gaussian trap should vanish and the three body recombination should be at a minimum. The relaxed cloud radius $R = \langle r^2 \rangle^{1/2}$ should be largely insensitive to the size of ΔE since it is a measure of the balance between the net kinetic and potential energy. However, the details of the attenuation of the cloud we would expect to be different. Higher frequency waves in the hyperradial direction will extend further from the trap center. To quantify this, let ΔE become large enough so that the typical eigenstates of energy E_0 have a radius $R(E_0)$ that exhibits a nonlinear behavior over the range $E_0 \pm \Delta E$. Specifically, if $R(E_0 + \epsilon) \approx R_0 + A(\epsilon - E_0) + B(\epsilon - E_0)^2$ then we expect a difference in the difference in the trap radius $\Delta R = R_{heating}(E_0) - R_{cooling}(E_0) \approx \frac{1}{12} B \Delta E$.

Interestingly, the most accurate measurements of the presumed equation of state (EoS) have been done during cooling [77]. It would be interesting to make a systematic study of the variation in experimental results based on cloud preparation and see if they correlate with history dependence from heating that introduces such internal persistent currents.

To enhance our ability to probe tunneling loss rates we can introduce a barrier potential by replacing the usual gaussian shaped laser beam with a cylindrical varying beam that generates a barrier potential of height V_0, with resonant states, $V(r) = V_0(\alpha e^{-a^2/r^2} - e^{-a^2/(r-b)^2} - e^{-a^2/(r+b)^2})$ This is most easily realized in 2D with a (not necessarily narrow) harmonic confinement in the z-direction. An advantageous property about this potential is that we can start with our usual gaussian trap and produce the the desired $\langle E \rangle$ and ΔE by the usual methods, then optically convert to this new potential. By adjusting $\langle E \rangle - V_0 \gtrsim \Delta E$ we can observe tunneling losses out of the trap at a rate much faster than three body recombination.

So far we have only discussed variations in the internal structure due to radial changes in the external potential. There are two other experimental handles at our disposal: interaction

strength and angular momentum. The possibilities for angular momentum to distribute itself were partially discussed in Sec. 5.4. Starting from a rotating elliptically deformed cloud of interacting bosons in a spherical trap the one-body function $\rho(x)$ will relax to an ellipsoidal deformed cloud. Hydrodynamics predicts a final rigid body cloud rotation but the strong internal curvature can raise the energy cost of vortex penetration too large for the initial angular momentum present to enter the bulk of the cloud. The barrier for this is lowered if the interaction strength is lowered or the thermal energy is increased. Each of these should make a change in the shape of the clouds, rate of evaporative losses and the ratio of angular momentum to mass loss carried with the flux of evaporated atoms.

The case of fermionic gases is special in several ways. Firstly, there is no natural reason for vorticity to correlate in them at low energies that would lead to some visible depression in the one-body density function $\rho(x)$. This leads to the opinion that they are not "superfluid" although it is unclear that "normal" fluid hydrodynamics governs their evolution either. Additionally, we can control the range of interaction over a much larger range while keeping the clouds stable thanks to the effect of antisymmetry that keeps amplitude low at the n-body diagonals where amplitude can get transferred to small bound states that leave the trap. Three body recombination is the dominant such process.

So far we have made extensive arguments that thermodynamics and hydrodynamics do not properly apply to bosonic ultracold gases. Fermionic gases are more complicated but similar arguments apply although the consideration of the distribution of angular momentum is evidently more complicated. For free bosons near their ground state in a trap we can have oscillations persist indefinitely and, due to Madelung reformulation of Schrödinger dynamics, these are hydrodynamic. Bosonic clouds with interactions exhibiting small oscillations also obey an Euler equation approximation for the evolution. For free fermions, a similar situation exists but it does not make itself evident in the one-body density function $\rho(x)$ due to the many frequencies that must compose it due to the antisymmetry of same spin label coordinates.

It is however very interesting that near unitarity, $a_{sc}k_F = 0$, hydrodynamic evolution seems to be recovered. The Euler equation gives "elliptic flow" in free expansion rather than the ballistic motion we would see for classical kinetics at low density or free fermion waves. Small oscillations correspondingly give long lifetimes of coherent motion for $\rho(x)$ which would rapidly become an undifferentiated static ellipsoid in the free case. The antisymmetry of the wavefunction drives the wavefunction to zero for all the $\mathcal{O}(N/2)^2$ same spin label diagonals. In a spin unpolarized gas, there are many more diagonals where the function gets driven to zero, specifically, all the pairs of coordinates where the spin labels are $(\uparrow, \downarrow)$. It seems that this is sufficient to drive the cloud to a restricted set of velocity fields and a stiffness of evolution so that the motion of $\rho(x)$ seems to closely track the case of the cloud under quasi-static multipolar shifts in the potential. We gave a similar argument for why interacting bosonic clouds do this Sec. 5.3.

In the case of bosons the interactions are strongly repulsive (else the cloud collapses through recombination). For fermions near unitarity we have attractive interactions that are just at the threshold for bound states to occur. If the interaction is too strong we have bound pairs that repel (due to the effect of symmetry that is still evident from their composite fermion structure). This seems not to be enough to enforce hydrodynamic behavior as these pairs get smaller. The threshold case gives long scattering lengths, $a_{sc} > n^{-1/3}$, so that the ground state curvature can enforce correlations that strongly constrain the evolution. It would be interesting to prepare a state with large ΔE so that the time varying currents are comparable to this E_s. Presumably, this would destroy hydrodynamic behavior faster for clouds with the same net energy and the same strength of interactions.

The question of damping is an important one. In hydrodynamics, it measure the time for oscillations and nonrigid rotation to settle down to a minimum energy state and is parameterized by the viscosity. Viscosity and vorticity are closely interrelated in that the final states tend to have uniform vorticity and even purely irrotational flows tend to pull in vorticity at the boundaries as a result of viscosity. Incompressible fluids without viscosity subject to conservative forces leave vorticity unchanged. In the case of our gas clouds, we must first ask what exactly is damping. Since we now have reason to believe in a history dependent structure hidden in the apparently stationary relaxed cloud density $\rho(x)$ we must ask what observable is damping. The most evident observable is the cloud density $\rho(x)$ itself.

Quantum treatments of damping typically begin with linear response theory, generally the Kubo formula. This can be thought of as a scattering based approach. It is interesting to consider the same problem from the standpoint of eigenstate superposition. As we argued for thermalization, some systems will tend to a local universality of current distributions and fluctuations that depend only on the energy density despite being very different distributions of eigenstates. Relaxation to such states is what we measure in damping. Because we expect this to be universal behavior that is independent of the eigenstate distributions it seems generally fruitless to approach it from such a point of view. However, for our cold gases that contain history dependent features this is not necessarily true. It is entirely possible that knowing the energy distribution of states with a small set of additional information about them that we could derive damping rates in terms of fundamental constants.

The density of states $g(E)$ is the function on which quantum thermostatistics is built. For a cloud in a fixed trap we can, more generally, consider the set of eigenstates partitioned based on other parameters such as mean radius R, angular momentum L, ellipticity η and so forth. By constructing typical initial data based on distributions of, not just the energy, but these other variables we can consider the damping rates of measurable features such as the distortion of the cloud, η, and the mean radial profile $\langle\rho(r)\rangle$. This seems to be the natural extension of thermo and hydro to trapped gases. As the distributions get larger we may be able to detect

a crossover and convergence to classical hydro and, for the first time, measure a quantum to classical hydrodynamic transition that clearly conserves angular momentum.

5.9 Harmonic Oscillations

There are variety of trapping configurations for holding ultracold gases. Laser and magnetic fields exploit the low field seeking property of some hyperfine states. Some of these are now done on chip sets which allow compactness of the device and manipulation features that are novel. However for optimal isolation and trap shape control optical lattices now dominate the subject. Although these beams typically have a gaussian profile, the lowest few percentiles of them are well described by harmonic potentials. This shape induces a high dimensional symmetry that allows a great simplification in the structure of the eigenspectrum. The gaussian traps were convenient for our discussion above where evaporation and internal currents were our main interest. However, the many-body shape of the cloud in such a trap is not simple. The isopotentials exhibit bulging away from the origin in the manner of the L^p spaces for $p > 1$ of analysis [112]. This makes the analysis of small oscillations very difficult and, for large N, will eventually create tight n-body "corners" where the curvature of the wavefunction cannot penetrate.

In contrast, the harmonic potential is exceptionally simple. To see why this is so consider that our 3N dimensional wavefunction feels an external potential given by $\sum_i^N V_{ext}(x_i)$. For a harmonic (and anisotropic) potential we see that its equipotentials are perfect hyperspheres. For contact potentials we can view the Hamiltonian as a free Hamiltonian over a space with modified boundary conditions along the two body diagonals. This has been exploited by Castin and Warner [135] to demonstrate that the eigenstates of the free and unitarity bounded systems form towers of states separated by $\Delta\omega = 2\omega_0$ where the ground state $E_{g'}$ of each tower varies. Further, they demonstrate that any eigenstate of the trap, when suddenly released or the trap begins to periodically oscillate obey a mathematically simple dynamic behavior [123].

For small radial cloud oscillations, this is often taken as proof of zero bulk viscosity in a unitary gas but it is good to reflect on this from the point of view of arbitrary superpositions and how this reflects on observables. We can choose some linear combination of the ground state and first excited state of a tower and obtain persistent $2\omega_0$ oscillations. However the magnitude of such oscillations is very small since all N particles share in the meager $2\omega_0\hbar$ energy. This is clearly below the threshold of an observable change in the density of our cloud $\rho(x)$. To get large energy oscillations we can take simple superpositions of the ground state and states with $E \sim N\hbar\omega_0$. These states are high frequency and therefore still low in amplitude. To generate the kind of relatively large amplitude ($\delta R \sim R_{trap}$) low frequency ($\omega \sim \omega_0$) motions we observe in experiment let us first consider how it works in the free particle case.

We can form the states $\psi_{2n}(x_i) + \alpha\psi_{2n+1}(x_i)$ for each coordinate where these are one-body states separated by energy $\epsilon = 2\hbar\omega_0$. If we do this over all states ψ_n up to twice the Fermi level and take an antisymmetrized product we will have our observables persistently oscillate at $\omega' = \epsilon/\hbar$. Expanding we see that we have a very large range of energy of the many-body eigenstates involved in the superposition. This distribution will be sharply peaked but the spread is important in obtaining oscillations that are measurably large and of low frequency. This introduces a time scale $\tau = \hbar/\Delta E$ from which we can find a damping rate for one-body observables. However, we must be careful in this interpretation. If I have a one dimensional wavefunction as the states in a square well and take a superposition of eigenstates with spread ΔE corresponding to a peak displaced from the center, then the center-of-mass never settles down to an equilibrium value. The "equilibration" of one-body observables evidently depends on the high dimensionality of the system. This is familiar from the case of classical kinetics where the 1D case of a gas of hard spheres may never relax.

An example just discussed [135] is the pure hyperradial oscillation of an interacting fermi gas in a harmonic trap never relaxes. If we choose our superposition to come from one tower of states (identified by the ground state $E_{g'}$) we have only hyperradial changes to the wavefunction and thus, even though we have some energy spread of eigenstates, the cloud width is a superposition of a one-parameter set of oscillations. Additionally, experience with interacting bosonic gases [104] show that equilibration in such cases does not happen. Therefore the actual superpositions involved for damped states must involve some change in the hyperangular motion as well. This gives the beginnings of what could be a condition on wavefunction superposition for damping of few body observables. The most important observation is that observable distortions of the the cloud will involve distributions of eigenstates over a broad energy scale and relaxation of some observables will be related to this spread of energy.

In the hydrodynamic picture of damping, viscosity provides the mechanism and we obtain

$$\rho\frac{v}{\tau} \approx \eta\frac{v}{l^2} \tag{5.18}$$

where τ is the characteristic damping time and v and l are typical velocities and length scales of the flow. From this we see $\tau \sim \rho l^2/\eta$. A dimensional observation that $[\eta/\rho] = [\hbar/m]$ suggests a way to relate the damping rate to the quantum of action. Such arguments are similar to reasoning for why viscosity has a quantum bound. If one is more skeptical that hydrodynamics is a suitable model for such a system, one can still arrive at such a relaxation time scale for oscillations of the cloud by using the above observation on the energy spread of the distribution of eigenstates involved at unitarity.

Using that the universal parameter for a unitary gas $\beta \sim \mathcal{O}(1)$, we can say the energy spread per particle of Ψ is $\Delta E \sim \frac{\hbar^2}{mL^3}l$ where L is the cloud size and l the deformation width of the

trap at the beginning of the oscillation. Assuming that there are many hyperangular excitations involved in this superposition so that it is not a 1D subset of the motion, as in the hyperradial expansion case, we have a relaxation time for the trap anisotropy of $\tau \sim \hbar/\Delta E \sim \frac{\hbar}{E}\frac{L}{l}$. This gives a quantum expression of damping that is independent of hydrodynamics. As noted above, this is the time for the one-body density function $\rho(x)$ to settle down in the trap. It does not imply that the internal currents and evaporation rates are the same as the cloud before it was released or the same as an evaporatively cooled cloud with the same energy.

Chapter 6

The Dilute Fermi Gas at Unitarity

In this chapter we will provide a brief introduction to the dilute Fermi gas at unitarity, and collect some basic physical scales and definitions that will be useful in the following sections. We consider a dilute gas of neutral spin $\frac{1}{2}$ particles with mass m. Because the gas is very dilute the details of the interaction are not relevant and we can model the two-body potential by a simple potential well, $V(r) = V_0\Theta(r_0 - r)$. This potential acts only between spin singlet pairs. Short range interactions in the triplet channel are suppressed by the Pauli principle. In three spatial dimensions this potential has at least one bound state if the depth V_0 exceeds a certain critical value V_{crit}. We will consider the case that $V_0 = V_{crit}$ and take the limit $r_0 \to 0$. This means that the potential has precisely one bound state with vanishing binding energy, and that the range of the potential is zero. This is called the unitary limit for reasons that we explain below when we discuss the connection to scattering theory.

In the zero-range limit the potential can also be modeled by a delta function, $V(r) = g\delta(r)$. The delta function is too singular to be used in the Schrödinger equation, and requires a regularization scheme. Many different schemes have been discussed in the literature. We note that in dimensional regularization the unitary limit corresponds to the limit $g \to \infty$.

The two-body interaction can also be characterized in terms of scattering theory. At low energy the spin singlet scattering amplitude is dominated by s-wave scattering and we can write

$$A = \frac{4\pi}{m}\frac{1}{k\cot(\delta(k)) - ik}\,, \tag{6.1}$$

where $\delta(k)$ is the scattering phase shift as a function of the relative momentum of the pair. The quantity $k\cot(\delta)$ can be expanded as a Taylor series in k. This expansion is called the effective range expansion

$$k\cot(\delta(k)) = -\frac{1}{a} + \frac{1}{2}rk^2 + \dots\,, \tag{6.2}$$

where a is the scattering length, r is the effective range, and the higher order terms are known as shape parameters. The limit of vanishing two-body binding energy and zero range corresponds to $a \to \infty$ and $r \to 0$. This is called the unitary limit because the s-wave scattering amplitude is completely determined by the ik term, which can be traced back to the unitarity of the S-matrix. In the unitary limit the s-wave scattering length also saturates the s-wave unitarity bound. In this sense, the unitary limit corresponds to the strongest possible two-body correlation.

Experimentally, the unitary limit is realized using two different hyperfine states of a neutral atom with half-integer total (nuclear plus electronic) spin. The interaction is tunable because the two "open" hyperfine states that are being studied couple to a third "closed" hyperfine state whose energy relative to the first two can be tuned using the coupling of the magnetic moment of the closed channel state to an applied magnetic field. The s-wave scattering length in the open channel diverges when a state in the closed channel is tuned to be degenerate with the scattering threshold in the open channel. This is called a Feshbach resonance.

We are interested in many-body systems of spin 1/2 particles interacting via the unitary two-body interaction. This is a very complicated, strongly correlated system. We introduce some of the relevant physical scales by considering a non-interacting Fermi gas. At zero temperature the Pauli principle leads to a ground states in which all non-interacting single particle states below the Fermi momentum k_F are occupied, and all states above k_F are empty. The density is given by

$$n = \frac{1}{3\pi^2} k_F^3 \,. \tag{6.3}$$

The energy of the highest occupied state is called the Fermi energy, $E_F = k_F^2/(2m)$. The total energy can be found by adding the energy of all the filled states. We get

$$E = \frac{3}{5} N E_F \,. \tag{6.4}$$

The energy per particle is 3/5 of the Fermi energy. The pressure of the gas is

$$P = \frac{2}{5} n E_F \,, \tag{6.5}$$

which is entirely due to degeneracy pressure. The Fermi energy determines a characteristic Temperature $T_F = E_F/k_B$, which is called the Fermi temperature. For $T \ll T_F$ the system is degenerate and the pressure is dominated by Fermi pressure. For $T \gg T_F$ the system is a classical Boltzmann gas and the pressure is approximately that of a classical gas, $P = nT$.

The interacting gas does not have a sharp Fermi surface, but we can use equ. (6.3) to define a Fermi momentum, and a corresponding Fermi energy and Fermi temperature. At unitarity the absence of any dimensionful scales associated with the interaction implies that the equation

of state $E = E(N)$ and $P = P(n)$ is still of the form given in equ. (6.6) and (6.5), but the overall numerical coefficient is different. In particular, we can write

$$E = \frac{3}{5}\,\xi N E_F\,, \tag{6.6}$$

where ξ is known as the Bertsch parameter. Experiments and quantum Monte Carlo calculations indicate that $\xi \simeq 0.38$. At zero temperature the attractive s-wave interaction leads to pairing and superfluidity. Dimensional analysis implies that the pairing gap must be proportional to the Fermi energy, $\Delta \sim E_F$, and the critical temperature is proportional to the Fermi temperature, $T_c \sim T_F$. The constants of proportionality are of order one, implying that the unitary Fermi gas is a high T_c superfluid. For comparison, the Fermi temperature of the electrons in a typical metal is a few thousand Kelvin.

More generally, we can use the dilute Fermi gas to study the crossover between a weak attractive interaction, without a bound state in the two-body channel, to a strongly coupled gas with a deeply bound two-body state. This is called the BCS-BEC crossover, because the weakly interacting gas exhibits Bardeen-Cooper-Schrieffer (BCS) pairing, whereas the strongly coupled gas shows Bose-Einstein condensation of preformed bosonic bound states. Experiments and numerical simulations show that the crossover is smooth, without an intervening phase transition. The unitary Fermi is between the BCS and BEC limits, but there are no singularities or discontinuities associated with the limit $a \to \infty$ [82]. A special feature of the unitary Fermi gas is exact scale invariance, the unitary Fermi gas therefore exhibits a large degree of universality. The unitary gas is also expected to have a short mean free path and good hydrodynamic behavior. In the BCS limit the microscopic interaction is weak and the mean free path is long. In the BEC limit the fundamental interaction is strong, but the gas forms small, tightly bound, pairs and the residual interaction between the pairs is weak. As a result the mean free path is also long. A short mean free path and universal, scale invariant, hydrodynamics therefore occurs for the unitary gas, at the BCS/BEC crossover.

Experiments are carried out using atoms confined in optical traps. The trapping potential is approximately harmonic

$$V = \frac{m}{2}\left(\omega_x^2 x^2 + \omega_y^2 y^2 + \omega_z^2 z^2\right)\,. \tag{6.7}$$

The trapping potential breaks the scale invariance of the unitary Fermi gas, but in a harmonic potential many exact relations remain, see [135]. In a harmonic trap the density is a function of position, and as a result the Fermi temperature becomes position dependent as well. In order to characterize experiments it is useful to assign a global Fermi temperature to the trapped gas. A common prescription is based on the the Fermi level of a trapped non-interacting gas.

Defining $k_B T_F^{trap} = E_F^{trap}$ leads to

$$T_F^{trap} = (3N)^{1/3} \bar{\omega} \,, \tag{6.8}$$

where $\bar{\omega} = (\omega_x \omega_y \omega_z)^{1/3}$ is the geometric mean of the trapping frequencies, and we again employ a system of units in which $\hbar = k_B = 1$.

Chapter 7

Scaling Flows

7.1 Introduction

The transition from noninteracting to interacting quantum gases hints at problems in the transition from quantum to classical gases and in the appearance of thermodynamic equilibrium in quantum systems in general. In the classical case we can always do some parcel averaging to get a 3D density and velocity function $(\rho(x), v(x))$. These may be far from equilibrium due to far from equilibrium initial data or strong external driving but the functions themselves are meaningful and a local description of the energy, momentum and other conserved quantities always exists. In the quantum case we can arrange solid boundaries to enforce such a well defined 3D shape but how the kinetic degrees of freedom are reduced to those of classical hydro/thermo is still a mystery. In the classical case, we can derive hydrodynamics from perturbations of the Boltzmann equations [68]. In the quantum case, we need both the kinetic degrees of freedom to be meaningful (i.e. propagated by the equations of motion) and the underlying quantum equations of motion to yield the Navier-Stokes equations for them.

This problem is even more urgent in the case of the partially degenerate and very isolated systems we study in ultracold gases. We know that at small enough numbers and energies, we have the full quantum degrees of freedom and dynamics with arbitrary correlations. It is generally assumed that once N becomes large thermodynamics becomes relevant. Unfortunately, as pointed out before, this is completely inconsistent with the quantum equations of motion which allow any superposition of eigenstates, forbid mixed states, and never "equilibrate". In the case of strongly interacting ultracold fermions, the hydrodynamic approximation seems to give a good approximation to the mass distribution in a trap and the frequencies of small oscillations. For this reason, a vast literature exists on damping based on hydrodynamics assumptions and kinetics.

The observable quantities, just and our freedom to manipulate the gases in these traps, is

rather sparse in relation to the degrees of freedom of such a high dimensional function: we can measure the one body density function and its motion during a trap release. This begs the question if the attenuation results we derive by the Kubo formula or other field theory means is just a reorganization of the dynamics into motions we don't see due our limited observables. This sounds sufficiently like the classical case to be comforting. The wrinkle here is in the case of angular momentum. A classical deformed ball of gas undergoing irrotational motion in a spherical trap will generate vorticity near the edges and damp to a rigid body rotation.

In the quantum case we expect that the many body amplitude and phase always exist. The introduction of vorticity to a wavefunction is very different that for a classical gas. Vorticity is in the form of singular 3N-2 dimensional hyperlines that produce local amplitude cancelation near them. As such, they are a more expensive proposition. Furthermore, the kinetic energy of such flows is logarithmic in the size of the body [106]. This makes their contribution nonextensive. A corresponding experiment for a quantum gas might "settle down" to an axially symmetric $\rho(x)$ function while hiding advancing correlated oscillation waves at the surface. We don't have a direct way to probe the velocity field $v(x)$ corresponding to $\rho(x)$ so the extent to which a rigid body rotation is the final state can only be inferred from the elliptical cloud deformation and kinetic energy that gets transferred to thermal expansion. As of yet, I know of no such attempt to extract such information from available data or a tailored experiment of this sort.

If the process of cooling or exciting the cloud energies gives a narrow enough energy distribution of the eigenstates composing it, we can assign an unambiguous temperature to it. The extent to which this generates history independent results (or has the property of equilibration with other such clouds) is uncertain but reproducible results have been obtained for statics and simple dynamics of these clouds that are consistent with a simply hydrodynamic model in the one body density function $\rho(x)$. For this reason we assume it holds rather generally.

In the case of classical kinetics we know the shear viscosity is related to the mean free path as

$$\eta = \frac{1}{3}\, npl_{mfp}\,, \tag{7.1}$$

where n is the density, p is the rms momentum of the particles, and l_{mfp} = is the mean free path and σ is the cross section. There has been success at predicting the viscosity of liquid ^{4}He through the quasiparticle interaction theory of Landau and Khalatnikov [71]. This is interesting since quasiparticles sometimes transfer no mass at all (as with phonons in solids) and the $|k\rangle$ value corresponding to them may not indicate the actual mass flux (momentum) when they do since it corresponds to quasimomentum not true momentum. These calculations allow for some ambiguity in the overall scale factor of the momentum transfer but it seems that this model is giving some valid picture of a thermally driven mass flux transverse to shear flow. These notions have been extended to the case of Fermi gases [117]. Using the above relation for

quasiparticles we have the cross section saturate the unitary bound, $\sigma = 4\pi/k^2$, where k is the relative scattering momentum. This suggests we should get unusually small damping/viscosity at unitarity.

The Heisenberg uncertainty relation can be construed to imposes a bound on the product of the average momentum and the mean free path, $pl_{mfp} \geq \hbar$. Danielewicz and Gyulassy demonstrated that $\eta/n \geq \hbar$ [40]. Holographic dualities in string theory gave a precise bound on η/s instead of η/n. Policastro, Son and Starinets showed that in $\mathcal{N} = 4$ supersymmetric QCD the strong coupling limit of $\eta/s = \hbar/(4\pi k_B)$ [103]. This was shown to be a universal bound in the strong coupling limit. It was later conjectured that $\eta/s \geq \hbar/(4\pi k_B)$ is a general lower bound, valid for all fluids [96].

The origin of viscosity in classical liquids is typically different than gases. In gases, there is a thermally driven mass transfer across the flows that acts to locally average the flow momentum, converting the rest of the energy into heat. There is no consensus on a microscopic understanding of liquids. This is a reason that the results of Landau and Khalatnikov have been so influential. Additionally the "mode-coupling" theories and their success at predicting critical exponents [60] gives support to the idea that quasiparticle kinetics is sufficient. From another point of view, liquids are locally a lot like solids. Elastic shear modes of solids seem to dissolve into a collection of short lived quasiparticles. On small scales liquids are even probed using shear waves [122]. This suggests that the transverse forces are due to elastic strain from transient bonds between the particles. Some reconciliation of these two points of views is highly desirable. There are cases where quasiparticle momentum can give real forces [88] but true momentum transfer ultimately arises from either mass transfer or an elastically strained or compressed medium.

To find a fluid in nature that violates or approaches the proposed bound must be strongly interacting because a long mean free path would give larger viscosity and a weak elastic stress would give little force. Since $\eta \approx hs$ in such a case we would tend to refer to such a fluid as "quantum" in some sense. Many of the model field theories that attain the bound in the strong coupling limit are scale invariant so this suggests the unitary fermi gas is a good place to find a very low value of η/s.

To be specific about what we mean when we describe flow as "hydrodynamic" we expect $\rho(x)$ to evolve according to Navier-Stokes. In the case of little damping that means that a fluid that starts with irrotational motion will maintain it and the changes are driven by a local pressure function. This is distinct from the evolution of a single body wavefunction where anisotropic forces due to curvature gradients matter as in the Madelung formulation of quantum evolution. This nonhydrodynamic but still irrotational flow is what we expect to see in the noninteracting case. Nearly ideal hydrodynamic flow in the unitary Fermi gas was first observed in [93]. Numerous experiments have been done since to calculate the shear viscosity of the unitary gas [65, 74, 64, 5, 4, 138, 8, 109].

Geometrically, the effect of turning up contact-like potentials near unitarity is to create long range curvature that propagates away from the two-body diagonals over many atomic spacings. The effect of these $\frac{N(N-1)}{2}$ interactions seems to overwhelm the tendency of the function to evolve as an antisymmetrized product and attain a rigidity so that it evolves in a very restricted parameter space. Given that the value of $\rho(x')$ is actually an integral over as 3N-3 dimensional subspace it is a little disingenuous to call its evolution "local" yet we define 3D local functions $P(x)$, $v(x)$, $T(x)$ to seek a complete set of variables to describe this. We don't even know that at high energies when a wavefunction of a gas will correspond to the evolution of a classical gas so the extent to which such a simple model works at low energies is especially compelling.

The presence of irrotational motion and hydrodynamic features begs the question of how far the parallel with macroscopic fluids will persist. Vortex motion is observed in Bose gases. The energy and angular momentum of these vortices indicates that the observed density or something proportional to it is all taking part in the irrotational motion as in the case of superfluid Helium. A noninteracting gas allows any number of "single body" vortices in any configuration. Near the ground state, strong interactions seem to force us to have exactly N of the same vortex for each boson. Thermal energy causes these to become larger and more diffuse. However this is just as observed in the projected $\rho(x)$ images. We expect that the phase still wraps around these vortices in an integral fashion (with associated $\frac{1}{r}$ velocity field) and it might be better to think of them as losing the coherence between them. Below T_λ Helium behaves according to the two-fluid model. This is still just a phenomenological model and how much of this is relevant to strongly interacting fermi gases is unclear, however, such systems seem like an excellent place to probe transitional behavior in that direction.

Below we give an overview and comparison of the hydrodynamic approaches used in these experiments. In this chapter we will not discuss superfluid hydrodynamics (as implied by the two-fluid model) but will comment on dissipative effects in a presumed superfluid phase (specifically below the critical temperature) in Sect. 7.3.1.

7.2 Scaling Flows

We begin by studying the ideal (Eulerian) fluid dynamics of a non-relativistic gas. The equations of continuity and of momentum conservation are given by

$$\frac{\partial n}{\partial t} + \vec{\nabla} \cdot (n\vec{v}) = 0, \tag{7.2}$$

$$mn\frac{\partial \vec{v}}{\partial t} + mn\left(\vec{v} \cdot \vec{\nabla}\right)\vec{v} = -\vec{\nabla}P - n\vec{\nabla}V, \tag{7.3}$$

where n is the number density, m is the mass of the atoms, $\vec{v}$ is the fluid velocity, P is the pressure and V is the external potential.

In general we can write the pressure, or any thermodynamic function, in the form

$$P(X,Y) = P_0(X,Y)\ \varsigma(\alpha(X,Y),\beta(X,Y))\,, \tag{7.4}$$

where (X,Y) are thermodynamic variables, (α,β) are dimensionless functions of them and ς is a function that attains the value "1" at some values and P_0 is the value the pressure takes at this point and is expressible in terms of the variables. Not any such pair of functions are consistent with the monotonicity and stability constraints of equilibrium but they can come from a large class of functions.

In the unitary limit we have universal constants like $\hbar,\ k_B,\ m\ \ldots$ but don't have any extra dimensionful parameters, since $a_{sc}\to\infty$, so the result degenerates to a single parameter. Specifically we can write the equation of state of the form

$$P(n,T) = \frac{n^{5/3}}{m} f\left(\frac{mT}{n^{2/3}}\right)\,, \tag{7.5}$$

where $f(y)$ is a universal function ($k_B=\hbar=1$). We note that $y = const\cdot(T/T_F^{hom})$, where $T_F^{hom} = (3\pi^2 n)^{2/3}/(2m)$ is the Fermi temperature of a homogeneous Fermi gas. In the high temperature limit, $y\gg 1$, we have $f(y)\simeq y$ and in the low temperature limit $f(y)\simeq (3\pi^2)^{2/3}\xi/5$, where the parameter $\xi = 0.40(2)$ has been determined in quantum Monte Carlo calculations [61]. Monte Carlo methods have also been used to determine $f(y)$ for all values of y [22, 91]. The critical temperature for superfluidity is $T_c/T_F^{hom}\simeq 0.15$, corresponding to $y_c\simeq 0.72$. An alternative representation of the pressure is

$$P(\mu,T) = \mu^{5/2} m^{3/2} g\left(\frac{T}{\mu}\right)\,, \tag{7.6}$$

where $g(z)$ is a universal function, related to $f(y)$ by thermodynamic identities. In the high temperature limit $g(z)\simeq 2z^{5/2}e^{1/z}/(2\pi)^{3/2}$ and in the low temperature limit $g(z)\simeq 2^{5/2}/(15\pi^2\xi^{3/2})$. The density is

$$n(\mu,T) = \mu^{3/2} m^{3/2} h\left(\frac{T}{\mu}\right)\,,\qquad h(z) = \frac{5}{2}g(z) - z g'(z)\,. \tag{7.7}$$

The high and low temperature limits of the function $h(z)$ are $h(z)\simeq 2z^{3/2}e^{1/z}/(2\pi)^{3/2}$ ($z\gg 1$) and $h(z)\simeq 2^{3/2}/(3\pi^2\xi^{3/2})$ ($z\ll 1$). The equilibrium distribution n_0 of a trapped atomic gas follows from the hydrostatic equation $\vec{\nabla}P_0 = -n_0\vec{\nabla}V$. The trapping potential is approximately harmonic

$$V(x) = \frac{m}{2}\sum_i \omega_i^2 x_i^2. \tag{7.8}$$

Using the Gibbs-Duhem relation $dP = nd\mu + sdT$ together with the fact that the equilibrium configuration is isothermal we can write the equation of hydrostatic equilibrium as $\vec{\nabla}\mu = -\vec{\nabla}V$. This implies that the equilibrium density is $n_0(x) = n(\mu(x), T)$ with

$$\mu(x) = \mu_0 - V(x) = \mu_0 \left(1 - \sum_i \frac{x_i^2}{R_i^2}\right), \qquad R_i^2 = \frac{2\mu_0}{m\omega_i^2}\,. \tag{7.9}$$

A scaling flow is a solution of the hydrodynamic equations in which the shape of the density distribution is preserved. Consider the ansatz $n(x,t) = n(\mu(x,t), T(t))$ where

$$\mu(x,t) = \mu_0(t) \left(1 - \frac{x^2}{R_x(t)^2} - \frac{y^2}{R_y(t)^2} - \frac{z^2}{R_z(t)^2} - \frac{xy}{R_{xy}(t)}\right), \tag{7.10}$$

and $T(t)/T(0) = \mu_0(t)/\mu_0(0)$. Without loss of generality we have restricted the ansatz to rotations in the xy-plane. We note that the fluid remains isothermal during the expansion. Scale invariance implies that properties of the fluid only depend on the dimensionless ratio T/μ. For any given fluid element this ratio does not change during the expansion. In particular, if the fluid element was in the superfluid or normal phase initially, it will stay in that phase throughout the expansion.

The velocity field created by the scaling expansion in equ. (7.10) is linear in the coordinates. We can write

$$\vec{v}(x,t) = \frac{1}{2}\vec{\nabla}\left(\alpha_x(t)x^2 + \alpha_y(t)y^2 + \alpha_z(t)z^2 + 2\alpha(t)xy\right) + \Omega(t)\hat{z} \times \vec{x}. \tag{7.11}$$

The parameters α_i, α and Ω are related to the parameters R_i, R_{xy} and μ_0 by the continuity equation. Remarkably, the continuity equation is independent of the universal function $h(z)$ in equ. (7.7). Introducing the dimensionless scale parameters

$$\bar{\mu}(t) = \frac{\mu_0(t)}{\mu_0(0)}, \qquad b_i(t) = \frac{R_i(t)}{R_i(0)}, \qquad a(t) = \frac{R_x(0)^2}{R_{xy}(t)}\,, \tag{7.12}$$

the continuity equation can be written as

$$\begin{aligned}
\dot{\bar{\mu}} + \frac{2}{3}\bar{\mu}\,(\alpha_x + \alpha_y + \alpha_z) &= 0\,, && (7.13)\\
\dot{a} + \frac{2(\alpha-\Omega)}{b_x^2} + \frac{2(\alpha+\Omega)}{\lambda^2 b_y^2} + a(\alpha_x + \alpha_y) &= 0\,, && (7.14)\\
\dot{b}_x - b_x\alpha_x - \frac{b_x^3 a}{2}(\alpha+\Omega) &= 0\,, && (7.15)\\
\dot{b}_y - b_y\alpha_y - \frac{b_y^3\lambda^2 a}{2}(\alpha-\Omega) &= 0\,, && (7.16)\\
\dot{b}_z - b_z\alpha_z &= 0\,, && (7.17)
\end{aligned}$$

where $\lambda = R_y(0)/R_x(0) = \omega_x/\omega_y$. These equations can be solved directly in the case that there is no rotation, $a(t) = 0$. Then $\alpha = \Omega = 0$ and

$$(\alpha_x, \alpha_y, \alpha_z) = \left(\frac{\dot{b}_x}{b_x}, \frac{\dot{b}_y}{b_y}, \frac{\dot{b}_z}{b_z}\right), \quad \bar{\mu} = \frac{1}{(b_x b_y b_z)^{2/3}}\,. \tag{7.18}$$

The velocity field is a simple "Hubble flow", $\vec{v} = (\alpha_x x, \alpha_y y, \alpha_z z)$. Finally, we note that the entropy density is given by $s = (m\mu)^{3/2} g'(T/\mu)$. Since the entropy density has the same functional form as the particle density we conclude that, in the case of scaling flows, the continuity equation implies entropy conservation,

$$\frac{\partial s}{\partial t} + \vec{\nabla}\cdot(\vec{v}s) = 0\,. \tag{7.19}$$

7.3 Elliptic Flow

The simplest scaling flow is the expansion of the cloud after the trapping potential is removed [90]. Since the cloud remains isothermal the Euler equation can be derived using the Gibbs-Duhem relation $dP = nd\mu$. This implies that the equation of motion is independent of the universal function $f(y)$ defined in equ. (7.5). We get

$$\ddot{b}_i = \frac{\omega_i^2}{(b_x b_y b_z)^{2/3}}\frac{1}{b_i}\,, \tag{7.20}$$

The total energy of the expanding system is given by the sum of internal energy and kinetic energy,

$$E = E_{int} + E_{kin} = \int d^3x\,\left(\mathcal{E}(x) + \frac{1}{2}\,mn\vec{v}^2\right)\,. \tag{7.21}$$

For the Fermi gas at unitarity the energy density $\mathcal{E}$ is related to the pressure by $\mathcal{E} = \frac{3}{2}P$. We find

$$E = E_{int}(0)\left\{\frac{1}{(b_x b_y b_z)^{2/3}} + \frac{1}{3}\left(\frac{\dot{b}_x^2}{\omega_x^2} + \frac{\dot{b}_y^2}{\omega_y^2} + \frac{\dot{b}_z^2}{\omega_z^2}\right)\right\}, \tag{7.22}$$

where $E_{int}(0)$ is the internal energy at $t = 0$. Conservation of energy immediately follows from the equation of motion, equ. (7.20). We note that the equation of hydrostatic equilibrium, $\vec{\nabla}P = -n\vec{\nabla}V$, implies the Virial theorem $\langle\mathcal{E}\rangle = \langle V\rangle$ [126], where $\langle V\rangle$ denotes the integral of the potential energy over the trap. This means that the total energy of the trapped gas is $E_0 = 2E_{int}(0)$, where the factor 2 is due to the contribution of the potential energy.

We are interested in an axially symmetric trap with $\omega_y = \omega_z = \omega_\perp$ and $\omega_x = \lambda\omega_\perp$. In this case we end up with two coupled equations for $b_\perp$ and b_x. If $\lambda \gg 1$ the evolution in the transverse direction is much faster and the equation for $b_\perp$ can be approximately decoupled,

$$\ddot{b}_\perp = \frac{\omega_\perp^2}{b_\perp^{7/3}}\,. \tag{7.23}$$

This equation has to be integrated numerically. The behavior at early and late times can be found analytically. We get

$$b_\perp(t) \simeq \begin{cases} 1 + \frac{1}{2}\,\omega_\perp^2 t^2 + O(t^4) & \omega_\perp t \ll 1\,, \\ \frac{\omega_\perp t}{\sqrt{\gamma}} + c_0 + O(t^{-1/3}) & \omega_\perp t \gg 1\,, \end{cases}\,, \tag{7.24}$$

where $\gamma = 2/3$ and c_0 is a constant that can be determined by matching the early and late time behavior. Numerically, we find $c_0 \simeq -1.3$. For the longitudinal expansion the early time behavior is $b_x(t) \simeq 1 + (\lambda\omega_\perp t)^2/2$, and at late times $b_x(t) \simeq const \cdot \lambda^2\omega_\perp t$.

The signature effect of hydrodynamics is that transverse pressure gradients cause the transverse radius to expand much faster than the longitudinal radius. This means that the two radii will eventually cross. This happens at a time

$$t_{cross} = \frac{\sqrt{\gamma}}{\omega_x}\left(1 + O(\lambda)\right)\,. \tag{7.25}$$

We note that the crossing time only depends on the trap parameters, and is independent of the initial energy or the number of particles.

7.3.1 Energy dissipation

We wish to understand how the expansion is affected by dissipation. The energy momentum tensor of a dissipative fluid is $\Pi_{ij} = P\delta_{ij} + mnv_iv_j + \delta\Pi_{ij}$ with

$$\delta\Pi_{ij} = \eta\left(\nabla_i v_j + \nabla_j v_i - \frac{2}{3}\delta_{ij}\nabla\cdot v\right) + \zeta\delta_{ij}\left(\nabla\cdot v\right) . \tag{7.26}$$

The energy current is $j_i^\epsilon = v_i(w + \frac{1}{2}mnv^2) + \delta j_i^\epsilon$ with $w = \mathcal{E} + P$ and $\delta j_i^\epsilon = \delta\Pi_{ij}v_j - \kappa\nabla_i T$. The unitary gas is scale invariant and $\zeta = 0$ [120]. Also, for an isentropic scaling expansion the temperature remains independent of position, and there is no contribution from the thermal conductivity κ. We will therefore concentrate on the role of shear viscosity.

Since the shear viscosity is small, we can take it into account perturbatively. The simplest idea it compute the amount of kinetic energy that is converted to heat. We have

$$\dot{E} = -\frac{1}{2}\int d^3x\,\eta\left(\nabla_i v_j + \nabla_j v_i - \frac{2}{3}\delta_{ij}\nabla\cdot v\right)^2 . \tag{7.27}$$

For the scaling expansion given in equ. (7.11) the result is particularly simple. We get

$$4\dot{E} = -\frac{4}{3}\left(\frac{\dot{b}_\perp}{b_\perp} - \frac{\dot{b}_x}{b_x}\right)^2\int d^3x\,\eta(x). \tag{7.28}$$

The total energy dissipated is given by the integral of equ. (7.28) over time. We first show that the spatial integral over $\eta(x)$ does not depend on time. In the local density approximation $\eta(x) = \eta(\mu(x), T)$. Scale invariance implies that

$$\eta(\mu, T) = n(\mu, T)\alpha_n\left(\frac{T}{\mu}\right) , \tag{7.29}$$

where $\alpha_n(z)$ is a universal function, and we have set $\hbar = 1$. In order to compare with the string theory bound it is also useful to define $\eta(\mu, T) = s(\mu, T)\alpha_s(T/\mu)$, where we have also set $k_B = 1$. We can write

$$\int d^3x\,\eta(x) = N\langle\alpha_n\rangle\,, \tag{7.30}$$

where

$$\langle\alpha_n\rangle = \frac{1}{N}\int d^3x\,n(x,t)\,\alpha_n\left(\frac{T(t)}{\mu(x,t)}\right) = \frac{1}{N}\int d^3x\,n_0(x)\,\alpha_n\left(\frac{T_0}{\mu(x,0)}\right) \tag{7.31}$$

is an average of α_n over the initial density distribution. Analogously, we can write the integral over $\eta(x)$ as $S\langle\alpha_s\rangle$, where S is the total entropy and $\langle\alpha_s\rangle$ is an average of α_s over the initial entropy density.

The time integral over $(\dot{b}_\perp/b_\perp - \dot{b}_x/b_x)^2$ is dominated by the regime $\omega_\perp t \sim 1$ and converges rapidly – the integral reaches 80% of its asymptotic value at $t_{diss} \simeq 5.9\,\omega_\perp^{-1}$. In the limit $\lambda \ll 1$ we can neglect the contribution from $\dot{b}_x$. On dimensional grounds the integral over $(\dot{b}_\perp/b_\perp)^2$ must be proportional to $\omega_\perp$. The constant of proportionality can be determined numerically. We find

$$\int_0^\infty dt \left(\frac{\dot{b}_\perp}{b_\perp}\right)^2 = 0.87\,\omega_\perp\,. \tag{7.32}$$

We can now compute the ratio $\Delta E/E_{int}$ of the dissipated energy to the initial internal energy of the system. In order to express the result in terms of experimentally measured quantities it is useful to introduce the energy $E_F = N\epsilon_F$ where $\epsilon_F = \bar{\omega}(3N)^{1/3}$ is the Fermi energy of the trapped gas and $\bar{\omega} = (\omega_x\omega_y\omega_z)^{1/3}$. We find

$$\frac{\Delta E}{E_{int}(0)} = -\frac{8}{3}\cdot 0.87\cdot\beta = -2.32\cdot\beta \tag{7.33}$$

where the parameter β is defined given by

$$\beta = \frac{\langle\alpha_n\rangle}{(3N\lambda)^{1/3}}\frac{1}{(E_0/E_F)} = \frac{\langle\alpha_s\rangle}{(3N\lambda)^{1/3}}\frac{(S/N)}{(E_0/E_F)}\,. \tag{7.34}$$

Dissipation slows down the transverse expansion of the system. For $(\omega_\perp t) \gg 1$ we have $(\delta\dot{b}_\perp/\dot{b}_\perp) = (\Delta E/E)/2$ and, up to terms that are higher order in λ, the change in the crossing time is directly related to the change in the expansion rate, $(\delta t/t)_{cross} = (\delta\dot{b}_\perp/\dot{b}_\perp)$.

The thermodynamic quantities S/N and E_0/E_F as a function of T/T_F were determined experimentally in [78]. Just above the critical temperature $S/N \simeq 2.2$ and $E_0/E_F \simeq 0.83$. The double ratio $[(S/N)/(E_0/E_F)]$ is only weakly dependent on T, changing by less than 15% between T_c and $4T_c$. In the flow experiment carried out by O'Hara et al. [93] the cloud contained $N = 2\cdot 10^5$ atoms and the asymmetry parameter was $\lambda = 0.045$. The predicted sensitivity of the crossing time to dissipative effects is

$$\left(\frac{\delta t}{t}\right)_{cross} = 0.008\left(\frac{\langle\alpha_s\rangle}{1/(4\pi)}\right)\left(\frac{2\cdot 10^5}{N}\right)^{1/3}\left(\frac{0.045}{\lambda}\right)^{1/3}\left(\frac{S/N}{2.2}\right)\left(\frac{0.83}{E_0/E_F}\right)\,. \tag{7.35}$$

For $\langle\alpha_s\rangle = 1/(4\pi)$ this is at the limit of what can be resolved experimentally, but for $\langle\alpha_s\rangle = 0.5$ the effect reaches about 5%. An example is shown in Fig. 7.1. The solid lines show the solution of the Euler equation (7.20), and the dashed lines show a solution of the Navier-Stokes equation (see Sect. 7.3.2) with $\langle\alpha_s\rangle = 0.5$. The main effect of shear viscosity is a suppression of the transverse expansion of the system. We find $(\delta t/t)_{cross} = 6.5\%$, in fairly good agreement with the estimate $(\delta t/t)_{cross} = 5\%$ from equ. (7.35).

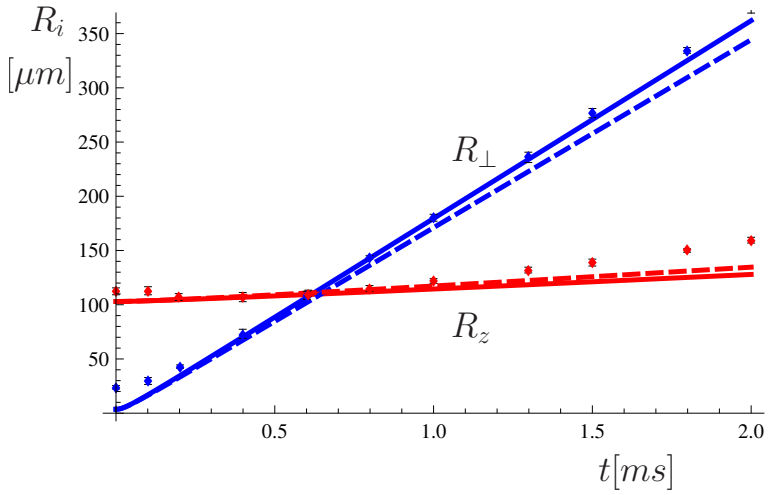

Figure 7.1: Expansion of the transverse and longitudinal radii after release from a harmonic trap. The data points are taken from [93]. The solid and dashed lines correspond to solutions of the Navier-Stokes equation with $\langle \alpha_s \rangle = 0$ (solid lines) and $\langle \alpha_s \rangle = 0.5$ (dashed lines).

The best fit to the data is provided by ideal hydrodynamics with $\langle \alpha_s \rangle = 0$. This is probably related to the fact that the data were taken significantly below T_c, at $T/T_F = 0.13 \pm 0.05$. In this regime the system is described by two-fluid hydrodynamics. The superfluid component has no shear viscosity but the viscosity of the normal component becomes very large as $T/T_F \to 0$ [113]. In a finite system, however, the large viscosity of the normal phase is likely to be suppressed by relaxation time effects, see Sect. 7.3.5. As a consequence one observes perfect superfluid hydrodynamics. The data in Fig. 7.1 show some deviations from hydrodynamics at very early and very late times. Discrepancies at early times are probably related to experimental resolution [93], while the differences at late times may be connected to the breakdown of hydrodynamics in the late stages of the expansion.

We can also compute the amount of entropy generated by dissipative effects. Using $dS = dQ/T$ we find

$$\frac{\Delta S}{N} = \frac{4}{3} \frac{\langle \alpha_n \rangle}{(3N\lambda)^{1/3}} \frac{1}{(T_0/T_F)} I_S \tag{7.36}$$

with

$$I_S = \omega_\perp^{-1} \int_0^\tau dt\, b_\perp^{-2/3} \left(\dot{b}_\perp \right)^2 . \tag{7.37}$$

For $\tau \simeq t_{diss}$ we find $I_s \simeq 2.6$ and the produced entropy is small, $(\Delta S/N) \simeq 0.27$ for the conditions given above. However, the integral diverges as $I_s \sim (\omega_\perp \tau)^{1/3}$ for $\tau \to \infty$. This result is not reliable since we expect hydrodynamics to break down at late times, see Sect. 7.3.4.

7.3.2 Moments of the Navier-Stokes equation

It is clearly desirable to study the role of dissipation more directly by solving the Navier-Stokes equation. The Navier-Stokes equation differs from the Euler equation by an extra term on the right hand side,

$$mn\left(\frac{\partial v_i}{\partial t}+\left(\vec{v}\cdot\vec{\nabla}\right)v_i\right)=-\nabla_i P-\nabla_j\,\delta\Pi_{ij}. \tag{7.38}$$

We will assume that the viscosity is small, so that derivatives with respect to thermodynamic variables can be computed at constant entropy. We will also assume that the entropy conservation equation, equ. (7.19), is not modified. Physically, this implies that we assume that there is a reservoir that removes the heat generated by dissipative effects. In this case, the only correction to the equations of hydrodynamics is the viscous force in the Navier-Stokes equation.

In general the inclusion of the Navier-Stokes term will break the simple scaling form of the flow. The Navier-Stokes equation also depends on the functional form of the pressure and the viscosity, that means we have to specify the functions $f(y)$ in equ. (7.5) and $\alpha_n(z)$ in equ. (7.29). A simple approach that avoids extensive numerical work as well as model assumptions about $f(y)$ and $\alpha_n(z)$ is to take moments of the Navier-Stokes equation. Consider the linear moments

$$m\int d^3x\,x_k n(x)\left(\frac{\partial v_i}{\partial t}+\left(\vec{v}\cdot\vec{\nabla}\right)v_i\right)=-\int d^3x\,x_k\Big(\nabla_i P+\nabla_j\,\delta\Pi_{ij}\Big)\,, \tag{7.39}$$

with $k=1,2,3$. Since the velocity field is linear in the coordinates we find that the ideal fluid terms involve second moments of the density. These moments are related to the potential energy in a harmonic trap and, by the virial theorem, to the total energy of the system. The Navier-Stokes term can be integrated by parts and is proportional to the integral over $\eta(x)$. As a consequence, the first moment of the Navier-Stokes equation depends only on the parameter β defined in equ. (7.34). We get

$$\ddot{b}_\perp = \frac{\omega_\perp^2}{(b_\perp^2 b_x)^{2/3}b_\perp}-\frac{2\beta\omega_\perp}{b_\perp}\left(\frac{\dot{b}_\perp}{b_\perp}-\frac{\dot{b}_x}{b_x}\right) \tag{7.40}$$

$$\ddot{b}_x = \frac{\omega_x^2}{(b_\perp^2 b_x)^{2/3}b_x}+\frac{4\beta\lambda\omega_x}{b_x}\left(\frac{\dot{b}_\perp}{b_\perp}-\frac{\dot{b}_x}{b_x}\right). \tag{7.41}$$

These equations of motion are consistent with the result in the previous section. We can compute the amount of energy dissipated from equ. (7.22) and (7.40,7.41). We find

$$\dot{E}=-\frac{8}{3}\beta E_{int}(0)\left(\frac{\dot{b}_\perp}{b_\perp}-\frac{\dot{b}_x}{b_x}\right)^2. \tag{7.42}$$

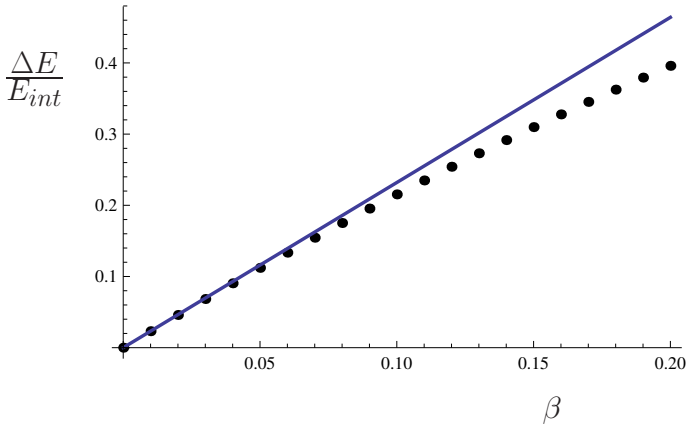

Figure 7.2: This figure show the ratio $(\Delta E)/E_{int}$ of the dissipated energy to the initial internal energy as a function of the parameter β defined in equ. (7.34). The dots show the result of a numerical solution of the Navier-Stokes equation (7.40, 7.41) in the limit $\omega_z/\omega_\perp \to 0$, and the line shows the estimate given in equ. (7.33).

We note that $b_\perp(t)$ and $b_z(t)$ are solutions of the Navier-Stokes equation and have an implicit dependence on β. As long as this dependence is smooth, $b_i(t,\beta) \to b_i(t,0)$ as $\beta \to 0$, equ. (7.42) reduces to equ. (7.28) at leading order in β. Since typical values of β are quite small, we expect the estimates in the previous section to be very accurate. This is studied in more detail in Fig. 7.2. We observe that the dissipated energy $(\Delta E)/E$ is very linear in β even for values of $(\Delta E)/E$ as large as 25%. We note that because of turbulence solutions of the Navier-Stokes equation do not in general approach solutions of the Euler equation in the limit that the shear viscosity goes to zero. Turbulence is not present in our analysis because we do not consider small fluctuations. We also note that there is no continuous forcing in the case of an expanding gas and it is not clear whether turbulence can develop even if fluctuations are included. We will estimate the Reynolds number of the flow in Sect. 7.3.4.

7.3.3 Scaling solution of the Navier-Stokes equation

In this section we discuss a specific model for the density dependence of the shear viscosity that preserves the scaling nature of the flow even if the viscosity is not zero. This model allows to compute the local amount of heat that is generated by dissipation, and to understand some of the shortcomings of the method discussed in Sections 7.3.1 and 7.3.2. Consider

$$\eta(n,T) = \eta_0 (mT)^{3/2} + \eta_1 \frac{P(n,T)}{T}, \tag{7.43}$$

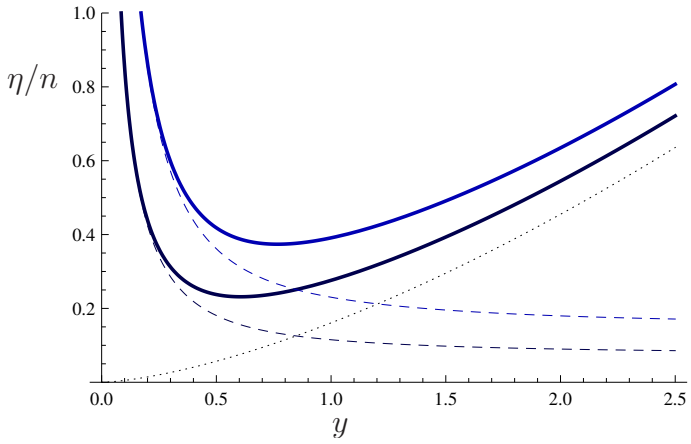

Figure 7.3: Ratio η/n as a function of $y = (mT)/n^{2/3}$ for the model defined in equ. (7.43). The two curves correspond to (from bottom to top) $\eta_1 = 1/(4\pi), 2/(4\pi)$ with $\eta_0 = 15/(32\sqrt{\pi})$. The dashed line shows the contribution from η_1, which is the term that contributes directly to the Navier-Stokes equation, and the dotted line is the contribution from η_0. Note that the critical point for the onset of superfluidity is $y_c \simeq 0.72$.

where $\eta_{0,1}$ are constants and $P(n,T)$ is the pressure. The first term dominates in the low density, high temperature limit. This is the regime in which a kinetic description in terms of weakly coupled atoms is applicable. Kinetic theory gives [51, 53]

$$\eta_0 = \frac{15}{32\sqrt{\pi}}\,. \tag{7.44}$$

The second term dominates in the high density, low temperature regime. The functional form of this term is not motivated by kinetic theory. We note, however, that η/n has a minimum as a function of T, as expected on theoretical [113] and phenomenological grounds [117].

The model given in equ. (7.43) has two remarkable features: First, the η_0 term does not contribute to the Navier-Stokes equation at all. The Navier-Stokes term $\nabla_j[\eta_0(mT)^{3/2}(\nabla_i v_j + \ldots)]$ vanishes since both T and $\nabla_i v_j$ are constant. Second, the η_1 term preserves the scaling flow. Using $T, \nabla_i v_j \sim const$ we see that $\nabla_j[\eta_1 P(n,T)/T\,(\nabla_i v_j + \ldots)]$ scales like the contribution from the pressure of an ideal fluid, $\nabla_i P(n,T)$. We get

$$\ddot{b}_\perp = \frac{\omega_\perp^2}{(b_\perp^2 b_x)^{2/3} b_\perp} - \frac{2\eta_1\omega_\perp^2}{3T_0 b_\perp}\left(\frac{\dot{b}_\perp}{b_\perp} - \frac{\dot{b}_x}{b_x}\right) \tag{7.45}$$

$$\ddot{b}_x = \frac{\omega_x^2}{(b_\perp^2 b_x)^{2/3} b_x} + \frac{4\eta_1\omega_x^2}{3T_0 b_x}\left(\frac{\dot{b}_\perp}{b_\perp} - \frac{\dot{b}_x}{b_x}\right). \tag{7.46}$$

We observe that these equations are identical to the moment equations (7.40,7.41) with $\beta = \eta_1\omega_\perp/(3T_0)$. This is not a surprise – the η_1 contribution to $\eta(n,T)$ vanishes as $n \to 0$ and the assumptions underlying the moment method are satisfied. The η_0 term, on the other hand, does not vanish as $n \to 0$, and it cannot be included in the moment equations (it makes an infinite contribution to the integral over $\eta(x)$).

Using the identification $\beta = \eta_1\omega_\perp/(3T_0)$ we can write

$$\beta = \frac{\eta_1}{3(3\lambda N)^{1/3}} \frac{1}{(T_0/T_F)}\,, \tag{7.47}$$

which shows that any bound on $\langle\alpha_n\rangle$ obtained using the methods of Sect. 7.3.2 can be translated into an estimate of η_1, $\eta_1 = 3(T_0/E_0)\langle\alpha_n\rangle$. Near T_c this implies that $\eta_1 \simeq 0.76\langle\alpha_n\rangle$. We note that the relation between η_1 and $\langle\alpha_n\rangle$ is precisely what one obtains if the trap average of $\eta(x)$ is computed from the η_1-term only. The situation is more complicated if the contribution from η_0 is taken into account. The ratio η/n is given by

$$\frac{\eta(n,T)}{n} = \eta_0 y^{3/2} + \frac{\eta_1}{y} f(y) \tag{7.48}$$

with $y = (mT)/n^{2/3}$. Since $f(0) = const$ and $f(y) \simeq y$ for $y \gg 1$ this function has a minimum, see Fig. 7.3. The figure also shows that $(\eta/n)_{min}$ receives significant contributions from η_0. It is clearly unsatisfactory that our analysis has no sensitivity to this term. We will return to this issue in Sect. 7.3.5.

Using the explicit form of $\eta(n,T)$ we can also address the question where the energy is being dissipated and how much reheating is taking place. We first consider the contribution from η_1. The energy dissipated is

$$\dot{\mathcal{E}} = -\frac{4\eta_1}{3}\left(\frac{\dot{b}_\perp}{b_\perp}\right)^2 \frac{P(n,T)}{T}\,. \tag{7.49}$$

For a Fermi gas at unitarity the energy density is related to the pressure by $\mathcal{E}(n,T) = (3/2)P(n,T)$. Equ. (7.49) implies that the energy dissipated is proportional to the local internal energy density. The source of the dissipated energy is the reduction in the kinetic energy density relative to its value in ideal hydrodynamics. The local kinetic energy density is

$$\mathcal{E}_{kin} = \frac{m}{2} n \left(\frac{\dot{b}_\perp}{b_\perp}\right)^2 x_\perp^2\,. \tag{7.50}$$

Since the kinetic energy density differs from the spatial distribution of the dissipated energy there has to be a dissipative contribution to the energy current. This current is given by $\delta\vec{j}^{\,\epsilon} =$

$(0, \delta j_y^\epsilon, \delta j_z^\epsilon)$ with

$$\delta j_z^\epsilon = v_z \delta \Pi_{zz} = -z \frac{2\eta_1 P(n,T)}{3T} \left(\frac{\dot{b}_\perp}{b_\perp} \right)^2 , \tag{7.51}$$

and $\delta j_y^\epsilon = \delta j_z^\epsilon (z \leftrightarrow y)$. The dissipative current flows from the outer edge of the cloud, where the kinetic energy is peaked, to the center of the cloud, where the pressure is largest.

Energy dissipation leads to reheating. The change in temperature is $\Delta T = (\Delta \mathcal{E})/c_V$. The time evolution of the temperature is governed by

$$\dot{T} = -\frac{4T_0}{3\, b_\perp^{4/3}} \left(\frac{\dot{b}_\perp}{b_\perp} \right) + \frac{\eta_1 P}{c_V T} \left(\frac{\dot{b}_\perp}{b_\perp} \right)^2 , \tag{7.52}$$

where the first term is related to the adiabatic expansion of the system, and the second term is the dissipative correction. Note that if $c_V \sim \mathcal{E}/T$, which is the case in the high temperature limit, then reheating will preserve the fact that the cloud is isothermal. In general the behavior of the specific heat is more complicated and dissipation produces a temperature gradient. The relative importance of reheating is governed by the parameter $(\eta_1 \omega_\perp / T_0)(P/(c_V T))$. In the high temperature limit we can use $P \sim c_V T$ and this expression reduces to the parameter β defined in equ. (7.47). Reheating becomes important at a time $\omega_\perp t \sim \beta^{-3}$. Since β is typically very small, this occurs very late during the evolution of the system.

A similar analysis of the effects of η_0 leads to a number of puzzles. The energy dissipated is independent of density, and the total energy dissipated over all space is infinite. There is no change in the kinetic energy, and the source of the dissipated energy is the viscous correction to the energy current. This current flows into the system from spatial infinity. The relative importance of reheating is governed by the parameter $(\eta_0 \omega_\perp / T_0)((mT)^{3/2}/n)$, which is always large in the dilute region of the cloud.

7.3.4 Breakdown of hydrodynamics

The constant term $\eta \sim \eta_0 (mT)^{3/2}$ in the shear viscosity dominates in the dilute outer regions of the cloud, and the difficulty in understanding the effects of this term must be related to the breakdown of hydrodynamics in the dilute regime. A standard criterion for the applicability of hydrodynamics is the condition that the Knudsen number $Kn = l_{mfp}/L$, the ratio of the mean free path to the system size, is much less than one. In the dilute regime the mean free path is given by

$$l_{mfp} = \frac{1}{n\sigma} = \frac{3}{4\pi} \frac{mT}{n} . \tag{7.53}$$

The density is given by equ. (7.7). In the dilute regime we can use the high temperature limit of $h(z)$, but the scaling arguments in the following are independent of the functional form of

$h(z)$. For a comoving observer the density scales as $n \sim (m\mu)^{3/2}$, and the mean free path scales as $l_{mfp} \sim T/(m^{1/2}\mu^{3/2})$. The evolution of T and μ is governed by the scaling relations discussed in Sect. 7.2. We may use, in particular, that $T/\mu \sim const$ and $\mu \sim \mu(0)/(b_\perp^2 b_x)^{2/3}$. We conclude that in a comoving fluid cell

$$Kn = \frac{l_{mfp}}{L} \sim \left(\frac{b_x}{b_\perp}\right)^{1/3} . \tag{7.54}$$

During the two-dimensional expansion the Knudsen number is dropping, which implies that the hydrodynamic description is becoming more accurate. In the late, three-dimensional stage, the Knudsen number is constant.

A more accurate criterion can be obtained by using a characteristic length or time scale derived from the flow profile. Hydrodynamics is based on a derivative expansion of the energy momentum tensor, and the validity of hydrodynamics requires that $\delta\Pi_{ij}$ is small compared to the ideal fluid stress tensor. Consider the ratio of the moments of the ideal and dissipative terms on the RHS of the Navier-Stokes equation

$$\frac{\langle x_k \nabla_k P\rangle}{\langle x_k \nabla_j \delta\Pi_{kj}\rangle} = \frac{\langle P\rangle}{\left\langle \frac{4}{3}\eta(\nabla_k v_k)\right\rangle} \tag{7.55}$$

where $\langle . \rangle$ denotes an integral over d^3x and the index k is fixed. The ratio $(\eta/P)(\nabla \cdot v)$ has a simple interpretation in kinetic theory. For a dilute gas $\eta \sim npl_{mfp} \sim \rho u^2 \tau_{mft}$ and $P \sim \rho u^2$, where n is the particle density, ρ is the mass density, p is the average quasi-particle momentum, u the average velocity, and τ_{mft} the mean free time. The ratio $\nabla \cdot v \sim \tau_{exp}^{-1}$ defines a characteristic expansion time. The quantity

$$\frac{\eta}{P}(\nabla \cdot v) \sim \frac{\tau_{mft}}{\tau_{exp}} \tag{7.56}$$

measures the ratio of the mean free time over the expansion time. Hydrodynamics is valid if $\tau_{mft} \ll \tau_{exp}$. We observe that for $\eta \sim P$ the freezeout criterion is independent of position and only a function of time. We get

$$\frac{\eta}{P}(\nabla_z v_z) = \frac{\eta_1}{T_0}\,(b_x b_\perp)^{1/3}\,\dot{b}_\perp \simeq \frac{\eta_1}{(3N)^{1/3}\lambda^{1/3}}\,\frac{1}{(T_0/T_F)}\,(\omega_\perp t)^{1/3} , \tag{7.57}$$

where we have assumed that the expansion is two-dimensional. We note that the relevant parameter is the quantity β defined in equ. (7.47). Freezeout occurs at $(\omega_\perp t_{fr}) \sim \beta^{-3}$. For typical values of β we find that $t_{fr} \gg t_{cross} \gg t_{diss}$, where $t_{cross} \sim (\omega_\perp \lambda)^{-1}$ is the crossing time, and $t_{diss} \sim 5.9\,\omega_\perp^{-1}$ is the characteristic time for dissipative effects.

The freezeout time defined by equ. (7.57) is very long, and the physical freezeout is determined by the viscous effects in the dilute part of the cloud. In the case of a spatially constant

shear viscosity we find

$$\frac{\eta}{P}(\nabla_z v_z) = \frac{\eta_0 (mT)^{3/2}}{P}\left(\frac{\dot{b}_\perp}{b_\perp}\right) \simeq \frac{45\pi}{8\sqrt{2}}\frac{(T_0/T_F)^2}{(3\lambda N)^{1/3}}\, b_\perp^{1/3}\dot{b}_\perp \exp\left(\sum_i \frac{x_i^2}{b_i^2 \bar{R}_i^2}\right), \tag{7.58}$$

where we have used $P = nT$ as well as the low density (high temperature) limit of $n_0(x)$, see equ. (7.7). The radius parameter $\bar{R}_i$ is defined as $\bar{R}_i^2 = 2T_0/(m\omega_i^2)$. The condition $(\eta/P)(\nabla_z v_z)$ determines a freezeout surface $x_{fr}(t)$. This surface is initially at $x_i \gg R_i$, but it moves inward as time increases and reaches the origin at a time $t_{fr} \sim \omega_\perp^{-1}(3\lambda N)(T_F/T_0)^6$. This time is also parametrically very long, but the freezeout time at a characteristic distance $x_i \simeq b_i \bar{R}_i$ is significantly smaller.

Finally, we wish to mention one more quantity that characterizes a viscous flow. The Reynolds number *Re* is defined as the ratio of inertial and viscous forces in the system. In the case of a scaling flow with $\eta \sim P$ this ratio is independent of position and only a function of time. We find

$$Re = \frac{T_0}{\eta_1 \omega_\perp^2}\, b_\perp \dot{b}_\perp \simeq \frac{\omega_\perp t}{\beta}\,. \tag{7.59}$$

The Reynolds number is zero initially, but it grows quickly, reaching $Re \simeq \beta^{-1}$ at $(\omega_\perp t) = 1$. For typical experimental parameters $\beta^{-1} \sim 100$, which is large but not large enough to cause instabilities. At later times even larger values of *Re* are reached, but at these late times the system is simply free streaming. A constant contribution to the viscosity does not lead to a viscous force, and does not directly contribute to the Reynolds number.

7.3.5 Relaxation time approach

The discussion in the previous section does not fully resolve the problems caused by the dilute regions of the cloud. If the shear viscosity is proportional to the pressure then the system freezes out at some time t_{fr}. For values of η/P implied by the data this time is much larger than the characteristic time for dissipative effects in the evolution of the system, and the estimates in Sect. 7.3.1-7.3.3 are internally consistent. If the shear viscosity is constant then there is a freezeout surface which moves inward as a function of time. This implies that the integral in equ. (7.28) and (7.39) should be restricted to the region enclosed by the freezeout surface. However, in order for energy to be conserved, and for viscosity to have an effect on the evolution of the system, we would have to include an external force on the freezeout surface.

An approach that can describe the effects of freezeout without the need to introduce an artificial surface is second order viscous hydrodynamic [79]. The second order formalism takes into account terms with two derivatives of the thermodynamic variables in the dissipative correction to the stress tensor and energy current. In general, the second order formalism

contains a large number of new transport coefficients. A phenomenological ansatz that has proven to be useful in many different applications is to treat the viscous part of the stress tensor as an independent hydrodynamical variable which satisfies a relaxation equation

$$\tau_R \frac{\partial}{\partial t} \delta\Pi_{ij} = -\delta\Pi_{ij} + \delta\Pi_{ij}^{NS} \,, \tag{7.60}$$

where τ_R is the relaxation time and $\delta\Pi_{ij}^{NS}$ is the Navier-Stokes expression for the viscous contribution to the stress tensor, equ. (7.26). An equation of this type was first introduced by Maxwell and Cattaneo in the context of heat transport. More recently, time or frequency dependent viscosities were considered in the study of Bose condensed gases in [92, 56]. In relativistic hydrodynamics relaxation equations for the viscous stress tensor are used in order to restore causality, see the review [111].

Scale invariance implies that $\tau_R(n,T) = w(mT/n^{2/3})/T$ where $w(y)$ is a universal function. In the dilute limit $y \gg 1$ the function $w(y)$ can be calculated in kinetic theory which gives $\tau_R = \eta/(nT)$ [52]. This result corresponds to the estimate for τ_{mft} given in equ. (7.56). The relaxation equation (7.60) requires an initial condition for the viscous stress $\delta\Pi_{ij}$. If is natural to assume that $\delta\Pi_{ij} = 0$ at $t = 0$. In the center of the cloud τ_R is small and the viscous stress quickly relaxes to the Navier-Stokes result. In the dilute region $\tau_R \to \infty$ and the viscous contribution to the stress tensor remains zero. This implies that even a spatially constant shear viscosity leads to a spatially varying $\delta\Pi_{ij}$ and a non-zero drag force. This drag force is largest near the freezeout surface and breaks the scaling nature of the flow. This means that a detailed study of the Israel-Stewart equations will require numerical solutions of the hydrodynamic equations. We can estimate the effect of the relaxation time by computing the energy dissipation. We have

$$\dot{E} = -\frac{1}{2} \int d^3x \, \delta\Pi_{ij} \left(\nabla_i v_j + \nabla_j v_i - \frac{2}{3} \delta_{ij} \nabla \cdot v \right) , \tag{7.61}$$

where $\delta\Pi_{ij}$ is determined by equ. (7.60). The simplest approximation is to set $\delta\Pi_{ij} = \delta\Pi_{ij}^{NS}$ inside the freezeout surface and $\delta\Pi_{ij} = 0$ outside.

In order to obtain more accurate estimates we have to solve the differential equation (7.60). As in Sect. 7.3.1 we may compute $\delta\Pi_{ij}^{NS}$ from the solution of ideal hydrodynamics. The relaxation time can be calculated using the high temperature result for the density profile. We find

$$\omega_\perp \tau_R = \frac{45\pi}{8\sqrt{2}} \frac{1}{(3\lambda N)^{1/3}} \left(\frac{T}{T_F} \right)^2 b_\perp^{4/3} \exp\left(\frac{x_\perp^2}{b_\perp^2 \bar{R}_\perp^2} + \frac{x_z^2}{\bar{R}_z^2} \right) , \tag{7.62}$$

which has the same functional form as the freezeout criterion in equ. (7.58). The viscous stress tensor $\delta\Pi_{ij}$ is determined by integrating equ. (7.60) and the dissipated energy can be computed from equ. (7.61). By comparing ΔE with equ. (7.28) we can express the result in terms of an

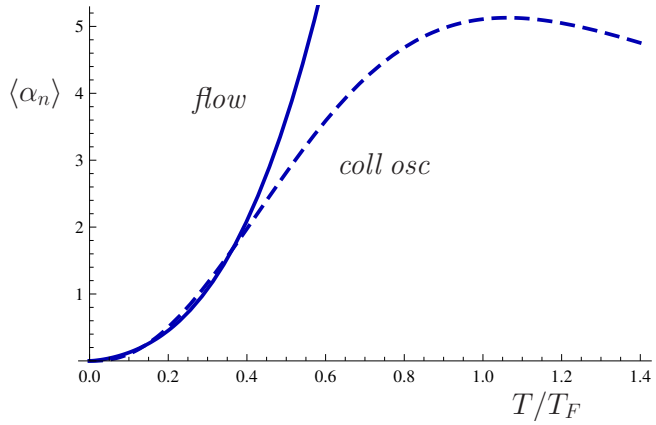

Figure 7.4: Trap average $\langle\alpha_n\rangle = \langle\eta\rangle/N$ computed from a relaxation time equation with $\eta = \eta_0(mT)^{3/2}$ and $\tau_R = \eta/(nT)$. Contrary to the pure Navier-Stokes case $\tau_R \to 0$ the ratio $\langle\eta\rangle/N$ depends on the number of particles and the trap geometry. Here we have chosen $N = 2\cdot 10^5$ and $\lambda = 0.045$. The solid shows the result for the elliptic flow field, and the dashed line corresponds to the transverse collective mode, see Sect. 7.5.

effective $\langle\alpha_n\rangle$. This quantity is shown in Fig. 7.4. We observe that $\langle\alpha_n\rangle$ grows with temperature as $\langle\alpha_n\rangle \sim T^3$, much faster than one would expect from the relation $\eta \sim T^{3/2}$.

There are no data for elliptic flow at temperatures above T_c, but we will compare the relaxation time result to collective mode data in Sect. 7.5. We note that at low temperature the effective $\langle\alpha_n\rangle$ is the same for expanding and oscillating systems, but that at high temperature the two systems behave differently. In the expanding system the hydrodynamic expansion time τ_{exp} continues to increase during the expansion, whereas the period of the oscillation provides a fixed hydrodynamic time scale in the case of the collective mode. The viscous relaxation time τ_R increases with temperature. This implies that for the collective mode we eventually get $\tau_R > \tau_{exp}$ and the effective $\langle\alpha_n\rangle$ starts to decrease. In the expanding system, on the other hand, the relaxation time can always match the expansion time and $\langle\alpha_n\rangle$ continues to grow with temperature.

7.4 Expansion from a rotating trap

The expansion from a rotating trap was studied in [8]. Rotating gases are of interest for a number of reasons. The quenching of the moment of inertia in a superfluid Bose gas was used as a signature of superfluidity [44]. The remarkable discovery in [8] is that in a Fermi gas at unitarity the suppression of the moment of inertia is also observed in the normal phase. It is clearly of interest to determine to what extent this discovery places constraints on the shear

viscosity [125].

7.4.1 Ideal fluid dynamics

The Euler equations for a Bose gas with $P \sim n$ were derived in [44]. The result is easily generalized to a Fermi gas at unitarity [8]. As in the case of a non-rotating trap the equations are independent of the temperature and the universal function $f(y)$ in equ. (7.5). We have

$$\dot{\alpha}_x + \alpha_x^2 + \alpha^2 - \Omega^2 = \frac{\bar{\mu}\omega_x^2}{b_x^2} \tag{7.63}$$

$$\dot{\alpha}_y + \alpha_y^2 + \alpha^2 - \Omega^2 = \frac{\bar{\mu}\omega_y^2}{b_y^2} \tag{7.64}$$

$$\dot{\alpha}_z + \alpha_z^2 = \frac{\bar{\mu}\omega_z^2}{b_z^2} \tag{7.65}$$

$$\dot{\alpha} + \alpha\left(\alpha_x + \alpha_y\right) = \frac{\bar{\mu}a\omega_x^2}{2} \tag{7.66}$$

$$\dot{\Omega} + \Omega\left(\alpha_x + \alpha_y\right) = 0\,. \tag{7.67}$$

These equations have to be solved together with the continuity equations (7.13-7.17). In all there are ten coupled equations. In the case of a rotating trap there is no initial expansion, $\alpha_i(0) = 0$, but either $\alpha(0)$ or $\Omega(0)$ (or both) are non-zero. If the initial flow is purely irrotational then $\alpha(0) = \omega_{rot}$, where ω_{rot} is the angular velocity of the trap. If the flow corresponds to rigid rotation then $\Omega(0) = \omega_{rot}$. Below the critical temperature the flow of the superfluid component must be irrotational, but above T_c both rotational and irrotational flows are possible.

The equations simplify in the experimentally relevant case of strongly deformed, slowly rotating traps, $\omega_{rot} < \omega_x \ll \omega_\perp$ with $\omega_\perp = \omega_y \simeq \omega_z$. In this limit the motion of the fluid is dominated by the transverse expansion of the system. Up to corrections of order $O(\lambda^2)$ or $O((\omega_{rot}/\omega_\perp)^2)$ we have

$$b_\perp(t) \simeq \begin{cases} 1 + \frac{1}{2}\omega_\perp^2 t^2 + O(t^4) & \omega_\perp t \ll 1\,, \\ \frac{\omega_\perp t}{\sqrt{\gamma}} + c_0 + O(t^{-1/3}) & \omega_\perp t \gg 1\,, \end{cases} \tag{7.68}$$

as in the case of a stationary trap. The orientation of the expanding cloud is described by the parameter a defined in equ. (7.12). We find

$$a(t) \simeq \begin{cases} -\frac{2\omega_{rot}t}{\lambda^2} & \omega_\perp t \ll 1\,, \\ -\frac{c_a\omega_{rot}}{\lambda^2\omega_\perp^2 t} & \omega_\perp t \gg 1 \;\; (t < t_{3d}), \end{cases} \tag{7.69}$$

where c_a is a constant. Below we will show that $c_a = \gamma$. At very late times, $t > t_{3d} \sim 1/(\lambda^2\omega_\perp)$,

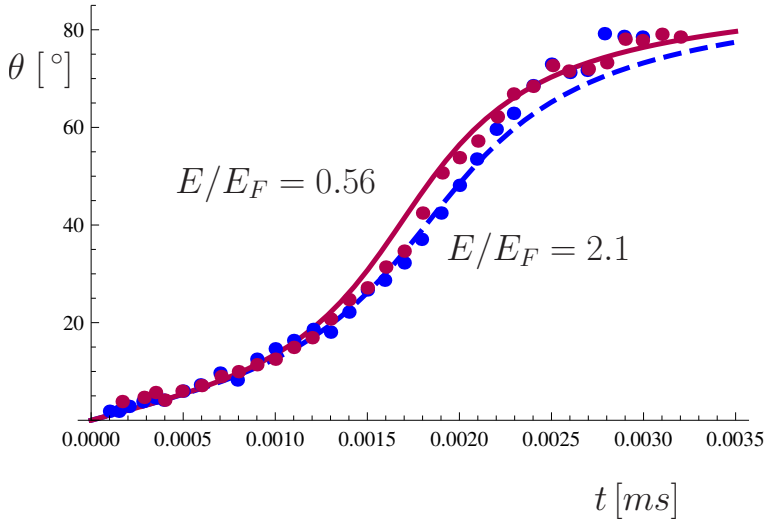

Figure 7.5: Time evolution of the angle of the major axis of a rotating expanding cloud after release from the trapping potential. The data are taken from [8]. The two data sets were obtained with initial energies $E/E_F = 0.56$ and 2.1. The solid line shows the prediction of ideal fluid dynamics, and the dashed lines shows the solution of the Navier-Stokes equation for $\beta = 0.061$. Using an entropy per particle $S/N \simeq 4.8$ this value of β implies a shear viscosity to entropy density ratio $\langle \alpha_s \rangle = 0.60$

we find $a(t) \sim 1/t^2$. The result (7.69) holds irrespective of the nature of the initial rotational flow. The parameter $a(t)$ can be related to the angle of the cloud with respect to the x-axis,

$$\tan(2\theta) = -\frac{a\lambda^2 b_x^2 b_y^2}{b_x^2 - \lambda^2 b_y^2}\,. \tag{7.70}$$

At early times, $\omega_x t \ll 1$, the angle is proportional to the rotational frequency of the trap, $\theta = \omega_{rot} t$. The angular motion speeds up as $b_y\lambda$ approaches b_x. The angle goes through 45° at

$$t_{45^\circ} = \frac{\sqrt{\gamma}}{\omega_x} \tag{7.71}$$

which is the identical to the crossing time in equ. (7.25). At late times, and up to corrections of $O(\omega_{rot}/\omega_\perp)$, the angle approaches 90°. The velocity field is dominated by the transverse expansion of the system. In the limit $\omega_{rot} < \omega_x \ll \omega_\perp$ the velocity fields α_i are identical to those in the non-rotating case. We have

$$\alpha_{y,z} \simeq \begin{cases} \omega_\perp^2 t & \omega_\perp t \ll 1\,, \\ 1/t & \omega_\perp t \gg 1\,, \end{cases} \tag{7.72}$$

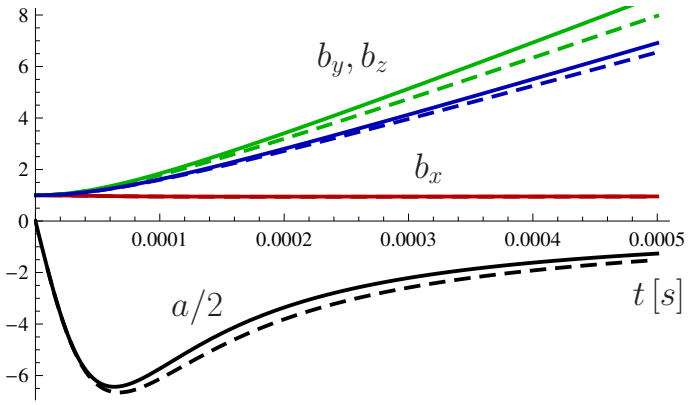

Figure 7.6: Time evolution of the parameters a, b_x, b_y, b_z that characterize the scaling expansion out of a rotating trap. Note that in this case ω_y and ω_z are not exactly equal, and that the time scale is different from Fig. 7.5. Here, we only show the early evolution of the system. Solid lines show the solution of the Euler equation, and dashed lines show the solution of the Navier-Stokes equation for $\beta = 0.077$.

and $\alpha_x = O(\lambda^2)$. The rotational components of the velocity field decay quickly. If the initial flow is irrotational, $\alpha(0) = \omega_{rot}$, then

$$\alpha(t) \simeq \omega_{rot}\left(1 - \omega_\perp^2 t^2\right) \tag{7.73}$$

for $(\omega_\perp t) < 1$. For $(\omega_\perp t) > 1$ the rotational component of the flow is small, $(\alpha/\omega_{rot}) \ll 1$, but the remaining flow decays slowly, $\alpha \sim t^{-1}$ for $t < t_{3d}$ and $\alpha \sim t^{-2}$ for $t > t_{3d}$. In ideal hydrodynamics an initially irrotational flow will remain irrotational, $\Omega(t) = 0$, for all t. If the initial flow corresponds to rigid rotation, $\Omega(0) = \omega_{rot}$, then the early time behavior is given by

$$\Omega(t) \simeq \omega_{rot}\left(1 - \frac{1}{2}\omega_\perp^2 t^2\right). \tag{7.74}$$

An initially rigid rotating flow induces a non-zero irrotational flow. For $(\omega_\perp t) > 1$ both components of the velocity field become much smaller than ω_{rot}.

The angular momentum is given by

$$L_z = \alpha m\langle n(x^2 - y^2)\rangle + \Omega m\langle n(x^2 + y^2)\rangle + (\alpha_x - \alpha_y)\, m\langle nxy\rangle, \tag{7.75}$$

where n is the density and $\langle . \rangle$ is an integral over the cloud. The moment of inertia of a rigid

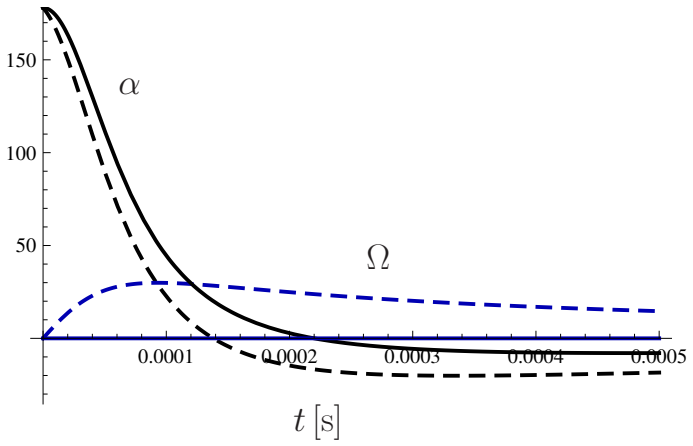

Figure 7.7: Time evolution of the parameters α and Ω which control the irrotational and rotational components of the velocity field. Parameters were chosen as in Fig. 7.6. Solid lines show the solution of the Euler equation, and dashed lines show the solution of the Navier-Stokes equation for $\beta = 0.077$.

rotor is $I_{rig} = m\langle x^2 + y^2\rangle$, and the irrotational moment of inertia is $I_{irr} = m\langle x^2 - y^2\rangle$. We have

$$m\langle nx^2\rangle = \frac{b_x^2}{1 - \frac{\lambda^2}{4}(ab_xb_y)^2}\,\frac{L_0}{\omega_x}\,, \tag{7.76}$$

$$m\langle ny^2\rangle = \frac{\lambda^2 b_y^2}{1 - \frac{\lambda^2}{4}(ab_xb_y)^2}\,\frac{L_0}{\omega_x}\,, \tag{7.77}$$

$$m\langle nxy\rangle = \frac{-\frac{\lambda^2}{2}ab_x^2b_y^2}{1 - \frac{\lambda^2}{4}(ab_xb_y)^2}\,\frac{L_0}{\omega_x}\,, \tag{7.78}$$

where the scale is set by

$$L_0 = \frac{N}{6}\frac{(3N)^{1/3}}{\lambda^{2/3}}\left(\frac{E_0}{E_F}\right)\,. \tag{7.79}$$

In the experiment of Clancy et al. $(\omega_{rot}/\omega_x) \simeq 0.4$ and $L_0/N \simeq 131(E_0/E_F)$. For $E_0/E_F = 1$, which is in the normal phase, the angular momentum per particle is $50\hbar$.

At early times the trap is strongly deformed and $I_{rig} \simeq I_{irr}$. When the cloud becomes almost spherical the irrotational moment is much smaller than the rigid moment of inertia, $I_{irr} \ll I_{rig}$. However, at times $(\omega_\perp t) > 1$ the angular momentum is mainly carried by the last term in equ. (7.75), which is related to the transverse expansion of the system. This is true irrespective of the nature of the initial rotational flow. For $(\omega_\perp t) > 1$ we have $\alpha_y m\langle nxy\rangle \simeq (c_a/\gamma)(\omega_{rot}/\omega_x)L_0$. Angular momentum conservation then fixes the constant c_a in equ. (7.69), $c_a = \gamma$. At very late time, $t > t_{3d}$, the angular momentum is shared among all the terms in equ. (7.75), and

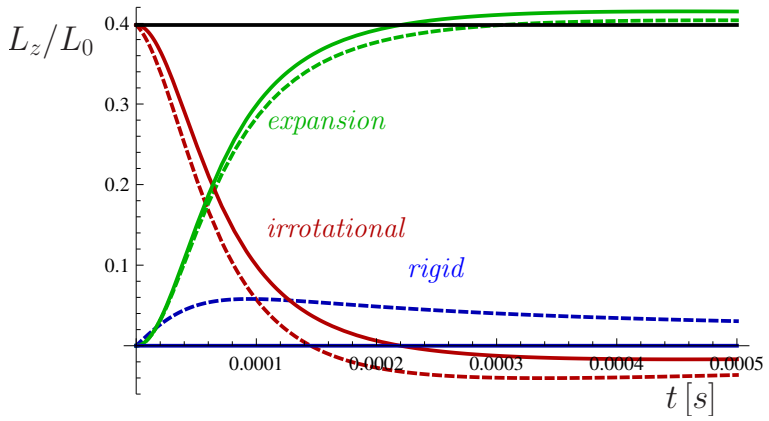

Figure 7.8: This figure shows different contribution to the total angular momentum of the expanding cloud as a function of time. The angular momentum is given in units of the quantity L_0 defined in the text. The curves labeled irrotational, rigid, and expansion show the $\langle x^2 - y^2\rangle$, $\langle x^2 + y^2\rangle$, and $\langle xy\rangle$ contributions. The solid and dashed lines correspond to ideal and viscous hydrodynamics, respectively. The solid black line shows the (conserved) total angular momentum.

the relative size of the different contributions depends on the initial conditions. In practice, of course, hydrodynamics is no longer applicable at $t > t_{3d}$.

7.4.2 Dissipation

The effects of dissipation on the expansion from a rotating trap can be studied in close analogy with Sect. 7.3.1-7.3.5. The rate of energy dissipation is

$$\dot{E} = -\frac{4}{3}\left(\alpha_x^2 + \alpha_y^2 + \alpha_z^2 - \alpha_x\alpha_y - \alpha_x\alpha_z - \alpha_y\alpha_z + 3\alpha^2\right)\int d^3x\,\eta(x)\,. \tag{7.80}$$

For $\alpha_x \simeq \alpha_y \gg \alpha_z, \alpha$ this expression reduces to the energy dissipated by the transverse expansion of cloud, see equ. (7.28). This implies that the main effect of dissipation is to slow the transverse expansion of the cloud, and to delay the time t_{45°. This delay is exactly the same as the delay in the crossing time in equ. (7.35). We have

$$\left(\frac{\delta t}{t}\right)_{45^\circ} = 0.009\left(\frac{\langle\alpha_s\rangle}{1/(4\pi)}\right)\left(\frac{1.3\cdot 10^5}{N}\right)^{1/3}\left(\frac{0.3}{\lambda}\right)^{1/3}\left(\frac{S/N}{4.8}\right)\left(\frac{2.1}{E_0/E_F}\right). \tag{7.81}$$

We can confirm this estimate by solving the Navier-Stokes equation. The Navier-Stokes equation can be derived using the moment method described in Sect. 7.3.2. As before, an equivalent set

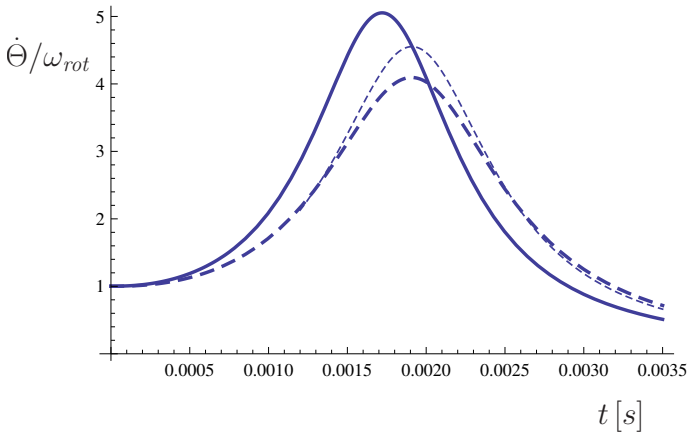

Figure 7.9: This figure shows the angular velocity of the rotating cloud as a function of time. The solid line shows the solution of the Euler equation, and the dashed line is the solution of the Navier-Stokes equation for $\beta = 0.077$. The thin dashed line shows the result for the angular velocity obtained by rescaling the solution of the Euler equation by a factor $1 + (\delta t/t)_{45^\circ} \simeq 1.1$. The discrepancy between the Navier-Stokes prediction and the rescaled Euler result in the regime where $\dot{\Theta}$ is large is due to the rotational component of the flow. We note that $I = L/\dot{\Theta}$ is the moment of inertia.

of equations can be obtained from the viscosity model given in equ. (7.43). We get [34]

$$\dot{\alpha}_x + \alpha_x^2 + \alpha^2 - \Omega^2 = \frac{\omega_x^2}{b_x^2}\left\{\bar{\mu} - \frac{6\beta}{\omega_\perp}\left[\frac{2}{3}\alpha_x - \frac{1}{3}\left(\alpha_y + \alpha_z\right) + \frac{1}{2}a b_x^2 \alpha\right]\right\} \tag{7.82}$$

$$\dot{\alpha}_y + \alpha_y^2 + \alpha^2 - \Omega^2 = \frac{\omega_y^2}{b_y^2}\left\{\bar{\mu} - \frac{6\beta}{\omega_\perp}\left[\frac{2}{3}\alpha_y - \frac{1}{3}\left(\alpha_x + \alpha_z\right) + \frac{1}{2}a\lambda^2 b_y^2 \alpha\right]\right\} \tag{7.83}$$

$$\dot{\alpha}_z + \alpha_z^2 = \frac{\omega_z^2}{b_z^2}\left\{\bar{\mu} - \frac{6\beta}{\omega_\perp}\left[\frac{2}{3}\alpha_z - \frac{1}{3}\left(\alpha_x + \alpha_y\right)\right]\right\} \tag{7.84}$$

$$\dot{\alpha} + \alpha\left(\alpha_x + \alpha_y\right) = \omega_x^2\left\{\frac{\bar{\mu}a}{2} - \frac{3\beta}{\omega_\perp}\left[\frac{a}{6}\left(\alpha_x + \alpha_y - 2\alpha_z\right) + \frac{b_x^2 + \lambda^2 b_y^2}{\lambda^2 b_x^2 b_y^2}\,\alpha\right]\right\} \tag{7.85}$$

$$\dot{\Omega} + \Omega\left(\alpha_x + \alpha_y\right) = \frac{3\beta\omega_x^2}{\omega_\perp}\left[\frac{a}{2}\left(\alpha_x - \alpha_y\right) + \frac{b_x^2 - \lambda^2 b_y^2}{\lambda^2 b_x^2 b_y^2}\,\alpha\right]. \tag{7.86}$$

These equations are independent of the functional form of the pressure. A solution of the Navier-Stokes equation for the trap parameters and initial conditions in [8] is shown in Fig. 7.5. The experimental data were taken at $E/E_F = 0.56$ which is in the superfluid phase, and $E/E_F = 2.1$ which is significantly above the phase transition. Similar to the low temperature data for pure transverse expansion in Fig. 7.1 the low temperature result for a rotating cloud shows no dissipative effects, and the best fit to the data is provided by ideal fluid dynamics.

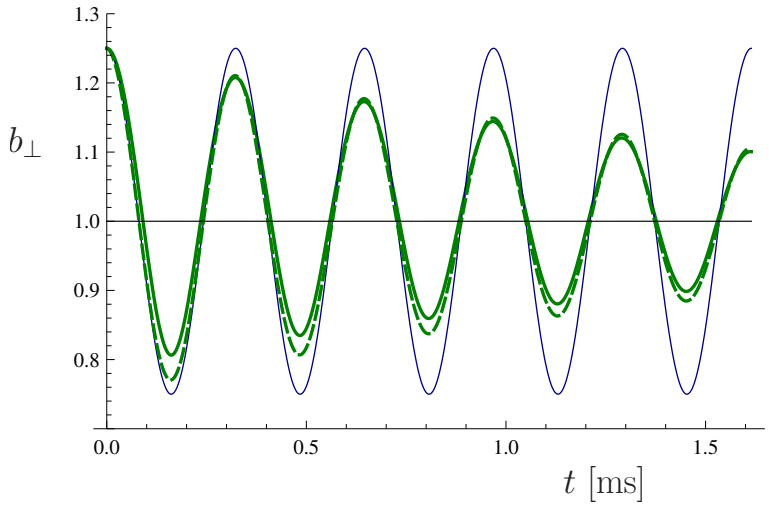

Figure 7.10: Time evolution of the amplitude of the transverse breathing mode. The black line shows the solution of the Euler equation and the solid green line is the solution of the Navier-Stokes equation for $\beta = 0.05$. The dashed green line is the damped cosine function given in equ. (7.91). The trap frequency was chosen to be $\omega_\perp = 1696$ Hz as in [64].

The data for $E/E_F = 2.1$ clearly show a delayed expansion. We find $(\delta t/t)_{45^\circ} \simeq 0.063$. Using $(\delta t/t) \simeq 1.16\beta$ from equ. (7.33) we estimate $\beta \simeq 0.057$. This estimate is quite accurate, the best fit of the Navier-Stokes solution to the data is obtained for $\beta = 0.061$. Using $N = 1.3 \cdot 10^5$, $\lambda = 0.03$ [8] and $(S/N) \simeq 4.8$ [78] we obtain $\langle \alpha_s \rangle \simeq 0.60$. The measurements were extended to values of E/E_F between 0.56 and 2.1 in [125]. This work reports values of η/s as small as $\langle \alpha_s \rangle \simeq (0.0 - 0.4)$. Note that in this regime it becomes very difficult to measure the viscosity accurately. A value of $\langle \alpha_s \rangle = 0.1$ affects the measured angle of the cloud by less than the with of the lines in Fig. 7.5.

A more detailed study of viscous effects on the evolution of the system is shown in Figs. 7.6-7.8. We observe that viscosity slows down the evolution of the scale parameters b_y, b_z and a. More interesting is the effect on the velocity fields α and Ω. Viscosity converts a fraction of the irrotational velocity field α into the rotational velocity field Ω. This is also seen in the breakdown of the angular momentum, see Fig. 7.8. The rotational component of L_z is not large, but it does lead to an observable effect in the angular velocity of the cloud. Fig. 7.9 shows that viscosity leads to a decrease in $\dot{\Theta}$. During most of the evolution this effect is dominated by the delayed expansion, but for $t \simeq t_{45^\circ}$ there is an extra reduction which is due to an increase of the effective moment of inertia $I = L/\dot{\Theta}$ caused by the rotational flow. Unfortunately, the experimental data are for $\Theta(t)$ are not sufficiently accurate to demonstrate this effect.

7.5 Collective Oscillations

In order to study collective oscillations we consider the Euler equation (7.20) in the presence of the trapping potential. The equation of motion is

$$\ddot{b}_i = \frac{\omega_i^2}{(b_x b_y b_z)^{2/3}} \frac{1}{b_i} - \omega_i^2 b_i \,. \tag{7.87}$$

The equilibrium solution is $b_x = b_y = b_z = 1$. We now consider small oscillations around the equilibrium, $b_i(t) = 1 + a_i e^{i\omega t}$. The linearized equation of motion gives

$$\omega^2 a_i = \omega_i^2 \left(2a_i + \gamma \sum_j a_j \right) , \tag{7.88}$$

which was derived in [59, 123, 21] using slightly different methods. For the radial breathing mode $a_y = a_z = a_\perp$, $a_x = 0$ we get $\omega^2 = 2(1+\gamma)\omega_\perp^2 = (10/3)\omega_\perp^2$. The energy dissipated can be computed from equ. (7.28). We find

$$\frac{\Delta E}{E_{osc}} = -4\pi \sqrt{\frac{3}{10}}\, \beta \simeq -6.88 \cdot \beta \,, \tag{7.89}$$

where ΔE is the energy dissipated per period, E_{osc} is the energy of the collective mode, and β is the parameter defined in equ. (7.34). We note that the amount of energy dissipated in one period of the transverse breathing mode is about three times larger than the energy dissipated by transverse expansion, see equ. (7.33).

We can also derive a Navier-Stokes equation, either by taking moments as in Sect. 7.3.2, or by using a simple scaling form of the shear viscosity as in Sect. 7.3.3. For the transverse breathing mode we find

$$\ddot{b}_\perp = \frac{\omega_\perp^2}{b_\perp^{7/3}} - \omega_\perp^2 b_\perp - \frac{2\beta\omega_\perp \dot{b}_\perp}{b_\perp^2} \,. \tag{7.90}$$

If β is small then this equation is approximately solved by a damped oscillating function. We have

$$b_\perp(t) = 1 + a_\perp \cos(\omega t) \exp(-\Gamma t) \,. \tag{7.91}$$

Comparison with equ. (7.89) gives $\Gamma = \beta\omega_\perp$. The main feature of collective modes is that the viscous term exponentiates so that even very small values of β are experimentally accessible. In Fig. (7.10) we show a comparison between an exact solution of equ. (7.90) for $\beta = 0.05$, $a_\perp(0) = 0.25$ and the approximate solution (7.91). We observe that the approximate solution is extremely accurate.

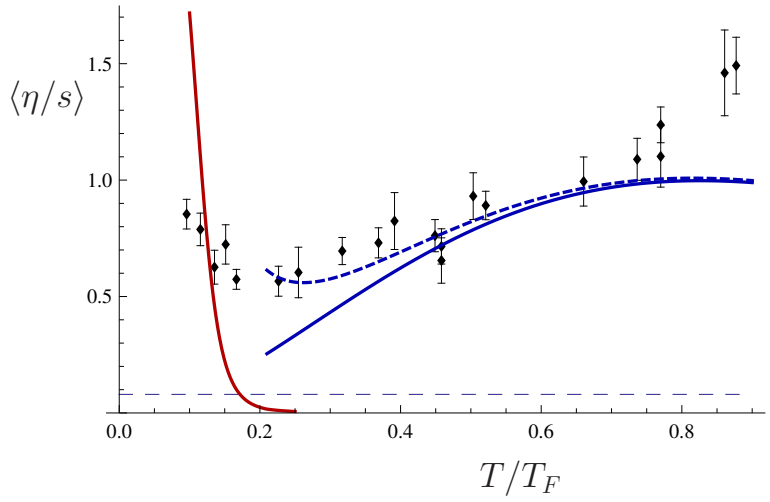

Figure 7.11: Trap average $\langle \alpha_s \rangle = \langle \eta/s \rangle$ extracted from the damping of the radial breathing mode. The data points were obtained using equ. (7.92) to analyze the data published by Kinast et al. [74]. The thermodynamic quantities (S/N) and E_0/E_F were taken from [78]. The solid red and blue lines show the expected low and high temperature limits. Both theory curves include relaxation time effects. The blue dashed curve is a phenomenological two-component model explained in the text.

The experimentally measured damping rate can be used to estimate $\langle \alpha_s \rangle$. We have

$$\langle \alpha_s \rangle = (3\lambda N)^{1/3} \left(\frac{\Gamma}{\omega_\perp} \right) \left(\frac{E_0}{E_F} \right) \left(\frac{N}{S} \right) . \tag{7.92}$$

In Fig. 7.11 we show an analysis of the data obtained by Kinast et al. [74] using equ. (7.92). This plot is very similar to our earlier analysis [114] (see also [54, 130]), except that the temperature calibration and thermodynamic data have been updated using the recent analysis published in [78].

There are a number of important checks on the interpretation of the damping date in terms of viscous hydrodynamics that should be, or have already been, performed. Viscous hydrodynamics predicts that the monopole mode in a spherical trap is not damped at all. This prediction is quite striking, but it has never been tested. Viscous hydrodynamics also predicts simple relationships between the damping constant of the radial breathing mode and the radial quadrupole as well as the scissors mode [114]. These predictions agree qualitatively with the data obtained by the Innsbruck group, but there are some structures in the data that do not fit a simple hydrodynamic description. Finally, hydrodynamics predicts that the damping rate decreases as $N^{-1/3}$. This prediction does not agree with the data published in [74]. We note,

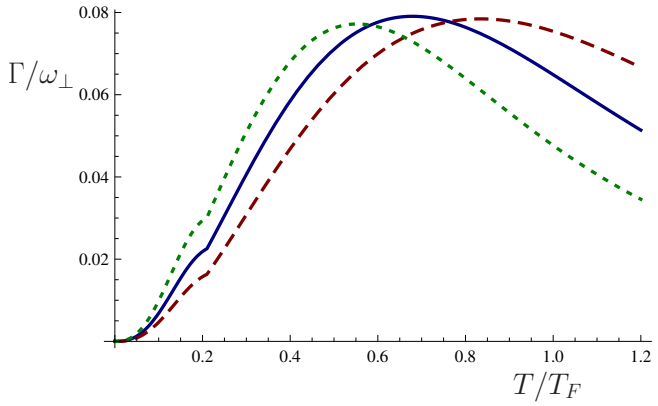

Figure 7.12: Damping rate of the radial breathing mode in units of the transverse trapping frequency. This figure only shows the contribution from the dilute corona, computed using the relaxation time approach. The solid line corresponds to $N \equiv N_0 = 2 \cdot 10^5$, $\lambda = 0.045$ as in [74]. The long dashed and short dashed lines corresponds to $N = 5N_0$ and $N = 0.2N_0$, respectively.

however, that Kinast et al. only checked the scaling behavior at very low temperature, and that relaxation time effects may modify the particle number scaling.

We can also compare the results in Fig. 7.11 to theoretical prediction for the shear viscosity in the low and high temperature limit. In the high temperature limit the viscosity is independent of density and the main source of dissipation is the finite relaxation time, see Sec. 7.3.5. In the case of periodic motion the relaxation time equation (7.60) is easily solved. The dissipated energy is given by equ. (7.34,7.89) with

$$\langle \alpha_n \rangle = \eta_0 (mT)^{3/2} \int d^3x \, \frac{1}{1 + \omega^2 \tau_R (n(x))^2}. \tag{7.93}$$

We will use the kinetic theory result $\tau_R(n) = \eta/(nT)$ with $\eta = \eta_0 (mT)^{3/2}$. In the high temperature (low density) limit we can use the classical expression for the density profile $n(x)$. In this case the integral over x can be done analytically. We find

$$\langle \alpha_n \rangle = -\frac{45\pi}{32} \left(\frac{T}{T_F}\right)^3 Li_{3/2}\left(-\left[\frac{const}{(\lambda N)^{2/3}} \left(\frac{T}{T_F}\right)^4 \right]^{-1} \right), \tag{7.94}$$

where $const = 1125 \cdot 3^{1/3}\pi^2/64 \simeq 250.1$, and $Li_\alpha(x)$ is the polylogarithm function. In the limit $T \ll T_F$ the result scales as $\langle \alpha_n \rangle \sim y^3 \log(y)^{3/2}$ with $y = T/T_F$. For $T \gg T_F$ we get $\langle \alpha_n \rangle \sim y^{-1}$. These results imply that both the temperature scaling and the particle number scaling differ from naive expectations. The shear viscosity scales as $\eta \sim T^{3/2}$, but $\langle \alpha_n \rangle \sim T^3 \log(T)^{3/2}$ at

low T, and $\langle\alpha_n\rangle \sim T^{-1}$ at high T. Also, the scaling of the damping rate with N is $\Gamma \sim N^{-1/3}\log(N)^{3/2}$ at low T and $\Gamma \sim N^{1/3}$ at high T, see Fig. 7.12. This implies that there are temperature regions in which the dependence of the damping rate on N is small.

The prediction of equ. (7.94) is shown as the solid blue line in Fig. 7.11. We observe that the relaxation time model agrees well with the data for $T \sim (0.5-0.8)T_F$. For temperature less than $0.5T_F$ the observed damping rate is bigger than the prediction of the relaxation model. At very low temperature the shear viscosity is expected to be dominated by the phonon contribution [113]

$$\eta = 0.018n\left(\frac{n^{2/3}}{mT}\right)^5 . \tag{7.95}$$

At low temperature we can compute the trap average by using the zero temperature profile. We find $\langle\alpha_n\rangle \simeq 1.5\cdot 10^{-5}(T_F/T)^5$. This result becomes large for $T/T_F < 0.1$. In this regime relaxation time effects are important, and $\langle\alpha_n\rangle$ at finite frequency goes to zero as $T \to 0$.

Neither the low temperature nor the high temperature result provide a good description of the data in the regime $T \simeq (0.15 - 0.40)T_F$. The dashed blue line in Fig. 7.11 shows a purely phenomenological fit based on the functional form $\eta = \eta_0(mT)^{3/2} + \eta_1 n^{5/3}/(mT)$ with $\eta_0 = 15/(32\sqrt{\pi}) \simeq 0.264$ and $\eta_1 \simeq 0.06$. In this case the minimum value of η/n is 0.24 which occurs below the phase transition at $mT/n^{2/3} \simeq 0.47$.

7.6 Summary and Outlook

A special feature of the hydrodynamics of a unitary Fermi gas is the existence of simple scaling solutions of the equations of ideal fluid dynamics. These solutions are independent of the equation of state, the initial temperature and the number of particles. The only time scales in the problem are the trap frequencies, see Fig. 7.13. The existence of scaling solutions is related to the constraints imposed by scale invariance on the equation of state, and to the harmonic character of the confinement potential.

The properties mentioned above make scaling flows an ideal class of solution to study the effects of shear viscosity. In this contribution we focused on three classes of experiments, expansion from a deformed trap ("elliptic flow"), expansion from a rotating trap, and damping of collective oscillations. These experiments provide somewhat complementary information, and they have different advantages and disadvantages:

- In the case of collective modes the effect of shear viscosity exponentiates, and as a consequence the damping of collective modes is sensitive to very small values of the shear viscosity. Collective modes also have the advantage that qualitatively the effect of dissipation is very simple: The kinetic energy of the collective mode is converted to heat, so that

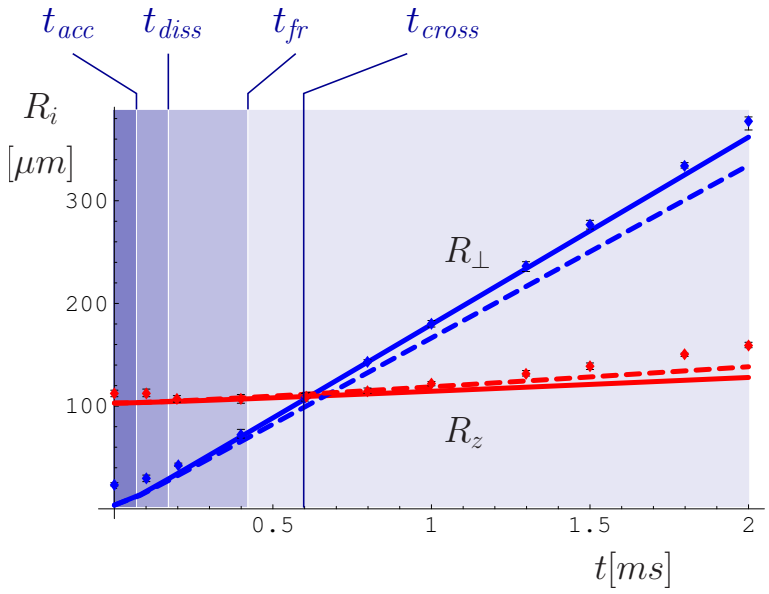

Figure 7.13: Time scales relevant to the expansion of a unitary Fermi gas from a deformed trap. The inverse trap frequency is $\omega_\perp^{-1} = 0.024\,ms$. The scale t_{acc} is the characteristic time for hydrodynamic acceleration, where we have defined $t = t_{acc}$ to be the time when 80% of the initial internal energy has been converted to kinetic energy. The characteristic time for viscous effects, t_{dis}, is determined by the condition that the dissipated energy ΔE has reached 80% of its asymptotic value. The freezeout time t_{fr} is quite uncertain. Here, we show the time at which, for $T_0/T_F = 0.21$, the freezeout surface reaches the point $x_\perp = b_\perp R_\perp$. The crossing time t_{cr} is the time at which the system becomes spherical. The time t_{3d} at which the expansion becomes three-dimensional is bigger by another factor λ^{-1}.

at the end of the evolution the system is again stationary, but the temperature is increased. In the case of flow experiments the situation is more complicated. Dissipation converts kinetic energy into heat but unless the system freezes out first, the internal energy is eventually converted back to kinetic energy. Because of the second law of thermodynamics, the final state of viscous hydrodynamics must differ from that of ideal hydrodynamics, but the differences can be subtle, manifesting themselves in violations of the simple scaling formulas for the density and the velocity field.

- The transverse expansion experiments provide detailed information about the time dependence of the density and flow profiles. This information can be used to understand the breakdown of hydrodynamics, for example by studying deviations from the simple linear velocity profile predicted by ideal fluid dynamics. Transverse flow experiments may also show a different, and possibly smaller, sensitivity to relaxation effects. Fig. 7.4 shows that, for $T/T_F < 0.4$, the relaxation time estimate of the trap averaged dissipation due to the

spatially constant part of the shear viscosity is similar for transverse flow and transverse collective modes. However, the local response of a rapidly expanding cloud is likely to be different from that of an oscillating system.

- The expansion of a rotating cloud is sensitive to a new viscous effect, the conversion of an irrotational flow $\vec{v} \sim \vec{\nabla}(xy)$ to a rotational flow $\vec{v} \sim \hat{z} \times \vec{x}$. Contrary to the slowdown of the transverse expansion, which could in principle be due to scale-breaking terms in the pressure or residual external potentials, this is a genuine dissipative effect, since vorticity is conserved in ideal hydrodynamics.

The main difficulty in extracting the shear viscosity from the analysis of scaling flows is associated with the role of the dilute corona of the cloud. Kinetic theory predicts that in the dilute limit the shear viscosity is independent of density and only depends on temperature. A simple analysis of the type presented in Sec. 7.3.3 then implies that the dilute corona does not generate a dissipative force. It nevertheless dissipates a large amount of energy. The analysis also suggests that freezeout only occurs very late, see Sec. 7.3.4. There are a number of aspects of this analysis that need to be improved:

- The Navier-Stokes equation is based on the assumption that the viscous correction to the stress tensor appears instantaneously. This is particularly problematic in the case of scaling flows, because the viscous contribution is spatially constant. The fact that the ideal stresses propagate outward with the expansion of the system whereas the dissipative stresses appear immediately indicates that causality is violated. This problem can be addressed by including a finite relaxation time, or by solving a more complete set of second order hydrodynamic equations.

- We have studied the effect of dissipative forces in the Navier-Stokes equations, but we have computed the non-dissipative forces (pressure gradients) based on an approximately isentropic expansion. This procedure neglects reheating, and violates energy conservation. Reheating is important in the dilute corona, and breaks the scaling nature of the expansion.

In addition to implementing these technical improvements it is important to consider other experimental setups that are directly sensitive to the spatially constant part of the shear viscosity. One option would be to measure the attenuation of sound propagating in a very long elongated trap. Another idea would be to directly measure the decay of a shear flow in a long channel.

Finally, we summarize the existing experimental constraints on the shear viscosity of the unitary Fermi gas:

- The damping of collective oscillations constrains the trap average $\langle\eta\rangle/S \equiv \langle\alpha_s\rangle$. We find that this quantity varies between $\langle\alpha_s\rangle \simeq 1$ at $T/T_F \simeq 0.8$ and $\langle\alpha_s\rangle \simeq 0.5$ at $T/T_F \simeq 0.2$. In the regime $0.4 \leq T/T_F \leq 0.8$ the temperature dependence is consistent with $\eta \sim (mT)^{3/2}$ and a relaxation time that scales as $\tau_R \sim \eta/(nT)$. At lower temperatures an additional contribution is needed. In a simple model the minimum of the shear viscosity to density ratio is $\eta/n \simeq 0.2$.

- The expansion of a rotating cloud gives $\langle\alpha_s\rangle \simeq 0.8$ at $T/T_F \simeq 0.8$, and $\langle\alpha_s\rangle \simeq (0.0 - 0.4)$ at $T/T_F \simeq 0.2$ [125]. The latter results are smaller than the values extracted from collective oscillations, although the errors are also somewhat larger. It will be important to determine whether this discrepancy is due to the effects of the dilute corona, and whether the smaller values of $\langle\alpha_s\rangle$ are more representative of the shear viscosity to entropy density ratio in the core.

Chapter 8

Fluctuations

8.1 Introduction

It is now widely appreciated that fluid dynamics can be viewed as an effective long-distance theory for a classical or quantum many-body system at non-zero temperature. Effective theories make systematic predictions for correlation functions order-by-order in a low-momentum expansion. These predictions depend on a small number of microscopic parameters. In the case of fluid dynamics the microscopic parameters are the equation of state and the transport coefficients.

Effective (field) theories are constructed using the following procedure: i) Identify the low energy degrees of freedoms. ii) Write down the most general local effective action consistent with the symmetries of the problem. This action is typically expressed in terms of low energy fields and their derivatives. The coefficients of allowed terms in the effective action are free parameters called low energy constants. iii) Determine what terms in the effective action have to be included in order to compute a correlation function to a given order in the low energy expansion. This is known as the "power counting". Typically, the leading contribution arises from tree level diagrams involving operators with the minimal number of derivatives, and higher order corrections arise both from higher derivative operators, and from loop diagrams generated by the leading order interactions. In some cases diagrams may have to be summed to all orders. For example, the sum of all tree diagrams corresponds to solving a classical field equation.

In fluid dynamics the low energy modes are fluctuations of the conserved charges. In the case of a one-component non-relativistic fluid the conserved charges are the particle density, the energy density, and the momentum density. The derivative expansion is implemented at the level of the constitutive equations. This means that the conserved currents are expressed in terms of derivatives of the thermodynamic variables. The effective theory without derivative terms in the currents is called ideal fluid dynamics, and the equation of motion at one-derivative

order is known as the Navier-Stokes equation. The validity of fluid dynamics requires that derivative corrections to the currents are small. This condition does not preclude the possibility that small corrections can exponentiate as one solves the equations of motion. Solutions of the Navier-Stokes equation are qualitatively different from solutions of ideal fluid dynamics. In ideal fluid dynamics the motion is time reversible, sound modes are not damped, and diffusive modes do not exist. This implies that in most cases one has to retain at least one-derivative terms in the constitutive equations. Two derivative terms have also been studied [79, 62], but the corrections are typically small. In relativistic fluid dynamics two-derivative terms improve the stability of equations of motion, and second order terms are now routinely included in hydrodynamic simulations of relativistic heavy ion collisions [111].

Loop corrections in fluid dynamics arise from thermal fluctuations. Fluctuations are known to be important in the vicinity of second order phase transitions [60], but they are rarely considered in the case of non-critical fluids. In this work we will consider the contribution of fluctuations to the correlation function of the stress tensor in a simple non-relativistic fluid. We study the implications of our results for the shear viscosity of the unitary Fermi gas. The unitary Fermi is known to have a very low viscosity [114, 26, 117, 2], close to the value obtained from the AdS/CFT (Anti-deSitter Space/Conformal Field Theory) correspondence, $\eta/s = \hbar/(4\pi k_B)$ [103, 96]. Here, η is the shear viscosity and s is the entropy density, $\hbar$ is Planck's constant and k_B is Boltzmann's constant. We will set $\hbar = k_B = 1$ in the following. We will show that the small shear viscosity enhances the role of fluctuations, but we also show that fluctuations imply a lower limit on how small the viscosity can get. We demonstrate that fluctuations lead to a non-analytic term in the viscous relaxation time in three spatial dimensions, and to a logarithmic divergence of the shear viscosity in two dimensions. Finally, we discuss the possibility of observing these non-analytic terms in experiments with trapped atomic gases.

Our work builds on a substantial literature related to fluctuations in fluid dynamics, beginning with the work of Landau [6]. The role of fluctuations in critical transport phenomena was summarized in the review article by Hohenberg and Halperin [60] and the text books by Ma and Onuki [85, 94]. Diagrammatic methods are discussed by a number of authors, for example in [95, 43, 72]. Our work closely follows a recent study of fluctuations in relativistic fluids, see [76, 100], the recent review [75], and the related work in [128].

8.2 Kubo Formula

In this section we will determine the low energy behavior of the retarded correlation function of the stress tensor using the classical equations of fluid dynamics at next-to-leading order in the gradient expansion. This result can be used to derive the standard Kubo formula for the shear viscosity, as well as a new Kubo formula for the viscous relaxation time. We will employ

the formalism developed in [121, 120, 63, 62], which is based on coupling the theory to a non-trivial background metric $g_{ij}(t,\vec{x})$. Correlation functions of the stress tensor can be computed by using linear response theory, and the requirements of Gallilean and conformal symmetry can be incorporated by requiring the equations of fluid dynamics to satisfy diffeomorphism and conformal invariance.

The retarded correlation function of the stress tensor Π^{ij} is defined by

$$G_R^{ijkl}(\omega,\mathbf{k}) = -i\int dt\int d\mathbf{x}\, e^{i\omega t - i\mathbf{k}\cdot\mathbf{x}}\Theta(t)\langle[\Pi^{ij}(t,\mathbf{x}),\Pi^{kl}(0,\mathbf{0})]\rangle\,. \tag{8.1}$$

G_R determines the stresses induced by a small perturbation $g_{ij}(t,\mathbf{x}) = \delta_{ij} + h_{ij}(t,\mathbf{x})$ around the flat metric. We have

$$\delta\Pi^{ij} = -\frac{1}{2}G_R^{ijkl}h_{kl}\,. \tag{8.2}$$

In fluid dynamics we expand the stress tensor in derivatives of the local thermodynamic variables $P,\rho,\mathbf{v}$, where P is the pressure, ρ is the density, and $\mathbf{v}$ is the fluid velocity. We write $\Pi_{ij} = \Pi^0_{ij} + \delta\Pi_{ij}$, where

$$\Pi^0_{ij} = \rho v_i v_j + P g_{ij} \tag{8.3}$$

is the ideal fluid part, and $\delta\Pi_{ij}$ is the viscous correction. In a conformally invariant fluid the leading term is $\delta\Pi_{ij} = -\eta\sigma_{ij}$ with

$$\sigma_{ij} = \nabla_i v_j + \nabla_j v_i + \dot{g}_{ij} - \frac{2}{3}g_{ij}\langle\sigma\rangle\,, \tag{8.4}$$

$$\langle\sigma\rangle = \nabla\cdot v + \frac{\dot{g}}{2g}\,, \tag{8.5}$$

where σ_{ij} is the shear stress tensor, η is the shear viscosity, $g_{ij}\langle\sigma\rangle$ is the bulk stress tensor, and ∇_i is the covariant derivative associated with g_{ij}. Note that the bulk viscosity of a conformal fluid is zero. In [62] we classified all terms up to second order in derivatives. We have

$$\begin{aligned}\delta\Pi_{ij} = {} & -\eta\sigma_{ij} + \eta\tau_R\left(g_{ik}\dot{\sigma}^k_j + v^k\nabla_k\sigma_{ij} + \frac{2}{3}\langle\sigma\rangle\sigma_{ij}\right) + \lambda_1\sigma_{\langle i}{}^k\sigma_{j\rangle k} + \lambda_2\sigma_{\langle i}{}^k\Omega_{j\rangle k} \\ & + \lambda_3\Omega_{\langle i}{}^k\Omega_{j\rangle k} + \gamma_1\nabla_{\langle i}T\nabla_{j\rangle}T + \gamma_2\nabla_{\langle i}P\nabla_{j\rangle}P + \gamma_3\nabla_{\langle i}T\nabla_{j\rangle}P \\ & + \gamma_4\nabla_{\langle i}\nabla_{j\rangle}T + \gamma_5\nabla_{\langle i}\nabla_{j\rangle}P + \kappa_R R_{\langle ij\rangle}\,,\end{aligned} \tag{8.6}$$

where τ_R is the viscous relaxation time, λ_i, γ_i, κ_R are second order transport coefficients, $\Omega_{ij} = \nabla_i v_j - \nabla_j v_i$ is the vorticity tensor, T is the temperature, and R_{ij} is the Ricci tensor associated with g_{ij}. Note that R_{ij} vanishes in flat space $g_{ij} = \delta_{ij}$, but keeping terms involving the curvature is crucial for obtaining the correct low energy expansion of G_R.

We will concentrate on the "pure shear" component G_R^{xyxy}. For this purpose we consider

a perturbation of the form $h_{xy}(z,t)$. From the linearized Euler equation we can see that the perturbation does not induce a shift in the density, temperature, or velocity. This means that we can directly read off $\delta\Pi_{ij}$ from equ. (8.6). We find

$$G_R^{xyxy}(\omega,k) = P - i\eta\omega + \tau_R\eta\omega^2 - \frac{\kappa_R}{2}k^2 + O(\omega^3,\omega k^2)\,, \tag{8.7}$$

which implies the familiar Kubo relation for the shear viscosity

$$\eta = -\lim_{\omega\to 0}\lim_{\mathbf{k}\to 0}\frac{d}{d\omega}\,\mathrm{Im}\,G_R^{xyxy}(\omega,\mathbf{k}) \tag{8.8}$$

as well as a new Kubo formula for the viscous relaxation time

$$\tau_R\eta = \lim_{\omega\to 0}\lim_{\mathbf{k}\to 0}\frac{1}{2}\frac{d^2}{d\omega^2}\,\mathrm{Re}\,G_R^{xyxy}(\omega,\mathbf{k})\,. \tag{8.9}$$

This result is simpler than the corresponding formula in relativistic hydrodynamics [9], which also involves a term proportional to κ_R. In the next Section we will show that in three dimensions fluctuations lead to a $\omega^{3/2}$ term in $\mathrm{Re}\,G_R^{xyxy}(\omega,0)$, see equ. (8.28). This term is cutoff independent and completely fixed by η. This implies that even if fluctuations are included τ_R can be defined in terms of a subtracted Kubo relation.

8.3 Hydrodynamic Fluctuations

In this section we will study the contribution of fluctuations to the retarded correlation function. For this purpose it is convenient to start from the symmetrized correlation function

$$G_S^{xyxy}(\omega,\mathbf{k}) = \int d^3x\int dt\, e^{i(\omega t-\mathbf{k}\cdot\mathbf{x})}\left\langle\frac{1}{2}\left\{\Pi_{xy}(t,\mathbf{x}),\Pi_{xy}(0,0)\right\}\right\rangle\,. \tag{8.10}$$

This function is related to the retarded correlator by the fluctuation dissipation theorem. For $\omega\to 0$ we have

$$G_S(\omega,\mathbf{k}) \simeq -\frac{2T}{\omega}\mathrm{Im}\,G_R(\omega,\mathbf{k})\,. \tag{8.11}$$

In the low frequency, low momentum limit we can use the form of the stress tensor in fluid dynamics, $\Pi_{xy} = \rho v_x v_y - \eta(\nabla_x v_y + \nabla_y v_x) + O(\nabla^2)$, and expand the hydrodynamic variables around their mean values, $\rho = \rho_0 + \delta\rho$ etc. We will use the Gaussian approximation and write expectation values of products of fluctuating fields as products of two point functions. The ideal (zero derivative) terms in the stress tensor give one and two loop graphs involving velocity-velocity and density-density correlation functions. We will show in A.1 that graphs with higher derivative vertices, as well as graphs with additional loops are suppressed by powers

of $\omega/(D_\eta K_{hyd}^2)$, where D_η is the momentum diffusion constant (see equ. (8.16)) and K_{hyd} is the breakdown scale of hydrodynamics which we will define in Sect. 8.4. We will therefore concentrate on the one-loop graph

$$G_S^{xyxy}(\omega,0) = \rho_0^2 \int \frac{d\omega'}{2\pi} \int \frac{d^3\mathbf{k}}{(2\pi)^3} \Big[\Delta_S^{xy}(\omega',\mathbf{k}) \Delta_S^{yx}(\omega-\omega',\mathbf{k}) + \Delta_S^{xx}(\omega',\mathbf{k}) \Delta_S^{yy}(\omega-\omega',\mathbf{k}) \Big] , \quad (8.12)$$

where Δ_S^{ij} is the symmetrized velocity correlation function

$$\Delta_S^{ij}(\omega,\mathbf{k}) = \int d^3x \int dt\, e^{i(\omega t - \mathbf{k}\cdot\mathbf{x})} \left\langle \frac{1}{2} \left\{ v^i(t,\mathbf{x}), v^j(0,0) \right\} \right\rangle . \quad (8.13)$$

We are ultimately interested in the retarded, not the symmetrized, correlation function. At low frequency the retarded function can be written as

$$\begin{aligned} G_R^{xyxy}(\omega,0) \;=\; & \rho_0^2 \int \frac{d\omega'}{2\pi} \int \frac{d^3\mathbf{k}}{(2\pi)^3} \Big[\Delta_R^{xy}(\omega',\mathbf{k}) \Delta_S^{yx}(\omega-\omega',\mathbf{k}) + \Delta_S^{xy}(\omega',\mathbf{k}) \Delta_R^{yx}(\omega-\omega',\mathbf{k}) \\ & + \Delta_R^{xx}(\omega',\mathbf{k}) \Delta_S^{yy}(\omega-\omega',\mathbf{k}) + \Delta_S^{xx}(\omega',\mathbf{k}) \Delta_R^{yy}(\omega-\omega',\mathbf{k}) \Big] , \end{aligned} \quad (8.14)$$

where we have used the fluctuation dissipation relation (8.11). This relation generalizes: retarded correlation functions of hydrodynamic variables have diagrammatic expansions in terms of retarded and symmetrized correlation functions [85, 95, 60, 43, 72, 94, 75].

The velocity correlation function can be decomposed into longitudinal and transverse parts

$$\Delta_{S,R}^{ij}(\omega,\mathbf{k}) = \left(\delta^{ij} - \hat{\mathbf{k}}^i \hat{\mathbf{k}}^j \right) \Delta_{S,R}^T(\omega,\mathbf{k}) + \hat{\mathbf{k}}^i \hat{\mathbf{k}}^j \Delta_{S,R}^L(\omega,\mathbf{k}) . \quad (8.15)$$

The transverse part is purely diffusive. The symmetrized correlation function is [6]

$$\Delta_S^T(\omega,\mathbf{k}) = \frac{2T}{\rho} \frac{D_\eta k^2}{\omega^2 + (D_\eta k^2)^2} , \quad (8.16)$$

where $k = |\mathbf{k}|$ and $D_\eta = \eta/\rho$ is the momentum diffusion constant, also known as the kinetic viscosity. The retarded correlation function is given by

$$\Delta_R^T(\omega,\mathbf{k}) = \frac{1}{\rho} \frac{-D_\eta k^2}{-i\omega + D_\eta k^2} . \quad (8.17)$$

The longitudinal correlation function can be reconstructed from the density-density correlation function (the dynamic structure factor) using current conservation, $i\omega\delta\rho = i\rho\mathbf{k}\cdot\mathbf{v}_L$, where

$\mathbf{v} = \mathbf{v}_L + \mathbf{v}_T$ with $\mathbf{k} \cdot \mathbf{v}_T = 0$ and $\mathbf{k} \times \mathbf{v}_L = 0$. We find

$$\begin{aligned}\Delta_S^L(\omega, \mathbf{k}) &= \frac{2T}{\rho}\left\{ \frac{\Gamma\omega k^2}{\left(\omega^2 - c_s^2 k^2\right)^2 + \left(\Gamma\omega k^2\right)^2} + \left(\frac{c_p}{c_v} - 1\right)\frac{1}{c_s^2}\frac{D_T\omega^2}{\omega^2 + \left(D_T k^2\right)^2} \right. \\ &\quad \left. - \left(\frac{c_p}{c_v} - 1\right)\frac{1}{c_s^2}\frac{(\omega^2 - c_s^2 k^2) D_T\omega^2}{\left(\omega^2 - c_s^2 k^2\right)^2 + \left(\Gamma\omega k^2\right)^2} \right\}. \end{aligned} \tag{8.18}$$

The first two terms have a clear physical interpretation as the contributions from propagating sound waves and diffusive heat transport. The third term is required to satisfy sum rules. This term is suppressed near the sound pole $\omega^2 \simeq c_s^2 k^2$. In equ. (8.18) c_s is the speed of sound, Γ is the sound attenuation constant, $D_T = \kappa/(c_p\rho)$ is the thermal diffusion constant, κ is the thermal conductivity, c_p is the specific heat per unit mass at constant pressure and c_v is the specific heat at constant volume. The sound attenuation constant is

$$\Gamma = \frac{4}{3}\frac{\eta}{\rho} + \frac{\zeta}{\rho} + \frac{\kappa}{\rho}\left(\frac{1}{c_v} - \frac{1}{c_p}\right) = \frac{4}{3}\frac{\eta}{\rho}\left[1 + \frac{3}{4}\frac{\zeta}{\eta} + \frac{3}{4}\frac{\Delta c_p}{Pr}\right], \tag{8.19}$$

where $\Delta c_p = (c_p - c_v)/c_v$ and $Pr = (c_p\eta)/\kappa$ is the Prandtl number, the ratio of momentum to thermal diffusion. At high temperature $\Delta c_p = 2/3$ and $Pr = 2/3$ [17], and at low temperature $\Delta c_p/Pr \to 0$. In the case of a conformal fluid the bulk viscosity vanishes, $\zeta = 0$. This implies that $\Gamma = \frac{7}{3}D_\eta$ at high temperature, and $\Gamma = \frac{4}{3}D_\eta$ at low temperature.

At low frequency and momentum the symmetrized correlation function can be further simplified. We illustrate the result in the case of the sound pole. We can write

$$\Delta_S^{sound}(\omega, \mathbf{k}) \simeq \frac{\Gamma T k^2}{2\rho}\left\{ \frac{1}{(\omega - c_s k)^2 + \left(\frac{\Gamma k^2}{2}\right)^2} + \frac{1}{(\omega + c_s k)^2 + \left(\frac{\Gamma k^2}{2}\right)^2} \right\}, \tag{8.20}$$

which is correct up to terms of order $\Gamma k/c_s$. The retarded correlator is

$$\Delta_R^{sound}(\omega, \mathbf{k}) \simeq \frac{\omega}{2\rho}\left\{ \frac{1}{\omega - c_s k + i\frac{\Gamma k^2}{2}} + \frac{1}{\omega + c_s k + i\frac{\Gamma k^2}{2}} \right\}, \tag{8.21}$$

and an analogous expression holds for the sum rule term in equ. (8.18).

We can insert the decomposition of the velocity correlation function given in equ. (8.15) into the one-loop result for the retarded correlation function, equ. (8.14). This gives a series of terms which correspond to the contribution from a pair of shear modes, a pair of sound modes, a mixed shear and sound term, and finally diffusive heat modes, see Fig. 8.1. We discuss these contributions in turn:

1. Shear modes: This is the contribution which is easiest to compute. The frequency integral

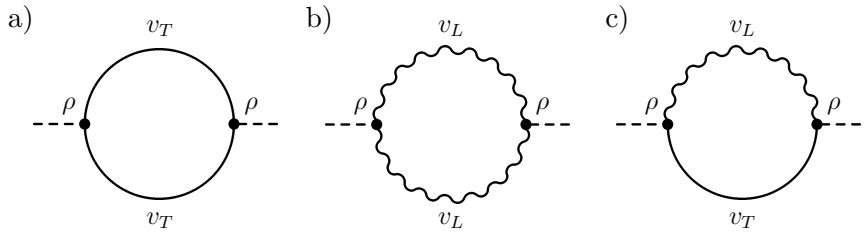

Figure 8.1: Diagrammatic representation of the leading contribution of thermal fluctuations to the stress tensor correlation function. Solid lines labeled v_T denote the transverse velocity correlator, dominated by the shear pole, and wavy lines labeled v_L denote the longitudinal velocity correlator, governed by the sound pole and the diffusive heat mode.

can be done by contour integration. We find

$$G_R^{xyxy}(\omega,0)\big|_{shear} = -\frac{7T}{30\pi^2}\int dk\,\frac{k^4}{k^2 - i\omega/(2D_\eta)}\,. \tag{8.22}$$

This integral is UV divergent. We regulate the divergence by introducing a momentum cutoff Λ. We then expand the integral in the low frequency regime. We get

$$G_R^{xyxy}(\omega,0)\big|_{shear} = -\frac{7}{90\pi^2}T\Lambda^3 - i\omega\,\frac{7T\Lambda}{60\pi^2 D_\eta} + (1+i)\omega^{3/2}\frac{7T}{240\pi D_\eta^{3/2}} + O(\omega^{5/2})\,. \tag{8.23}$$

The physical meaning of these terms can be understood by comparing with the Kubo relation in equ. (8.7). The first term is a fluctuation contribution to the pressure, and the second term is a correction to the shear viscosity. The imaginary part of the third term can be viewed as a frequency dependent correction to the shear viscosity, and the real part is a frequency dependent contribution to the relaxation time which diverges as $\omega^{-1/2}$ in the low frequency limit. The existence of this term is sometimes interpreted as an indication that hydrodynamics breaks down beyond the Navier-Stokes (one-derivative) order.

2. Sound modes: In order to calculate the contribution from sound modes we use equ. (8.20) and (8.21). This leads to two types of terms, depending on whether the real parts of the poles of the propagators in the ω-plane have the same or opposite sign. The contribution from terms with opposite real parts has the same structure as the shear mode term. We get

$$G_R^{xyxy}(\omega,0)\big|_{sound} = \frac{1}{90\pi^2}T\Lambda^3 - i\omega\,\frac{T\Lambda}{30\pi^2\Gamma} + (1+i)\omega^{3/2}\frac{\sqrt{2}T}{120\pi\Gamma^{3/2}} + O(\omega^{5/2})\,. \tag{8.24}$$

The contribution from terms with real parts of the same sign is not infrared sensitive and does not contribute to the retarded correlation function at $O(\omega)$ or $O(\omega^{3/2})$.

3. Shear-sound contribution: The shear-sound contribution has the structure

$$G_R^{xyxy}(\omega,0)\big|_{sh-so} \sim \int_{-\Lambda}^{\Lambda} dk\, \frac{k^4}{k^2 + i(\omega - c_s k)/D_s}\,, \tag{8.25}$$

where $D_s = D_\eta + \Gamma/2$ and the range of the k-integral is $[-\Lambda, \Lambda]$ because of the $k \leftrightarrow -k$ symmetry of the sound propagator in equ. (8.20). We get

$$G_R^{xyxy}(\omega,0)\big|_{sh-so} \sim \frac{D_s^2\Lambda^5}{c_s^2} + i\omega\frac{D_s\Lambda^3}{c_s^2} + O(\omega^2)\,, \tag{8.26}$$

which is suppressed relative to the pure shear and sound contributions by a factor $D_s\Lambda/c_s \ll 1$ (see Sec. 8.4). We also note that the mixed shear-sound term does not give non-analytic terms of the form $\omega^{3/2}$.

4. Diffusive heat modes: The contribution of diffusive heat modes is very similar to the shear term, but the residue of the heat mode is proportional to ω^2/c_s^2 instead of k^2. In the diffusive regime $\omega^2 \ll c_s^2 k^2$. We find

$$G_R^{xyxy}(\omega,0)\big|_{heat} \sim \frac{\omega^2 D_T^2}{c_s^4}\int dk\, \frac{k^2}{k^2 - i\omega/(2D_T)} \sim \frac{\omega^2 D_T^2\Lambda^3}{c_s^4}\,, \tag{8.27}$$

which is much smaller than the shear term.

We conclude that the main contribution arises from the pure shear and sound terms. We will combine these two contributions using the approximation $\Gamma \simeq \frac{4}{3}D_\eta$, which corresponds to the low temperature regime. This is the more interesting regime because D_η is small and the role of fluctuations is enhanced. We find

$$G_R^{xyxy}(\omega,0)\big|_{tot} = const - i\omega\,\frac{17T\Lambda}{120\pi^2 D_\eta} + (1+i)\omega^{3/2}T\frac{7+\left(\frac{3}{2}\right)^{3/2}}{240\pi D_\eta^{3/2}} + O(\omega^2)\,. \tag{8.28}$$

As noted above the $i\omega$ term is a contribution to the shear viscosity. This term is cutoff dependent, but the physical viscosity must be independent of an arbitrary cutoff. This implies that the bare viscosity must be cutoff dependent too, and that the cutoff dependence of the bare viscosity is governed by a renormalization group equation. It is important for the consistency of hydrodynamics as an effective theory that the non-analytic $\omega^{3/2}$ term is not cutoff dependent, because any cutoff dependence in this contribution cannot be absorbed into the parameters of hydrodynamics.

8.4 Phenomenological estimates

In this section we study phenomenological implications of the results derived in the previous section. We have seen that the $i\omega$ term in the retarded correlation function can be combined with the bare shear viscosity to give a physical viscosity

$$\eta_{phys} = \eta + \frac{17}{120\pi^2}\frac{\rho T \Lambda}{\eta}\,. \tag{8.29}$$

An interesting consequence of this result is the fact that the physical viscosity cannot be arbitrary small [76], because equ. (8.29) has a minimum as long as the bare viscosity is positive. The bare viscosity must be positive for the hydrodynamic expansion to be well defined. The value at the minimum depends on the value of the cutoff; the larger the cutoff the stronger the bound on η becomes. The largest possible value of the cutoff is determined by the condition that the gradient expansion on which hydrodynamics is based must be valid for all $k \lesssim \Lambda$. In the following we will study this condition separately in the shear and sound channel.

1. Shear channel: Shear modes are characterized by $\omega \sim D_\eta k^2$. Corrections arise from higher order terms in the derivative expansion. For non-zero frequency the leading correction is due to the relaxation time. We have $\omega \sim D_\eta k^2 \ll \tau_R^{-1}$. For this relation to be maintained for all $k < \Lambda$ we need to require that $\Lambda \lesssim K_{hyd}$ with $K_{hyd} = (\tau_R D_\eta)^{-1/2}$. In kinetic theory $\tau_R = \eta/P$ [52, 63, 62] and

$$K_{hyd} \simeq \frac{1}{D_\eta}\left(\frac{P}{\rho}\right)^{1/2}\,. \tag{8.30}$$

2. Sound channel: In the sound channel we have $\omega \sim c_s k \ll \Gamma k^2$. Using $\Gamma \simeq \frac{4}{3} D_\eta$ we find

$$K_{hyd} \simeq \frac{3}{4D_\eta}\left(\frac{\partial P}{\partial \rho}\right)_s^{1/2}\,. \tag{8.31}$$

For a weakly interacting gas $(\partial P)/(\partial\rho)_s \simeq (5P)/(3\rho)$, and equ. (8.30) differs from equ. (8.31) by a factor very close to one, $\sqrt{16/15} \simeq 1.03$. In the following we will use equ. (8.30) as our estimate for the cutoff. We note that near a critical point the speed of sound can go to zero, and the contribution of sound waves is strongly suppressed relative to shear modes.

It is interesting to consider the microscopic meaning of the ultraviolet scale K_{hyd}. In kinetic theory $\eta \sim n\bar{p} l_{mfp}$, where $\bar{p} \sim \sqrt{mT}$ is the mean momentum, and l_{mfp} is the mean free path. For a weakly interacting gas $P \simeq nT$ and the ultraviolet scale is $K_{hyd} = (\rho/\eta)(P/\rho)^{1/2} \sim l_{mfp}^{-1}$. This is physically reasonable: It does not make sense to consider hydrodynamic fluctuations with wavelengths shorter than the mean free path.

We can illustrate this result further by using the leading order kinetic theory result as an estimate for the bare viscosity. This is consistent because kinetic theory takes into account

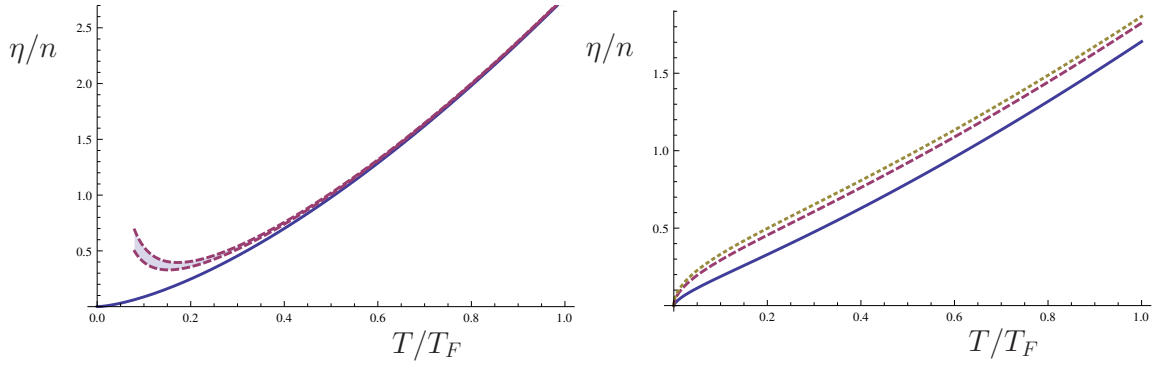

Figure 8.2: Shear viscosity to density ratio η/n as a function of T/T_F, where T_F is the local Fermi temperature. The left panel shows η/n for the unitary gas in three dimensions. The solid line is the result in kinetic theory and the dashed line includes fluctuations. The band shows the uncertainty if the cutoff is varied in the regime $\Lambda = (0.25 - 0.75)K_{hyd}$. The right panel shows the two-dimensional gas at the crossover point $T_{a,2d} = T_F$. The solid line is the kinetic result. The dashed and dotted lines include fluctuations where we have used $\Lambda = K_{hyd}$ and ω was taken to be the frequency of the quadrupole mode in a harmonic trap with $N = 10^4$ and $N = 10^5$ particles.

effects at distances $l \lesssim l_{mfp}$ but, unless stochastic forces are included, it does not take into account fluctuations on length scales $l \gtrsim l_{mfp}$. The kinetic theory result is [97]

$$\eta = \frac{15}{32\sqrt{\pi}} (mT)^{3/2} . \tag{8.32}$$

In Fig. 8.2 we show the bare viscosity and the physical viscosity including the effects of fluctuations. The band shows the uncertainty if the cutoff is varied in the regime $\Lambda = (0.25-0.75)K_{hyd}$. We observe that the viscosity has a minimum $\eta/n \simeq 0.5$ at a temperature $T \simeq 0.2T_F$, close to the critical temperature $T_c = 0.167(13)T_F$ [77]. Note that the increase of the shear viscosity at low temperature does not imply a breakdown of the hydrodynamic expansion: In this regime the one-loop graph is large compared to the bare viscosity, but the power counting discussed in A.1 ensures that graphs with more loops are suppressed.

The increase of the shear viscosity in the low temperature regime is related to a non-analytic frequency dependence of $\eta(\omega) = -\mathrm{Im}\, G_R^{xyxy}(\omega, \mathbf{k}{=}0)$. Equ. (8.28) implies that for small ω

$$\eta(\omega) = \eta - \sqrt{\omega}\, T\, \frac{7 + \left(\frac{3}{2}\right)^{3/2}}{240\pi D_\eta^{3/2}} . \tag{8.33}$$

The width of the non-analytic structure in the spectral function can be estimated by assuming that the fluctuation term in the physical shear viscosity, the second term in equ. (8.29), is due

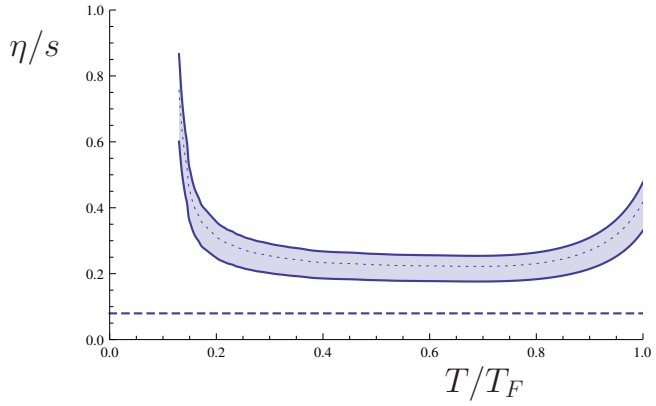

Figure 8.3: Bound on the shear viscosity to entropy density ratio η/s as a function of T/T_F, where T_F is the local Fermi temperature. This figure shows the bound given in equ. (8.35) evaluated using measurements of thermodynamic properties reported in [77]. The band around the dotted line shows the sensitivity to variations in the cutoff in the range $\Lambda = (0.5 \pm 0.25) K_{hyd}$. The dashed line shows the string theory bound $\eta/s = 1/(4\pi)$.

to the non-analytic term in the spectral function. This assumption leads to $\Delta\omega \simeq 0.3T(n/\eta)$, where we have used $\Lambda \simeq 0.5 K_{hyd}$.

8.5 The bound on η/s

The model discussed in the previous section shows that even if the bare viscosity goes to zero the physical viscosity always finite. In this section we show that there is a lower bound on η/s which does not depend on assumptions about the temperature dependence of the bare viscosity. Equ. (8.29) implies

$$\left(\frac{\eta}{s}\right)_{phys} = \frac{\eta}{s} + \frac{17}{\sqrt{2}\,80}\left(\frac{s}{\eta}\right)^2\left(\frac{T}{T_F}\right)^{3/2}\left(\frac{n}{s}\right)^3\left(\frac{P}{nT}\right)^{1/2}\left(\frac{\Lambda}{K_{hyd}}\right). \tag{8.34}$$

Minimizing this expression with respect to the bare viscosity we find

$$\left(\frac{\eta}{s}\right)_{phys} \gtrsim 1.005\left(\frac{T}{T_F}\right)^{1/2}\left(\frac{n}{s}\right)\left(\frac{P}{nT}\right)^{1/6}\left(\frac{\Lambda}{K_{hyd}}\right)^{1/3}. \tag{8.35}$$

This expression depends on the thermodynamic quantities s/n and $P/(nT)$, but we note that the bound on $(\eta/s)_{phys}$ always has a minimum at some temperature of order T_c. To see this we note that $(s/n) \sim T^3$ and $P/(nT) \sim n^{1/3}/(mT)$ for $T \ll T_c$, whereas $(s/n) \sim \log(T)$ and $P/(nT) \sim 1$ for $T \gg T_c$. This implies that the bound scales as $T^{-16/6}$ at low T, and as

$T^{1/2}/\log(T)$ at high T. In order to be more quantitative we have evaluated equ. (8.35) using the equation of state measured by the MIT group [77], see Fig. 8.3.

The remaining uncertainty is related to the value of the cutoff. The validity of hydrodynamics implies that Λ cannot be much smaller than K_{hyd}. This statement can be quantified by analyzing the data on collective modes published by the Duke group [64]. For the specific trap parameters used in that experiment the radial breathing mode was found to behave hydrodynamically for temperatures $T \lesssim 0.8 T_F$, see [116]. This implies that[1] $\omega/(D_\eta \Lambda^2) \gtrsim \omega/(D_\eta K_{hyd}^2) \simeq 0.5$. In order for the expansion parameter to satisfy $\omega/(D_\eta\Lambda^2) < 1$ the cutoff Λ cannot be much smaller than K_{hyd}. On the other hand, Λ also cannot be much bigger than K_{hyd} because then higher loop corrections are not suppressed, see A.1. In Fig. 8.3 we have used $\Lambda/K_{hyd} = 0.5 \pm 0.25$. We note that the bound on η/s scales as $(\Lambda/K_{hyd})^{1/3}$, and is only weakly sensitive to the uncertainty in the cutoff.

We obtain a fairly broad minimum $(\eta/s)_{phys} \gtrsim 0.2$ in the regime $T/T_F \sim (0.3 - 0.9)$. The bound on η/s becomes large as $T \to 0$ and $T \to \infty$, consistent with the expectation from kinetic theory which predicts $\eta/s \sim (T_F/T)^8$ at low temperature and $\eta/s \sim (T/T_F)^{3/2}/\log(T/T_F)$ at high temperature [97, 113, 87]. The bound is compatible with the experimental results reported by Cao et al. [26] and the T-matrix calculation of Enss et al. [124], but lager than the Path Integral Monte Carlo (PIMC) results obtained by Wlazlowski et al. [136]. These authors find $(\eta/s)_{min} \sim 0.2$ at temperatures $0.15 T_F \lesssim T \lesssim 0.25 T_F$. A possible reason for the discrepancy is that for the lattice spacing used in [136] one cannot resolve the non-analytic behavior of the spectral function given in equ. (8.33).

8.6 Two dimensional systems

It is interesting to consider the role of fluctuations in two dimensional systems. The results in Sect. 8.3 are easily generalized to two spatial dimensions. Aside from the obvious substitution $d^3k/(2\pi)^3 \to d^2k/(2\pi)^2$ the only difference is that in two spatial dimensions the shear contribution to the sound attenuation constant is $\Gamma = D_\eta$ instead of $\Gamma = \frac{4}{3} D_\eta$. In both two and three dimensions the dominant contribution to G_R^{xyxy} arises from the one loop diagram involving either a pair of shear modes or a pair of sound modes. In $d = 2$ the loop integral is logarithmically divergent and

$$G_R^{xyxy}(\omega, 0)\big|_{tot} = const - i\omega \, \frac{T}{16\pi D_\eta} \left[\log\left(\frac{\sqrt{2} D_\eta \Lambda^2}{\omega} \right) + i \frac{\pi}{2} \right] . \tag{8.36}$$

[1] We have used the trap parameters given in Sect. 8.7 below.

The imaginary part can be interpreted as a correction to the shear viscosity. We find

$$\eta_{phys} = \eta + \frac{mT}{16\pi}\frac{n}{\eta}\log\left(\frac{\sqrt{2}\Lambda^2}{m\omega}\frac{\eta}{n}\right) \tag{8.37}$$

which diverges logarithmically as $\omega \to 0$. This divergence is well known [46, 49, 73], and it has been observed in molecular dynamics and lattice gas simulations [3, 69]. To the best of our knowledge it has not been observed experimentally. Equ. (8.37) shows that the effect is large in systems that have a small value of the bare shear viscosity.

The shear viscosity of a dilute two-dimensional Fermi gas was recently computed in [115, 19]. The result is

$$\eta = \frac{mT}{2\pi^2}\left(\left[\log\left(\frac{5T}{2T_{a,2d}}\right)\right]^2 + \pi^2\right), \tag{8.38}$$

where $T_{a,2d} = 1/(ma_{2d})^2$ and a_{2d} is the scattering length in two dimensions [107]. In two dimensions there is no scale invariant fluid except in the non-interacting limit $a_{2d} \to 0$. The most strongly correlated fluid corresponds to $T_{a,2d} \simeq T_F$, which implies that the dimer binding energy is equal to the Fermi energy. The viscosity of the two dimensional gas was recently studied by measuring the damping of the quadrupole mode [132] in a harmonic potential. The frequency of this mode is $\omega = \sqrt{2}\omega_\perp$, where $\omega_\perp$ is the two dimensional oscillator frequency. The confinement frequency sets the scale for the Fermi temperature of the trap, $T_F^{trap} = N^{1/2}\omega^\perp$. We can use these relations to translate the frequency dependence of the shear viscosity into the dependence on the number of particles. In Fig. 8.2 we show the kinetic theory result as well as the viscosity with fluctuations included for two different values of the particle number. The main dependence on N is of the form $(\eta/n)_{phys} \sim \frac{1}{16\pi}\log(N)$. We observe that fluctuations make a significant contribution to the shear viscosity, but the logarithmic divergence with N is fairly slow, and one will need significantly larger numbers of particles than what is available in current experiments ($N \simeq 4 \cdot 10^3$ in [132]) to see the effect clearly.

8.7 Trapped atomic gases

In this section we will try to make contact with experiments that study the damping of collective modes in trapped Fermi gases. We are interested in the question whether it is possible to establish the role of hydrodynamic fluctuations by studying the scaling of the damping constant with temperature or particle number. A review of the hydrodynamic theory of collective modes can be found in [116].

Consider a trapped gas with N particles in a harmonic potential with trapping frequencies $\omega_x = \omega_y = \omega_\perp$ and $\omega_z = \lambda\omega_\perp$. In a typical experiment $N = (10^5 - 10^6)$ and $\lambda = (0.02 - 0.05)$

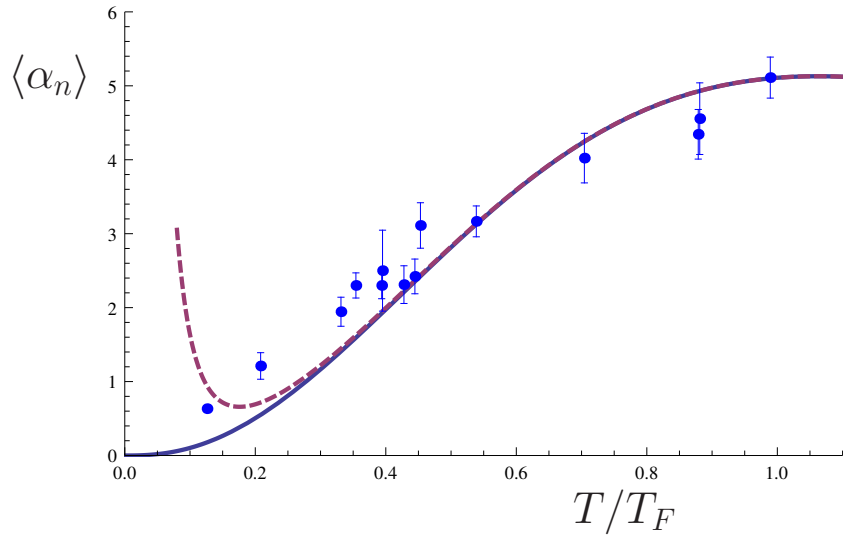

Figure 8.4: Trap averaged shear viscosity to density ratio $\langle \alpha_n \rangle$. We show $\langle \alpha_n \rangle$ as a function of T/T_F^{trap}, where $T_F^{trap} = (3\lambda N)^{1/3}\omega_\perp$ is the Fermi temperature of the trap. We have chosen $N = 2 \cdot 10^5$ and $\lambda = 0.045$ as in [64]. The solid line shows the kinetic theory result, the dashed line includes fluctuation corrections to the shear viscosity. The data are from [27], which is a reanalysis of the results reported in [64]. We do not show data in the superfluid regime $T \ll T_c$.

[74, 11, 64, 5]. The transverse breathing mode has a frequency $\omega = \sqrt{10/3}\,\omega_\perp$ and the damping constant is

$$\Gamma_{br} = \frac{\langle \alpha_n \rangle}{(3N\lambda)^{1/3}} \frac{\omega_\perp}{(E_0/[N\epsilon_F])}\,, \tag{8.39}$$

where E_0 is the total (potential and internal) energy of the trapped gas, $\epsilon_F = (3N\lambda)^{1/3}\omega_\perp$ is the Fermi energy of the trapped system, and $\langle \alpha_n \rangle = \frac{1}{N}\int d^3x\, \eta(x)$ is the trap average of the shear viscosity. Taking into account relaxation time effects we have

$$\langle \alpha_n \rangle = \frac{1}{N}\int d^3x\, \frac{\eta(x)}{1+\omega^2\tau_R(x)^2}\,. \tag{8.40}$$

We take the bare shear viscosity from kinetic theory, equ. (8.32), and compute the physical viscosity from equ. (8.34). We note that the bare viscosity only depends on T, which is independent of the position in the trap. The fluctuation term is largest at the center of the trap. We also use kinetic theory to determine the bare relaxation time, $\tau_R = \eta/P$, and use equ. (8.28) to determine the physical relaxation time. This corresponds to

$$(\tau_R\eta)_{phys} = \tau_R\eta + \frac{\left[7 + \left(\frac{3}{2}\right)^{3/2}\right] T}{240\pi\omega^{1/2}} \left(\frac{\rho}{\eta}\right)^{3/2}\,. \tag{8.41}$$

We note that the bare relaxation time is inversely proportional to the local pressure and depends on the position in the trap. In particular, $\tau_R\eta$ is large in the dilute part of the cloud. Fluctuations, on the other hand, increase the relaxation time near the center of the trap.

In the following we will use the high temperature approximation for the density of the cloud. This is consistent with using kinetic theory for the bare shear viscosity and relaxation time. It also provides a very accurate description of the tail of the density distribution at essentially all temperatures. We have

$$n(x) = N\left(\frac{m\bar{\omega}^2}{2\pi T}\right)^{3/2} \exp\left(-\sum_i \frac{m\omega_i^2 x_i^2}{2T}\right), \tag{8.42}$$

where $\bar{\omega} = (\omega_\perp^2\omega_z)^{1/3}$. Results for $\langle\alpha_n\rangle$ as a function of T/T_F^{trap} with $T_F^{trap} = (3N\lambda)^{1/3}\omega_\perp$ are shown in Fig. 8.4. We have used $N = 2\cdot 10^5$ and $\lambda = 0.045$ as in the experiment of Kinast et al. [64]. The solid line shows the result using kinetic theory for η and τ_R, and the dashed line includes the fluctuation term in η. We find that for the parameters considered here corrections to the relaxation time are very small.

We observe that kinetic theory describes the data for $T \gtrsim 0.4T_F^{trap}$ well. Fluctuations are important for $T \lesssim 0.2T_F^{trap}$, leading to a minimum in $\langle\alpha_n\rangle$. We note that the critical temperature is $T_c \simeq 0.2T_F^{trap}$ [83], and we do not expect the theory used in this section, which is based on kinetic theory in the dilute limit, to reproduce experiment for $T \ll T_c$. It was recently suggested that the data in this regime are dominated by the transition from hydrodynamic to ballistic behavior [84].

Finally, we have looked at the role of fluctuations in the experiment of Vogt et al. [132]. In this experiment the damping of two dimensional quadrupole mode was measured for $N = 4\cdot 10^3$. The dependence on the scattering length was studied for $\log(k_F a_{2d}) > 0$ at $T/T_F = 0.48$, and the temperature dependence was studied in the range $T/T_F^{trap} = (0.3 - 0.8)$ for $\log(k_F a_{2d}) = (2.7 - 42)$. We find that for this range of parameters the role of fluctuations is always small. Fluctuations lead to a significant enhancement of the damping constant if $\log(k_F a_{2d}) \sim 0$ and $N \gtrsim 10^5$. This enhancement grow as $\log(N)$, but the logarithmic growth is difficult to disentangle from a $\log(N)$ term related to the dilute corona, see [115].

8.8 Conclusions and outlook

We have studied the role of hydrodynamics fluctuations in the dilute Fermi gas. Our main findings are:

1. Hydrodynamic fluctuations imply the existence of a minimum in the shear viscosity. The physical origin of the minimum is the contribution of shear and sound modes to momen-

tum transport. If the bare viscosity is small, then sound and shear modes are weakly damped and the contribution of hydrodynamic modes to momentum transport is large. The magnitude of the minimum shear viscosity is weakly dependent on the cutoff scale of the hydrodynamic description. Allowing for a factor of two uncertainty in our estimate of Λ we find $\eta/s \gtrsim 0.2$. The uncertainty can be reduced by computing higher loop corrections. Our estimate is consistent with trap averaged measurements of η/s reported in [26], but not with recent lattice calculations [136].

2. Contrary to the proposed string theory limit $\eta/s \geq 1/(4\pi)$ the bound is not universal. It depends on thermodynamic properties and the breakdown scale of hydrodynamics. We note that the bound itself is purely classical, $\hbar$ only enters though thermodynamic quantities. Ignoring numerical factors we have $\eta/s \gtrsim (n/s)(mT/n^{2/3})^{1/2}(P/(nT))^{1/6}$. At large temperature the ratio n/s depends weakly on T and the bound grows as $T^{1/2}$. At low T the entropy per particle increases sharply when the system reaches quantum degeneracy, which corresponds to $mT \sim \hbar^2 n^{2/3}$. This implies that at the minimum $\eta/s \sim \hbar$.

3. Fluctuations cause a $1/\sqrt{\omega}$ divergence of the viscous relaxation time in three dimensions, and a $\log(\omega)$ divergence of the shear viscosity in two dimensions. These effects are independent of the cutoff and only depend on the value of the bare shear viscosity. The existence of non-analytic terms implies that, strictly speaking, the two dimensional Navier-Stokes equation as well as the three dimensional second order (Burnett) equations are not consistent unless fluctuating forces are taken into account. We note, however, that real flows that can be studied in experiment involve finite frequencies or time scales, and fluctuating forces may not be important.

4. We have studied the importance of fluctuations for the damping of trapped Fermi gases. The corrections are generally small for the conditions that have been experimentally investigated. A possible exception is the three dimensional unitary gas near T_c. In this case fluctuations may lead to enhanced damping[2]. Fluctuations lead to a $\log(N)$ divergence in the damping constant of the two dimensional Fermi gas, but this effect is difficult to observe unless the number of particles is varied by more than an order of magnitude.

There are a number of interesting formal questions that we have not studied in this paper. In order to study higher order corrections it is useful to start from an effective action for hydrodynamic fluctuations. This could be done using the methods developed in [72, 75]. The effective

[2]Note that we have not considered the role of critical fluctuations. The superfluid transition is described by model F in the classification of Hohenberg and Halperin [60]. This model does not contain direct couplings between the order parameter and the momentum density, and the calculation discussed in our work is not directly affected by critical fluctuations.

action might also be useful for studying the renormalization group evolution in more detail. In this work we have simply assumed that the bare shear viscosity can be computed in kinetic theory. It would be desirable to provide a more rigorous justification for this approximation by studying the matching between kinetic theory and hydrodynamics. Finally, in this work we have restricted ourselves to studying the effect of fluctuations on the damping of collective modes. In this case it is straightforward to take into account a frequency dependent shear viscosity and relaxation time. If one considers hydrodynamic flows that are not periodic in time, for example the elliptic flow experiment described in [26], one has to solve the hydrodynamic equations with fluctuating forces. This method has been studied in the context of microfluidic systems, see [10] and references therein.

We have shown that hydrodynamic fluctuations are important if the bare viscosity is small in the low temperature limit. The main physical question is whether this scenario is realized in the unitary Fermi gas near T_c, or whether other effects, like pairing correlations, a pseudo-gap or phonons are more important [124, 20, 57, 58]. This question is probably difficult to address experimentally, but it can be studied by analyzing the spectral function of the stress tensor. For this purpose it is necessary to construct models of the spectral function that include fluctuations. These models can be confronted with quantum Monte Carlo data, for example the recent work of Wlazlowski et al. [136].

Chapter 9

Outlook

Ultracold gases have given us access to quantum many-body systems in which the number of particles, their interactions, and the external potential can be experimentally controlled. Typical systems are dilute so that the interaction is dominated by short range two-body forces that can be modelled in terms of very simple effective interactions. Despite the diluteness of the gas and the simplicity of the interaction ultracold Fermi gases can be used to explore the regime of strong correlations. In this regime the many-body function is not well described by Hartree-Fock or similar approximations, the mean free path is short, and hydrodynamic behavior is observed even in very small systems. The simplest system in which strong correlations have been realized is the dilute Fermi gas at unitarity. As a consequence is serves as a model for strong correlations in many fields of physics, from neutron stars to high T_c superconductors and quark gluon plasmas.

The conceptual schism between statistical mechanics, classical mechanics and many-body quantum mechanics puts us in a weak position to investigate the extent to which hydrodynamic and thermodynamic variables are relevant to such systems. Certainly, we have ways of altering the internal energy that is evocative of heating. Near unitarity, fermionic gases exhibit hydrodynamic behavior in the one-body density function. From here we can pursue the origins of the classical behavior further using these systems as probes for crossover from quantum to classical evolution. Alternately, one can embrace the evidence for such classical motion and apply the symmetry constraints and established response theory to constrain their behavior. The most celebrated aspect of this later program is the proposed quantum bound on the viscosity to entropy density ratio η/s.

Ultimately, both approaches have value. The latter one is the most pursued in theory and experiment. We have argued here that these systems should often hold some history dependent features that are inconsistent with a thermodynamic description. The foundation of this argument is that a single wavefunction picture (pure state) is sufficient for a robust explanation of

the classical world and thermodynamics when the observed kinematic constraints are present in the initial many-body states. The opportunity here is to find what states do correspond to a well defined temperature and how the others attain this for large N and sufficiently large internal energy. This amounts to a claim that the "thermodynamic limit" is not just one of large N but of sufficiently large and varied internal excitation. The anisotropy induced by the confining potentials also provide an opportunity to probe for nonextensive thermodynamics, generally only considered for self bound systems too large to examine, and when there is a minimum scale on which temperature can meaningfully be defined.

Hydrodynamics is a local statement of momentum conservation but, for gases, its kinematics is intrinsically tied up with thermodynamic properties. Viscosity depends on thermal mass transport on faster scales than defined by the bulk flow. The classical gas expansions have run into problems with convergence both in the Chapman-Enskog theory and the BBGKY hierarchy. A study of fluctuations, that has been so successful in the analysis of universality classes and critical points of liquids, when extended to viscous flow, implies a minimum in the viscosity to entropy density ratio and a more subtle nonanalytic failure of such expansions at fractional order. One way to interpret this is to is that hydro "breaks."

This is a little unsatisfying and it is not clear if such arguments are relevant to such small traps. In any case, some extended set of continuum variables seems like it should extend the expansion in a meaningful way since we don't expect discontinuous behavior for such a large dense gaseous system. Extended thermodynamics is on approach used to solve causality problems in thermo. Diffusive quantities like temperature are revived as hyperbolic functions as in the Cattaneo equation [28]. This runs into the same problems found in the radiation reaction problem of electrodynamics [110]. There are now an unphysical number of degrees of freedom. Attempts to repair this universally introduce some acausal behavior.

The use of pseudomomentum to extract real forces is always tricky and, while sometimes successful, many failures have resulted. Field theoretic methods using quasiparticles invariably involve pseudomomentum conservation among diagrams. This is probably the one most important area where this method of calculation could be improved. The term "liquid" gets used by quantum theorists and most scientists in different ways. The electron sea of a metal is sometimes referred to as a quantum liquid since it is highly correlated. A molecular liquid, like water, is a largely incompressible entity that we usually think of when looking for examples for hydrodynamics. The forces across this kind of liquid are invariably dominated by bond strain. The mass transport the mediates viscosity in gases in minuscule here due to the short mean free paths. Pseudomomentum can mix momentum transport and stresses in nonintuitive ways. For ultracold gases thermal transport can be very low. Damping stress might be mediated by the molecular bonding in the gas. A more concrete understanding of how this relates to the fluctuations would be desirable.

The notion of damping in quantum systems is not intuitive. Any system can be decomposed in terms of eigenstates so that it is not clear that attenuation occurs. As an example we can think of conduction in a perfect crystal. The electron eigenstates are traveling waves (equivalently, pairs of out-of-phase standing waves). Introduction of defects eventually leads to Anderson localization where no percolating traveling waves exists. Traveling packets will eventually rebound and degenerate into a high frequency noise. For this reason, linear response theory makes most sense as a kind of scattering result where transverse motions would have to be highly occupied to give opposing currents to the incident current being scattered.

For the oscillations of trapped ultracold gas clouds, damping must similarly give a measure of the extent that observable radial motions degenerate into high frequency radial and angular motions. This informs us that the decomposition into eigenstates of these bulk motions must involve many frequencies of many states. It is not immediately obvious how to describe this as a scattering theory but the condition equ. 4.2 gives a suggestion. The currents at the two-body scattering centers must be imbalances and scatter in some incoherent fashion so that they are not destructively cancelled. This seems like a promising direction for further work that would show the extent to which the more phenomenological hydrodynamic approaches and more intrinsically quantum (but less computationally tractable) approaches overlap.

REFERENCES

[1] R. H. Abraham and J. E. Marsden. *Foundations of Mechanics*. AMS Chelsea publishing. AMS Chelsea Pub./American Mathematical Society, 2008.

[2] A. Adams, L. D. Carr, T. Schäfer, P. Steinberg, and J. E. Thomas. 'strongly correlated quantum fluids: Ultracold quantum gases, quantum chromodynamic plasmas, and holographic duality. *New J. Phys.*, **14**:115009, 2012.

[3] B. J. Alder and T. E. Wainwright. Velocity autocorrelations for hard spheres. *Phys. Rev. Lett.*, **18**:988, 1967.

[4] A. Altmeyer, S. Riedl, C. Kohstall, M. Wright, J. Hecker Denschlag, and R. Grimm. Note on collective excitations of a degenerate gas at.... *Phys. Rev. Lett.*, **98**:103602, 2007.

[5] A. Altmeyer, S. Riedl, C. Kohstall, M. Wright, R. Geursen, M. Bartenstein, C. Chin, J. Hecker Denschlag, and R. Grimm. Precision measurements of coll. oscillations in the bec-bcs crossover. *Phys. Rev. Lett.*, **98**:040401, 2007.

[6] L. D. Landau and E. M. Lifshitz. *Statistical Mechanics, Part II, Part II Course of Theoretical Physics, Vol.IX*. Pergamon Press, 1981.

[7] N. W. Ashcroft and N. D. Mermin. *Solid State Physics*. Saunders College, Philadelphia, 1976.

[8] J. E. Thomas B. Clancy, L. Luo. Observation of nearly perfect irrotational flow in normal and superfluid strongly interacting fermi gases. *Phys. Rev. Lett.*, **99**:140401, 2007.

[9] R. Baier, P. Romatschke, D. T. Son, A. O. Starinets, and M. A. Stephanov. Relativistic viscous hydrodynamics, conformal invariance, and holography. *JHEP*, **0804**:100, 2008.

[10] F. B. Balboa, J. B. Bell, R. Delgado-Buscalioni, A. Donev, T. G. Fai, B. E. Griffith, and C. S. Peskin. Staggered schemes for fluctuating hydrodynamics. 2011.

[11] M. Bartenstein, A. Altmeyer, S. Riedl, S. Jochim, and C. Chin. Collective excitiations of a degenerate gas at the bec-bcs crossover. *Phys. Rev. Lett.*, 92:203201, 2004.

[12] G. K. Batchelor. *An Introduction to Fluid Dynamics*. February 2000.

[13] J. S. Bell. On the problem of hidden variables in quantum mechanics. *Reviews of Modern Physics*, 38:447–452, July 1966.

[14] N. N. Bogoliubov. A new method in the theory of superconductivity. *Sov. Phys. JETP*, 46, June 1958.

[15] N. Bohr and L. Rosenfeld. Field and charge measurements in quantum electrodynamics. *Phys. Rev.*, 78(6):794–798, June 1950.

[16] Ludwig Boltzmann. *Lectures on Gas Theory*. University of California Press, english edition edition, 1964.

[17] M. Braby, J. Chao, and T. Schäfer. Thermal conductivity and sound attenuation in dilute atomic fermi gases. *Phys. Rev. A*, **82**:033619, 2010.

[18] D. C Brody, D. W Hook, and L. P Hughston. Microcanonical distributions for quantum systems. *eprint arXiv:quant-ph/0506163*, June 2005.

[19] G. M. Bruun. Shear viscosity and spin-diffusion coefficient of a two-dimensional fermi gas: Evolution from cooper pairing to bose condensation. *Phys. Rev. B*, **41**:327, 1990.

[20] G. M. Bruun and H. Smith. Shear viscosity and damping for a fermi gas in the unitarity limit. *Phys. Rev. A*, **75**:043612, 2007.

[21] A. Bulgac and G. F. Bertsch. Collective oscillations of a trapped fermi gas near the unitary limit'. *Phys. Rev. Lett.*, **94**:070401, 2005.

[22] A. Bulgac, J. E. Drut, and P. Magierski. Quantum monte carlo simulations of the bcs-bec crossover at finite temperature. *Phys. Rev. A*, **78**:0233625, 2008.

[23] C. P. Burgess. Goldstone and pseudo-goldstone bosons in nuclear, particle and condensed matter physics. *Phys. Rept.*, **330**:193, 2000.

[24] F. Laloe C. Cohen-Tannoudji, B. Diu, editor. *Quantum Mechanics*, volume 1. Wiley, New York, 1977. Two volumes.

[25] A. O. Caldeira and A. J. Leggett. Influence of dissipation on quantum tunneling in macroscopic systems. *Physical Review Letters*, 46:211–214, January 1981.

[26] C. Cao, E. Elliott, and H. Wu J. Joseph. Observation of universal temperature scaling in the quantum viscosity of a unitary fermi gas. *arXiv:1007.2625 [cond-mat.quant-gas]*, 2011.

[27] C. Cao, E. Elliott, H. Wu, and J. E. Thomas. Searching for perfect fluids: Quantum viscosity in a universal fermi gas. *New J. Phys.*, **13**:075007, 2011.

[28] C. Cattaneo, J.K. de Fériet, and Académie des sciences (France). *Sur une forme de l'équation de la chaleur éliminant le paradoxe d'une propagation instantanée*. Comptes rendus hebdomadaires des séances de l'Académie des sciences. Gauthier-Villars, 1958.

[29] D. M. Ceperley. Fermion nodes. *Journal of Statistical Physics*, 63:1237–1267, June 1991.

[30] C. Chafin and T. Schaefer. Scale breaking and fluid dynamics in a dilute two-dimensional Fermi gas. *ArXiv e-prints*, August 2013.

[31] C. Chafin and T. Schäfer. Hydrodynamic fluctuations and the minimum shear viscosity of the dilute Fermi gas at unitarity. *Phys. Rev. A*, 87(2):023629, February 2013.

[32] S. Chapman and T. G. Cowling. *The mathematical theory of non-uniform gases*. Cambridge University Press, Cambridge, 3 edition, 1990.

[33] Alexandre Joel Chorin and Jerrold E. Marsden. *A mathematical introduction to fluid mechanics*. Universitext. Springer-Verlag, New York, N.Y., Heidelberg, Berlin, 1979.

[34] B. Clancy. *Hydrodynamics of a Rotating Strongly Interacting Fermi Gas*. PhD thesis, Duke U., 2008.

[35] E. G .D. Cohen, editor. *Fundamental Problems in Statistical Mechanics*, volume 5. North Holland, 1980.

[36] E.G.D. Cohen. Fifty years of kinetic theory. *Physica A: Statistical Mechanics and its Applications*, 194(1):229–257, 1993.

[37] M. Cozzini and S. Stringari. Fermi Gases in Slowly Rotating Traps: Superfluid versus Collisional Hydrodynamics. *Physical Review Letters*, 91(7):070401, August 2003.

[38] M. J. Savage D. B. Kaplan and M. B. Wise. A new expansion for nucleon-nucleon interactions. *Phys. Lett. B*, **424**:390, 1998.

[39] F. Dalfovo, S. Giorgini, L. P. Pitaevskii, and S. Stringari. Theory of bose-einstein condensation in trapped gases. *Rev. Mod. Phys.*, 71:463–512, Apr 1999.

[40] P. Danielewicz and M. Gyulassy. Dissipative phenomena in quark gluon plasmas. *Phys. Rev. D*, **31**:53, 1985.

[41] L. Desvillettes and C. Villani. On the trend to global equilibrium for spatially inhomogeneous kinetic systems: The boltzmann equation. *Comm. Pure Appl. Math*, 54:1–42, 2003.

[42] P. A. M. Dirac. *The Principles of Quantum Mechanics*. Number 27 in The International Series of Monographs on Physics. Clarendon Press, Oxford, 4 edition, 1967.

[43] C. De Dominicis and L. Peliti. Field theory renormalization and critical dynamics above t_c: Helium, antiferromagnets and liquid gas systems. *Phys. Rev. B*, **18**:353, 1978.

[44] M. Edwards, C. W. Clark, P. Pedri, L. Pitaevskii, and S. Stringari. Consequence of superfluidity on the expansion of a rotating bose-einstein condensate. *Phys. Rev. Lett.*, **88**:070405, 2002.

[45] A. Einstein, B. Podolsky, and N. Rosen. Can quantum-mechanical description of physical reality be considered complete? *Physical Review*, 47:777–780, May 1935.

[46] M. H. Ernst, E. H. Hauge, and J. M. J. van Leeuwen. Large-distance and long-time properties of a randomly stirred fluid. *Phys. Rev. A*, **16**:732, 1977.

[47] J. Esteve, J.-B. Trebbia, T. Schumm, A. Aspect, C. I. Westbrook, and I. Bouchoule. Observations of density fluctuations in an elongated bose gas: Ideal gas and quasicondensate regimes. *Physical Review Letters*, 96(13):130403, April 2006.

[48] H. Everett. "Relative state" formulation of quantum mechanics. *Reviews of Modern Physics*, 29:454–462, July 1957.

[49] D. Forster, D. R. Nelson, and M. J. Stephen. Large-distance and long-time properties of a randomly stirred fluid. *Phys. Rev. A*, **16**:732, 1977.

[50] R. F. Fox and G. E. Uhlenbeck. Contributions to non-equilibrium thermodynamics. i. theory of hydrodynamical fluctuations. *Phys. Fluids*, **13**:1893, 1970.

[51] H. Smith G. M. Bruun. Viscosity and thermal relaxation for a resonantly interacting gas. *Phys. Rev. A*, **72**:043605, 2005.

[52] H. Smith G. M. Bruun. Frequency and damping of the scissors mode of a fermi gas. *Phys. Rev. A*, **76**:045602, 2007.

[53] H. Smith G. M. Bruun. Shear viscosity and damping for a fermi gas in the unitarity limit. *Phys. Rev. A*, **75**:043612, 2007.

[54] B. A. Gelman, E. V. Shuryak, and I. Zahed. An ultracold strongly coupled gas: a near-ideal liquid. *Phys. Rev. A*, **72**:043601, 2005.

[55] S. Goldstein, J. L. Lebowitz, C. Mastrodonato, R. Tumulka, and N. Zanghi. Approach to thermal equilibrium of macroscopic quantum systems. *Phys. Rev. E*, 81(1), January 2010.

[56] A. Griffin, T. Nikuni, and E. Zaremba. *Bose-condensed gases at finite temperature*. Cambridge University Press, 2009.

[57] C. C. Chien H. Guo, D. Wulin and K. Levin. Microscopic approach to shear viscosities in superfluid gases: From bcs to bec. *Phys. Rev. Lett.*, **107**:020403, 2011.

[58] C.-C. Chien H. Guo, D. Wulin and K. Levin. Perfect fluids and bad metals: Transport analogies between ultracold fermi gases and high t_c superconductors. *New J. Phys.*, **13**:075011, 2011.

[59] H. Heiselberg. Collective modes of trapped gases at the bec-bcs crossover. *Phys. Rev. Lett.*, **108**:249904, 2012.

[60] P. C. Hohenberg and B. I. Halperin. Theory of dynamic critical phenomena. *Rev. Mod. Phys.*, **49**:435, 1977.

[61] S. Reddy J. Carlson. Asymmetric two-component fermion systems in strong coupling. *Phys. Rev. Lett.*, **95**:060401, 2005.

[62] T. Schäfer J. Chao. Conformal symmetry and non-relativistic second order fluid dynamics. *Annals Phys.*, **327**:1852, 2012.

[63] T. Schäfer J. Chao, M. Braby. Viscosity spectral functions of the dilute fermi gas in kinetic theory,. *New J. Phys.*, **13**:035014, 2011.

[64] J. E. Thomas J. Kinast, A. Turlapov. Two transitions in the damping of a unitary fermi gas. *Phys. Rev. Lett.*, **94**:170404, 2005.

[65] M. E. Gehm J. Kinast, S. L. Hemmer. Evidence for superfluidity in a resonantly interacting fermi gas. *Phys. Rev. Lett.*, **92**:150402, 2004.

[66] Max Jammer. *The Philosophy of Quantum Mechanics; the Interpretations of Quantum Mechanics in Historical Perspective*. Wiley, 1974.

[67] C. Jarzynski. Nonequilibrium work relations: foundations and applications. *The European Physical Journal B - Condensed Matter and Complex Systems*, 64(3):331–340, 2008.

[68] J.H. Jeans. *The Dynamical Theory of Gases*. The University Press, 1904.

[69] L. P. Kadanoff, G. R. McNamara, and G. Zanetti. From automata to fluid flow: Comparisons of simulation and theory. *Phys. Rev. A*, **40**:4527, 1989.

[70] N. G. Van Kampen. The case against linear response theory. *Phys. Norv.*, 5:279, 1971.

[71] I. M. Khalatnikov. *Introduction to the Theory of Superfluidity*. Benjamin, New York, 1965.

[72] I. M. Khalatnikov, V. V. Lebedev, and A. I. Sukhorukov. Diagram technique for calculating long wave fluctuation effects. *Phys. Lett. A*, **94**:271, 1983.

[73] I. M. Khalatnikov, V. V. Lebedev, and A. I. Sukhorukov. Fluctuation effects in two-dimensional hydrodynamic systems. *Physica A*, **126**:135, 1984.

[74] J. Kinast, A. Turlapov, and J. E. Thomas. Breakdown of hydrodynamics in the radial breathing mode of a strongly-interacting fermi gas. *Phys. Rev. A*, 70:051401(R), 2004.

[75] P. Kovtun. Lectures on hydrodynamic fluctuations in relativistic theories. *J. Phys. A: Math. Theor.*, **45**:473001, 2012.

[76] P. Kovtun, G. D. Moore, and P. Romatschke. The stickiness of sound: An absolute lower limit on viscosity and the breakdown of second order relativistic hydrodynamics. *Phys. Rev. D*, **84**:025006, 2011.

[77] M. J. H. Ku, A. T. Somme, L. W. Cheuk, and M. W. Zwierlein. Revealing the superfluid lambda transition in the universal thermodynamics of a unitary fermi gas. *Science*, 335:563, 2012.

[78] J. E. Thomas L. Luo. Thermodynamic measurements in a strongly interacting fermi gas. *J. Low Temp. Phys.*, **154**:1, 2009.

[79] F. J. Uribea L. S. Garcia-Colina, R. M. Velascoa. Beyond the navier-stokes equations: Burnett hydrodynamics. *Phys. Rep.*, **465**:149, 2008.

[80] L. D. Landau and E. M. Lifshitz. *Statistical Physics Part 1*. Pergamon, Oxford, third edition, 1989.

[81] T. D. Lee, K. Huang, and C. N. Yang. Eigenvalues and eigenfunctions of a bose system of hard spheres and its low-temperature properties. *Physical Review*, 106:1135–1145, June 1957.

[82] Anthony J. Leggett. Cooper pairing in spin-polarized fermi systems. *J. Phys. Colloques*, 41(C7):C7–19 – C7–26, July 1980.

[83] L. Luo and J. E. Thomas. Thermodynamic measurements in a strongly interacting fermi gas. *J. Low Temp. Phys.*, **154**:1, 2009.

[84] C. Manuel M. Mannarelli and L. Tolos. Shear viscosity in a superfluid cold fermi gas at unitarity. 2012.

[85] S.-K. Ma. *Modern Theory Of Critical Phenomena*. W. A. Benjamin, 1976.

[86] Andrew J. Majda, Andrea L. Bertozzi, and D. G. Crighton. *Vorticity and Incompressible Flow*. Cambridge Univ. Press, Cambridge, 2001.

[87] C. Manuel and L. Tolos. Shear viscosity due to phonons in superfluid neutron stars. *Phys. Rev. D*, **84**:123007, 2011.

[88] M. E. McIntyre. On the 'wave momentum' myth. *J. Fluid Mech.*, 106:331–337, 1981.

[89] J. Meineke, J.-P. Brantut, D. Stadler, T. Müller, H. Moritz, and T. Esslinger. Interferometric measurement of local spin-fluctuations in a quantum gas. *ArXiv e-prints*, February 2012.

[90] C. Menotti, P. Pedri, and S. Stringari. Expansion of an interacting fermi gas. *Phys. Rev. Lett.*, **89**:250402, 2002.

[91] S. Nascimbene, N. Navon, K. Jiang, F. Chevy, and C Salomon. Exploring the thermodynamics of a universal fermi gas. *Nature*, **463**:1057, 2010.

[92] T. Nikuni and A. Griffin. Frequency and damping of hydrodynamic modes in a trapped bose-condensed gas. *Phys. Rev. A*, **69**:023604, 2004.

[93] K. M. O'Hara, S. L. Hemmer, M. E. Gehm, S. R. Granade, and J. E. Thomas. Observation of a strongly-interacting degenerate fermi gas of atoms. *Science*, **298**:2179, 2002.

[94] A. Onuki. *Phase Transition Dynamics*. Cambridge University Press, 2002.

[95] E. D. Siggia P. C. Martin and H. A. Rose. Statistical dynamics of classical systems. *Phys. Rev. A*, **8**:423, 1973.

[96] D. T. Son P. Kovtun and A. O. Starinets. Viscosity in strongly interacting quantum field theories from black hole physics. *Rev. Mod. Phys.*, **94**:111601, 2005.

[97] H. Smith P. Massignan, G. M. Bruun. Viscous relaxation and collective oscillations in a trapped fermi gas near the unitarity limit. *Phys. Rev. A*, **71**:033607, 2007.

[98] R. E. Peierls and J. Yoccoz. The collective model of nuclear motion. *Proceedings of the Physical Society A*, 70:381–387, May 1957.

[99] Rudolf Peierls. *Surprises in Theoretical Physics*. Princeton University Press, Princeton, N.J., 1979.

[100] J. Peralta-Ramos and E. Calzetta. Shear viscosity from thermal fluctuations in relativistic conformal fluid dynamics. *JHEP*, **1202**:085, 2012.

[101] Michael Edward Peskin and Daniel V. Schroeder. *An introduction to quantum field theory*. Advanced book program. Westview Press Reading (Mass.), Boulder (Colo.), 1995. Autre tirage : 1997.

[102] K. Petersen. *Ergodic Theory*. Cambridge U. Press, Cambridge, 1990.

[103] G. Policastro, D. T. Son, and A. O. Starinets. The shear viscosity of strongly coupled n = 4 supersymmetric yang-mills plasma. *Rev. Mod. Phys.*, **87**:081601, 2001.

[104] A. Polkovnikov, K. Sengupta, A. Silva, and M. Vengalattore. Colloquium: Nonequilibrium dynamics of closed interacting quantum systems. *Reviews of Modern Physics*, 83:863–883, July 2011.

[105] S. Popescu, A. J. Short, and A. Winter. The foundations of statistical mechanics from entanglement: Individual states vs. averages. *eprint arXiv:quant-ph/0511225*, November 2005.

[106] S. J. Putterman, editor. *Superfluid hydrodynamics*, volume 3, 1974.

[107] M. Randeria, J.-M. Duan, and L.-Y. Shieh. Superconductivity in a two-dimensional fermi gas: Evolution from cooper pairing to bose condensation. *Phys. Rev. B*, **41**:327, 1990.

[108] F. Reif. *Fundamentals of statistical and thermal physics*. McGraw–Hill, 1965.

[109] S. Riedl, E. R. Sanchez-Guajardo, C. Kohstall, A. Altmeyer, M. J. Wright, J. Hecker Denschlag, R. Grimm, G. M. Bruun, and H. Smith. Collective oscillations of a fermi gas in the unitarity limit: Temperature effects and the role of pair correlations. *Phys. Rev. A*, **78**,:053609, 2008.

[110] F. Rohrlich. *Classical Charged Particles*. World Scientific, 2007.

[111] P. Romatschke. New developments in relativistic viscous hydrodynamics. *IJMPE*, **19**:1, 2010.

[112] Walter Rudin. *Functional analysis*. McGraw-Hill Book Co., New York, 1973. McGraw-Hill Series in Higher Mathematics.

[113] G. Rupak and T. Schäfer. Shear viscosity of a superfluid fermi gas in the unitarity limit. *Phys. Rev. A*, **76**:053607, 2007.

[114] T. Schäfer. The shear viscosity to entropy density ratio of trapped fermions in the unitary limit. *Phys. Rev. Lett.*, **76**:063618, 2007.

[115] T. Schäfer. Shear viscosity and damping of collective modes in a two-dimensional fermi gas. *Phys. Rev. A*, **85**:033623, 2012.

[116] T. Schäfer and C. Chafin. Scaling flows and dissipation in the dilute fermi gas at unitarity. In *Springer Lecture Notes in Physics "BEC-BCS Crossover and the Unitary Fermi gas ""*. Springer, 2009.

[117] T. Schäfer and D. Teaney. Nearly perfect fluidity: From cold atomic gases to hot quark gluon plasmas. *Rept. Prog. Phys.*, **72**:126001, 2009.

[118] M. Schlosshauer. Decoherence, the measurement problem, and interpretations of quantum mechanics. *Reviews of Modern Physics*, 76:1267–1305, October 2004.

[119] Silvan S Schweber. *An introduction to relativistic quantum field theory*. Row and Peterson, Evanston, IL, 1961.

[120] D. T. Son. Vanishing bulk viscosities and conformal invariance of unitary fermi gas. *Phys. Rev. Lett.*, **98**:020604, 2007.

[121] D. T. Son and M. Wingate. General coordinate invariance and conformal invariance in nonrelativistic physics: Unitary fermi gas. *Annals Phys.*, **321**:197, 2006.

[122] B. P. Stoicheff and G. I. Stegeman. Light scattering from shear waves in liquids. *J. Acous. Soc. Am*, **45**:311, 1969.

[123] S. Stringari. Collective oscillations of a trapped superfluid fermi gas near a feshbach resonance. *Europhys. Lett.*, **65**:749, 2004.

[124] W. Zwerger T. Enss, R. Haussmann. Viscosity and scale invariance in the unitary fermi gas. *Annals Phys.*, **326**:770, 2011.

[125] J. E. Thomas. Is an ultra-cold strongly interacting fermi gas a perfect fluid? *Nuc. Phys. A*, **830**:665c, 2009.

[126] J. E. Thomas, J. Kinast, and A. Turlapov. Virial theorem and universality in a unitary fermi gas. *Phys. Rev. Lett.*, **95**:120402, 2005.

[127] Richard C. Tolman. *The Principles of Statistical Mechanics*. Dover, 1979.

[128] G. Torrieri. Viscosity of an ideal relativistic quantum fluid: A perturbative study. *Phys. Rev. D*, **85**:065006, 2012.

[129] Constantino. Tsallis. *Introduction to Nonextensive Statistical Mechanics: Approaching a Complex World /*. Springer New York,, New York, NY :, 2009.

[130] A. Turlapov, J. Kinast, B. Clancy, L. Luo, J. Joseph, and J. E. Thomas. Is a gas of strongly interacting atomic fermions a nearly perfect fluid. *J. Low Temp. Phys.*, **150**:567, 2007.

[131] B. Vacchini and K. Hornberger. Quantum linear Boltzmann equation. *Phys. Rep.*, 478:71–120, July 2009.

[132] E. Vogt, M. Feld, B. Frohlich, D. Pertot, M. Koschorreck, and M. Köhl. Scale invariance and viscosity of a two-dimensional fermi gas. *Phys. Rev. Lett.*, **108**:070404, 2012.

[133] J. von Neumann. *Mathematical Foundations of Quantum Mechanics*. Princeton University Press, Princeton, 1955.

[134] F. Werner. *Trapped cold atoms with resonant interactions: unitary gas and three-body problem*. PhD thesis, Ecole Normale Superieure, 2009.

[135] F. Werner and Y. Castin. Unitary gas in an isotropic harmonic trap: Symmetry properties and applications. *Phys. Rev. A*, 74(5):053604, November 2006.

[136] G. Wlazlowski, P. Magierski, and J. E. Drut. Shear viscosity of a unitary fermi gas. *Phys. Rev. Lett.*, **109**:020406, 2012.

[137] J. Wölk and R. Strey. Homogeneous nucleation of h2o and d2o in comparison: the isotope effect. *The Journal of Physical Chemistry B*, 105(47):11683–11701, 2001.

[138] M. J. Wright, S. Riedl, A. Altmeyer, C. Kohstall, E. R. Sanchez Guajardo, J. Hecker Denschlag, and R. Grimm. Finite-temperature collective dynamics of a fermi gas in the bec-bcs crossover. *Phys. Rev. Lett.*, **99**:150403, 2007.

[139] V. I. Yukalov and H. Kleinert. Gapless Hartree-Fock-Bogoliubov approximation for Bose gases. *Phys. Rev. A*, 73(6):063612, June 2006.

APPENDIX

Appendix A

Stress tensor correlation function in hydrodynamics

A.1 Low energy expansion

In this section we provide some additional details regarding the low energy expansion of the retarded stress tensor correlation function. Our starting point is the symmetrized correlation function

$$G_S^{xyxy}(\omega,\mathbf{k}) = \int d^3x \int dt\, e^{i(\omega t-\mathbf{k}\cdot\mathbf{x})} \left\langle \frac{1}{2}\left\{\Pi_{xy}(t,\mathbf{x}),\Pi_{xy}(0,0)\right\}\right\rangle . \tag{A.1}$$

We use the expression for the stress tensor in hydrodynamics and expand in small fluctuations, $\delta\rho, \delta T, v_i$, and in the number of derivatives. We get

$$\Pi_{xy} = \rho_0 v_x v_y - \eta_0\left(\nabla_x v_y + \nabla_y v_x\right) - \left[\left(\frac{\partial\eta}{\partial\rho}\right)_T \delta\rho + \left(\frac{\partial\eta}{\partial T}\right)_\rho \delta T\right]\left(\nabla_x v_y + \nabla_y v_x\right) + \ldots \tag{A.2}$$

where we have dropped terms of order $O(\delta^3)$ and $O(\nabla^2)$ (note that v_i is a quantity of $O(\delta)$). The diagrammatic expansion can be derived by inserting equ. (A.2) into equ. (A.1) and factorizing the expectation value into pairs of fluctuating fields. The retarded correlation function is obtained by replacing one of the symmetrized functions by a retarded function. In Section 8.3 we computed the one loop diagram that arises from the first term in equ. (A.2). This term has no spatial derivatives, and we find a contribution of the form

$$G_R^{xyxy}(\omega,0) \sim T\Lambda^3\left\{1 + c_1\frac{\omega}{D_\eta\Lambda^2} + c_{3/2}\frac{\omega^{3/2}}{D_\eta^{3/2}\Lambda^3} + \ldots\right\}, \tag{A.3}$$

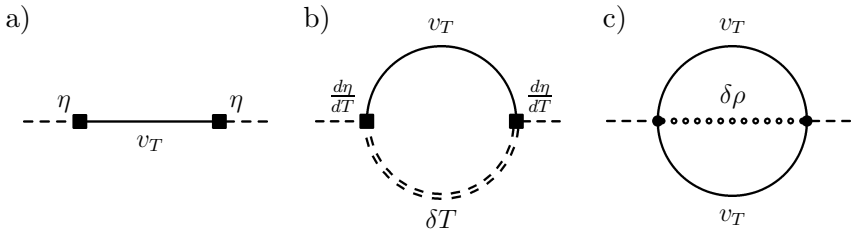

Figure A.1: Diagrammatic representation of higher order fluctuation contributions to the stress tensor correlation function. Solid lines labeled v_T denote the transverse velocity correlator, wavy lines labeled v_L denote the longitudinal velocity correlator. Temperature fluctuations are shown as double dashed lines, and density fluctuations are shown as dotted lines. Vertices shown as dots contain no derivatives, whereas vertices labeled by squares contain spatial derivatives.

where c_1 and $c_{3/2}$ are numerical constants. We observe that the low energy expansion involves powers of $\omega/(D_\eta \Lambda^2)$.

The second term contains spatial derivatives, and it gives rise to a tree diagram (Fig. A.1a) which vanishes as $k \to 0$. The third term in equ. (A.2) involves derivatives of the shear viscosity with respect to ρ and T. In kinetic theory $[(\partial\eta)/(\partial\rho)]_T$ vanishes at leading order in $n\lambda_{dB}^3$, where λ_{dB} is the de Broglie wave length. The dominant term therefore involves fluctuations of the temperature, $G_S \sim [(\partial\eta)/(\partial T)]^2 \langle \delta T \delta T \rangle \langle \nabla_x v_y \nabla_x v_y \rangle$ (plus permutations $x \to y$), see Fig. A.1b. This is a one-loop graph with vertices that contain one spatial derivative. For non-zero external momenta this graph gives a contribution to G_R which is suppressed by k^2/K_{hyd}^2 relative to equ. (A.3). For zero external momentum the diagram has power divergences which contribute at $O(\Lambda^2/K_{hyd}^2)$. This is not small if $\Lambda \sim K_{hyd}$, but power divergences can be absorbed into the transport coefficients[1].

The leading no-derivative contribution of order δ^3 in the stress tensor is of the form $\Pi_{xy} = (\delta\rho) v_x v_y$. This term generates the two-loop diagram shown in Fig. A.1c. The extra loop integral involves three powers of momentum, and the extra propagator is proportional to $1/\rho$. As a consequence, the graph is suppressed by Λ^3/k_F^3. This can be written as $(\Lambda/k_F)^3 \lesssim (K_{hyd}/k_F)^3 \simeq 1/(n l_{mfp}^3)$, where we have used the kinetic theory estimate $\eta \simeq n(mT)^{1/2} l_{mfp}$.

In summary, the hydrodynamic expansion of the correlation function $G_R^{xy}(\omega, \mathbf{k})$ involves powers of k/K_{hyd}, where $K_{hyd} = (P/\rho)^{1/2} D_\eta^{-1} \sim l_{mfp}^{-1}$ is the breakdown scale defined in Section

[1]It is well known that power counting is not manifest in effective field theories regularized by a momentum cutoff [23]. This problem can be circumvented using dimensional regularization (DR), which automatically eliminates all power divergent terms. In our context this is a disadvantage because we find that the leading one loop divergence in the stress tensor correlation function represents an important physical effect. The linear divergence is preserved in a modified version of dimensional regularization called "power divergence subtraction" (PDS) [38], which keeps the pole corresponding to the logarithmic divergence in two spatial dimensions.

8.4. Since $G_R^{xy}(\omega, \mathbf{k})$ is diffusive the frequency scales as $\omega \sim D_\eta k^2$ and the frequency expansion involves $(\omega/[D_\eta K_{hyd}^2])$. Powers of k/K_{hyd} arise from higher derivative terms in the currents or from loop graphs. Loop graphs are additionally suppressed by $(K_{hyd}/k_F)^3 \simeq 1/(nl_{mfp}^3)$. Loop graphs are important because they lead to non-analytic effects, logarithms and fractional powers of ω and k^2. For low viscosity fluids the mean free path is short, $nl_{mfp}^3 \sim 1$, and there is no suppression of loops relative to gradient terms.

A.2 Contact terms

The symmetrized correlation function contains a contact term which can be determined using the fluctuation-dissipation theorem [6, 50]

$$\left\langle \frac{1}{2}\left\{\Pi_{xy}(t,\mathbf{x}),\Pi_{xy}(t',\mathbf{x}')\right\}\right\rangle = 2\eta T\delta(t-t')\delta(\mathbf{x}-\mathbf{x}')\,. \tag{A.4}$$

In frequency space this gives the contribution of the bare shear viscosity to the retarded correlation function, $G_R = i\omega\eta$. The result therefore justifies combining the bare and loop corrections as in equ. (8.29). The contact term can also be obtained using the velocity correlation function combined with the conservation laws [76]. Momentum conservation implies $\nabla_i \Pi^{ij} = -\frac{\partial}{\partial t}(\rho v^j)$ and

$$k_x^2 G_S^{xyxy}(\omega,k_x) = \omega^2 \Delta_S^{yy}(\omega,k_x)\,. \tag{A.5}$$

Using the explicit form of the velocity correlation function we find

$$G_S^{xyxy}(\omega,k_x) = 2\eta T\left\{1-\frac{(D_\eta k_x^2)^2}{\omega^2+(D_\eta k_x^2)^2}\right\}\,, \tag{A.6}$$

which contains the contact term $2\eta T$.